DEVELOPMENT AND VALIDATION OF AN INSOLE BASED WEARABLE SYSTEM FOR GAIT AND ACTIVITY MONITORING

by

NAGARAJ HEGDE

EDWARD SAZONOV, COMMITTEE CHAIR
PHILIP A. BISHOP
DANIEL J. FONSECA
FEI HU
EDWARD MELANSON

A DISSERTATION

Submitted in partial fulfillment of the requirements
for the degree of Doctor of Philosophy
in the Department of Electrical & Computer Engineering
in the Graduate School of
The University of Alabama

TUSCALOOSA, ALABAMA

2017

ABSTRACT

Footwear based wearable sensors are used in applications such as activity monitoring, gait analysis, post-stroke rehabilitation, body weight measurements, and energy expenditure estimation. Such wearable sensors typically required the modification or alteration of the shoe, which is not typically feasible for large populations without the direct involvement of shoe manufacturers. This dissertation presents an insole-based wearable sensor (SmartStep) that has its electronics fully embedded into a generic insole, which can be used with a large variety of shoes and, thus, resolves the need for shoe modification. The SmartStep is an always-on electronic device that comprises of inertial sensors and resistive pressure sensors implemented around a system on chip with Bluetooth low energy (BLE) connectivity. The dissertation explains a novel Android application methodology to interface multiple BLE sensors. As a part of the research, SmartStep's predecessor, SmartShoe, was tested in an application scenario of gait monitoring of children with cerebral palsy. Novel signal processing algorithms were developed to deal with the effect of orthotics on pressure sensors. Machine learning models were used to recognize 3 major activities (sitting, standing and walking) with greater than 95% accuracy. The gait parameter estimation resulted in average error less than 6% across a range of temporal gait parameters. The SmartStep device was utilized in a study for recognizing activities of daily living (ADL) in adults. An upper-body, wrist-worn sensor was also utilized in the same study to compare the effectiveness of upper and lower body-worn sensors in recognizing ADL. The indirect calorimetry data from a portable metabolic system (Cosmed K4b), collected in the same study, were used to develop energy expenditure (EE) estimation

models. Two different sets of steady state activity branched models were developed, along with models for transition activities. The EE models were validated on the data from a room calorimeter. SmartStep was 90% accurate in recognizing a broad set of nine ADLs, including household activities; while having 6% validation error in estimating total energy expenditure. These results suggest that SmartStep is accurate in recognizing multiple activities of daily living and in energy expenditure estimation.

DEDICATION

This work is dedicated to my beloved parents, brother, wife, friends and all my teachers.

LIST OF ABBREVIATIONS AND SYMBOLS

FSR	Force sensitive resistor
EE	Energy expenditure
MCU	Microcontroller unit
BLE	Bluetooth low energy
MLD	Multinomial logistic discrimination
GRF	Ground reactive force
ACC	Accelerometer
PS	Pressure sensor
DR	Dara retrieved
DL	Data loss
NTS	Number of timestamps received
LTS	Last timestamp received
FTS	First timestamp received
CP	Cerebral palsy
SVM	Support vector machines
ANN	Artificial neural network
MALE	Most affected lower extremity
LALE	Least affected lower extremity
RMSE	Root mean square error
AP	ActivPAL

ACKNOWLEDGMENTS

My time spent at University of Alabama has been an opportunity to grow in many ways academically, personally, and spiritually. I would like to express my deepest gratitude to those who contributed to the fulfillment of this dream. First and foremost, I want to thank the supreme divinity (whom we call as Radha – Krishna in our tradition) for guiding my path, and providing the strength to purse my goals. Likewise, to my parents for always encouraging me to do better in life, be my inspiration, and continue to provide their unconditional love and support. I want to express my deepest gratitude and love to my dear wife – Raji, who supported me all throughout this journey.

My deepest gratitude to my advisor Dr. Edward Sazonov, whose guidance and constant support made this work possible. Dr. Sazonov was always available, very helpful, motivating, patient and immensely knowledgeable. I also want to acknowledge the help and support of my dissertation committee comprising of Dr. Daniel J. Fonseca, Dr. Fei Hu, Dr Philip A. Bishop and Dr Edward Melanson for their insightful comments and constructive criticism in writing of this work.

I have been blessed with many friends that I got to know during my stay at UA and made this journey even more interesting. First, I would like to express my humble gratitude to those friends that stood by me in times of uncertainty and always found a way to lift me up: Muhammad Farooq, Sayeed Doulah, Masudul Imtiaz, Yogendra Patel, Ting Zhang, Dr. Paulo Lopez-Meyer, Dr. Sawal Ali and Dr. Raul Ramos, Dr Juan Fontana for their support and fruitful discussion which always led me to better solutions to the problems at hand. My deepest gratitude to Prajakta and Suguna for helping me in proof reading of this manuscript. I would also like to thank the community members in Tuscaloosa who were kind hearted, friendly and made me feel at home. I would like to express my sincere gratitude to UA Vedic society, which is a student community focused on Yoga and meditation, which I was honored to serve for 3 years as president. I am very grateful to all my T-town friends namely Joseph Paul, William McGavin, Lauren, Paige, Prof. Chris, Gillian, Mohammad Firouz and all other members of UA Vedic society. I would like to thank Ms Connie Sol from Science of fitness, for helping me to conduct the controlled experiments utilizing SmartStep and the Cosmed K4B2 mask. I thank Praveen KR, Ganapati, Preetham and all my childhood friends for encouraging me in my life. My deepest gratitude to HLS Rao Sir, Ms Veena, Purnananand Sir for helping me to learn Mathematics and Physics in my life.

CONTENTS

LIST OF FIGURES

LIST OF TABLES

CHAPTER 1 INTRODUCTION

1.1 Motivation and Goals

Improving the quality of life is a fundamental goal of science and technology. Quality of life can be greatly affected by old age, obesity epidemic, disability and other factors. More than half of the U.S. population is overweight or obese [1]. Stroke is the third leading cause of death in the U.S and more than 140,000 people die each year from stroke [2]. Aged people represent 14% of the U.S. population [3]. Given these statistics, we can clearly see that there is immense potential in creating technology that can help these individuals.

With the exponential growth of electronics industry, wearable systems have become a part of modern everyday life. Wearable systems find their way in multiple different applications related to healthcare. Some of these application areas include, but are not limited to, post stroke rehabilitation, weight management programs, and fall risk applications.

Today, there are wearable systems that are socially acceptable but are not clinically accurate and clinically accurate systems that are not socially acceptable or are laboratory bound most of the time. This dissertation involved development and validation of an insole based wearable system that can be used in measures of accurate gait and activity monitoring, and energy expenditure estimation. The goal was to design and develop a socially acceptable, unobtrusive, low power, completely wireless insole based system that could be manufactured for any shoe size; and validate that system both in the laboratory as well as in free living conditions. This dissertation describes a review of the existing footwear based systems, system development aspects of the proposed insole based monitor (SmartStep) and challenges addressed in wireless communication. Along with these, description of future studies and data processing methodologies are also described.

1.2 The Big Picture

This dissertation builds upon some of the previous works carried out in our lab, in developing a clinically accurate activity and gait monitoring system that can be used in community living. SmartShoe systems[4]–[6] were one of the first systems in the field, which were utilized in gait and activity monitoring, and energy expenditure estimation studies in laboratory environments. SmartShoe systems are comprised of an insole with pressure sensors embedded and a shoe clip-on that housed all the electronics including interface for wireless connectivity. This solution was highly accurate clinically; however, SmartShoes had low social

acceptability, low power operation and lack of user friendly design, all of which play an important role in utilizing wearable systems for community living. The SmartStep insoles of the present study were the logical way forward addressing all these challenges (detailed later in Chapter 2 and 3). In developing a versatile, insole based wearable system, SmartStep, for

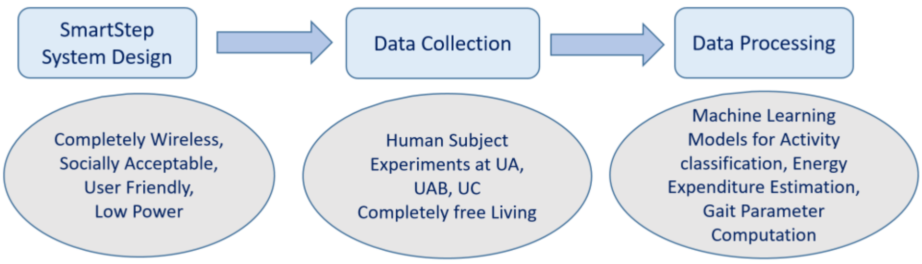

Figure 1-1. Overall design process.

applications such as physical activity monitoring, energy expenditure estimation and gait monitoring, this work had many components as shown in Figure 1-1.

SmartStep is an insole based wearable system, and the development of SmartStep involved intelligent hardware and firmware designs to make it user friendly while being a low power system. SmartStep's electronics are comprised of accelerometer, gyroscope, pressure sensors, flash memory, Bluetooth Low Energy (BLE) connectivity and the battery, all integrated in an insole. The system is utilized in human subject studies to collect the sensor data from the SmartStep. On the collected data, machine learning algorithms were developed offline, for activity prediction, gait monitoring, and for energy expenditure estimation. Once these final models are developed, they can be implemented in a smartphone for real time monitoring of daily activities, energy expenditure or in providing biofeedback to help the people in their daily living.

Chapter 2 gives a background on the existing footwear based wearable systems and possible future directions in the field. Chapter 3 details the hardware and firmware design challenges addressed in the development of the SmartStep, designing it to be a socially acceptable, user friendly and low power system. Chapter 4 describes a novel methodology developed to interface 2 or more BLE sensors to Android smartphones, a methodology which is essential in the human subject experiments proposed in this dissertation. Chapter 5 describes a human subject study conducted to develop activity and gait monitoring models for the children with cerebral palsy (CP). Chapter 6 describes a human subject study conducted in utilizing the SmartStep for monitoring a broader set of activities of daily living (ADL). Chapter 7 describes some initial results of utilizing SmartStep as a means for monitoring energy expenditure in daily living. Chapter 8 concludes the dissertation and gives future directions.

CHAPTER 2 A COMPARATIVE REVIEW OF FOOTWEAR-BASED WEARABLE SYSTEMS

Published: N. Hegde, M. Bries, E. Sazonov, "A Comparative Review of Footwear Based Wearable Systems" Electronics 2016, 5(3), 48; doi:10.3390/electronics5030048

This chapter describes a full review of the existing footwear based technologies for a wide range of applications such as gait monitoring, plantar pressure measurement, activity and energy expenditure estimation among others.

2.1 Introduction

Footwear is a vital part of human life across the globe. While the initial purpose was to protect the feet [1], they have also become a symbol of style and personality [2]. Footwear acts as the interface between the ground and the wearer's foot. Much information can be gleaned from observing this interaction. Attempts to capture this information by integrating sensing elements and electronics in the footwear began in the 1990s, both for academic research purposes and in commercial products [3]. In recent times, development of low power, wireless, unobtrusive and socially acceptable wearable computing systems has become an increasingly important research goal. This trend is aided by the exponential growth in the electronics industry, which is driving rapid advancements in microfabrication processes, wireless communication, and sensor systems.

The applications for footwear-based systems range from simple step counting systems to more advanced systems intended for use in rehabilitation programs for disabled subjects. Footwear-based systems available on the market or in research laboratories today vary in their sensor modalities and data acquisition methodologies in order to meet different application requirements. Typically, these systems consist of pressure sensors for plantar pressure measurement, inertial sensors (accelerometer and/or gyroscope) for movement detection and a wired or wireless connection for data acquisition. The signal processing of this collected data varies depending on the application, can range from lightweight signal processing methodologies (for example, binary decision trees) running on a handheld device to complex signal processing/machine learning models (for example, Support Vector Machines or neural networks) running on a personal computer.

Several vital biomechanical parameters can be estimated using sensors placed in the footwear. For example, by placing pressure-sensitive elements in the footwear, foot plantar pressure can be measured. By utilizing pressure-sensitive elements along with inertial sensors, several gait parameters can be calculated. Additionally, actuators in the footwear and measuring gait patterns, can generate biofeedback to assist patients suffering from stroke. The same set of pressure sensors and inertial sensors can also be used in tracking posture and activity recognition and energy expenditure estimation. These and other important applications have driven footwear wearable technology to its present state and continue to drive the technology even further.

In this chapter we review advancements in footwear-based wearable systems based on their target applications. Applications described in the chapter include those that focus on gait monitoring, plantar pressure measurement, posture and activity classification, body weight and energy expenditure estimation, biofeedback, navigation, and fall risk. For each application, example systems are taken from published research and consumer products.

Keywords such as ‘gait monitoring systems’, ‘plantar pressure measurement’, and others were searched in databases such as IEEE Xplore, PubMed, and Google Scholar.

Literature that described portable or wearable systems that have sensors embedded in the shoes, insoles, sandals, or socks were included and the stationary systems were excluded from the review.

The chapter discusses the existing systems with respect to their hardware, sensor modalities, modes of data acquisition and data processing methodologies. Merits/demerits of each system are also pointed out. The work also attempts to shine a light on some of the most recent advancements in the field, as well as on the future direction for footwear-based wearable systems.

2.2 Applications for Footwear-Based Wearable Systems

2.2.1 Gait Analysis

A person's walk is characterized by their gait, which involves a repetitious sequence of limb motions to move the body forward while simultaneously maintaining stability [7]. Having a normal gait allows someone to remain agile so that they may easily change directions, walk up or down stairs, and avoid obstacles. Patients with neuromuscular disorders are likely to have abnormal gaits and suffer in their ability to perform locomotive activities. Objective measurement and analysis of gait patterns can help in the rehabilitation of disabled individuals.

Figure 2-1a shows an illustration of an instrumented insole developed for gait monitoring by Crea et al. [8]. There are two kinds of parameters that are computed in gait monitoring applications: temporal and spatial. Some of the examples of the temporal gait parameters are cadence, stance time, step time, single support time, and double support time; while step length and stride length are examples for spatial gait parameters. Gait monitoring is one field of wearable computing where there is a high number of footwear-based systems deployed. There are force plates available for gait analysis [9], and there are also systems that make use of the Kinect (Microsoft Inc, Redmond, USA) [10], [11]; but footwear-based solutions are much better suited for uncontrolled free living conditions outside the laboratory environment. Footwear is also an ideal location to measure the gait parameters as these applications measure the parameters involved in the movement of foot.

By utilizing pressure-sensitive elements such as force sensitive resistors (FSR) for gait monitoring, temporal parameters such as cadence, step time, stance time and others can be computed. This is done utilizing the heel strike and toe off time events (Figure 2-1b). The gait monitoring applications extract gait event information from the changes in pressure sensor readings and not the absolute pressure. Hence, the pressure sensing does not need high spatial resolution, so only a few pressure elements are used in such applications. High pressure measurement precision is not needed, and for that reason, sometimes these are called foot switches. In Table 2-1 we are comparing many such footwear based gait analysis systems.

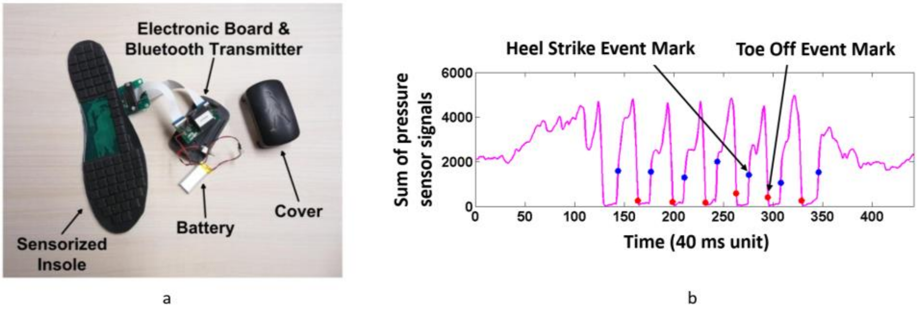

Figure 2-1. (a) Instrumented footwear for gait monitoring presented by and Crea et al. [8]; (b) Marking of heel strike and toe off time instances from the pressure sensor signals.

For computation of temporal gait parameters, a higher sampling frequency means better time resolution, resulting in higher accuracy in the computed parameters. However, there is a tradeoff between battery life, sampling frequency, and accuracy (applicable to all of the systems discussed in this work). A higher sensor sampling frequency will result in higher power consumption by the system, resulting in a shortened battery life; whereas a lower sampling frequency may decrease the accuracy of the system. Crea et al. [8] used 18.75 Hz, however it has not yet been fully validated. In [5], it was shown that 25 Hz is sufficient for gait parameter extraction for walking at the speed of 2 km/h or less. However, our ongoing work suggests that for computation of parameters such as double support time, especially during walking at speeds more than 4 km/h or running, 25 Hz is insufficient. Sampling frequencies of greater than 50 Hz, as reported by Leunkeu et al [12], will provide a better accuracy for all the gait parameter computations.

Inertial sensors such as an accelerometer in conjunction with gyroscope, can be used in the computation of distance or elevation. Hence, these inertial sensors are utilized in the computation of spatial gait parameters such as step length or stride length, as shown in cite [12].

Only a couple of the papers discussed the expected battery life for their systems. Wu et al. [8] reported that a battery life of about 20 h is achievable, which can enable almost two days of wear in real life situations. In [20], 10 h of usage time on single charge is reported, which can enable one day of wear on full charge. However, in [20], having this particular lithium polymer battery under the foot may be potentially hazardous.

From connectivity perspective, Bluetooth is quite commonly used in many of the footwear-based systems as done in several papers [5,10,18]. A lower power consumption version of Bluetooth, named Bluetooth Low Energy (BLE), is coming to prominence in the recent years and there are a few footwear-based systems that have utilized BLE, [21], [22], which will be discussed in the later sections. The study in [21] has reported more than two orders of magnitude in power savings when utilizing BLE compared to traditional Bluetooth

Table 2-1. Comparison of footwear systems in gait analysis

	Bamberg et al.[12]	Sazonov et al. [5]	Chen et al. [13]	Mariani et al. [14]	Leunkeu et al. [15]	Huang et al. [16]
Sensing element	FSR, polyvinyliden fluoride strip, accelerometer, gyroscope	FSR, accelerometer	FSR, accelerometer, gyroscope	Accelerometer and gyroscope	Parotec plantar pressure insoles	Pressure sensor, tilt angle sensor, accelerometer, gyroscope, bend sensor
Sampling frequency	75 Hz	25 Hz	50 Hz	200 Hz	150 Hz	50 Hz
Data transmission method	RF to PC	Bluetooth to Smartphone	RF to PC	SD card logged	SD card logged	RF to PC
Data analysis method	PC post processing to compute gait parameters	PC post processing to compute gait parameters	PC post processing to predict abnormal gait	PC post processing to compute gait parameters	PC post processing	PC post processing for gait modeling to identify humans based on their gait
Real time gait monitoring	NA	NA	NA	NA	NA	visualization of sensor signals in PC
Clinical/ Validation Study	Computed gait parameters of 10 healthy subjects and 5 PD patients	Computed gait parameters of 16 healthy subjects and 7 post stroke patients	NA	Computed gait parameters of 10 PD patients and 10 healthy subjects	Computed gait parameters of 15 CP and 10 normal children	Identified a human subject based on his gait against 8 other human subjects
Gait analysis performed	Computed maximum pitch, minimum pitch, stride length, stride time, % stance time	Computed cadence, step time, cycle time, swing %, stance %, single support %, double support %	Classified 5 different gait types: Normal, toe in, toe out, over supination and heel walking	Computed turning angle, stride velocity, stride length, swing width, path length	Computed step duration, double support time, ground contact time, velocity, step frequency and stride length	Computed individual human gait model using cascade neural network
Criterion Comparison	Validated against MGH BMLs Selspot II	Validated against GaitRite	NA	Validated against optical system by Vicon Motion Systems Ltd	NA	NA
Accuracy	Highest mean percentage change of 15.6% in maximum pitch	Highest relative error of 18.7% for step time and least relative error of 2.7% for cycle time	Highest accuracy of 97% for detecting over supination and least accuracy of 82.3% for toe in	Stride velocity and stride length accuracy ± precision of 2.8±2.4 cm/s and 1.3±3.0 cm	NA	97% accuracy for correct human identification from gait model

	Kong et al. [17]	Liu et al. [18]	González et al. [19]	Crea et al. [8]	Wu et al. [20]
Sensing element	Custom air pressure sensor	Triaxial force sensors for measuring GRF and COP	FSR and accelerometer	Optoelectronic sensing	Fiber based pressure sensors
Sampling frequency	200 Hz	100 Hz	50 Hz	18.75 Hz	30 Hz
Data transmission method	NI CompactRio was used for data acquisition	Storing data in MCU's SRAM and offline uploading to PC	Bluetooth to Smartphone	Bluetooth to PC	SD card logging
Data analysis method	PC post processing	PC post processing	PC post processing	PC post processing	PC post processing
Real time gait monitoring	NA	NA	Android smartphone	Real time display of sensor signals and gait phase.	NA
Clinical/ Validation Study	NA	Validated on 7 healthy subjects.	Validated on 6 healthy subjects.	Validated on 2 healthy subjects	NA
Gait analysis performed	Fuzzy logic based gait phase abnormality detection	Average coefficient of variation for three-directional GRF to evaluate walking extrinsic gait variability	A fuzzy rule-based inference algorithm implemented on a smartphone, used to detect each of the gait phases.	Computed stance and swing duration of both feet; duration of the double-support phases; and step cadence of both feet.	Methodology for local randomized selective sensing based on pressure signal maps.
Criterion Measure Comparison	NA	Validated against Kyowa force plate and optical motion analysis system by NAC Image Tech	NA	Validated against AMTI force plate	NA
Accuracy	Proposed sensing unit showed a repeatability of 97%. Abnormal gait monitoring results were not quantified	RMS error of 7.2% ± 0.8% and 9.0% ± 1% for transverse component of ground reaction force and 1.5% ± 0.9% for vertical component	92% cross validation accuracy for the probabilistic classifier	Pearson correlation 0.89 ± 0.03 with the force plate	Normalized mean square error of the proposed sensing methodology is within 10%, compared against actual signal

With regard to data processing, many gait monitoring applications in their current form rely on collecting the data from human subject experiments and a PC performing post processing, as in most of the cases as shown in Table 2-1. Real-time gait monitoring and visual feedback can help in clinical applications and González et al. [19], Ferrari et al. [23], and Crea et al. [8] have taken this into account.

There are a few studies that have used gait information obtained from footwear-based systems in pattern recognition. Huang et al. [16] identified a human subject based on the wearer's gait compared to eight other human subjects. Klucken et al. [24] were able to successfully distinguish Parkinson's Disease patients from healthy subjects with an accuracy of 81%. Barth et al. [25] have presented a methodology to search for patterns matching a pre-defined stride template from footwear sensor data, to automatically segment single strides from continuous movement sequences.

All of the footwear-based solutions listed are research prototypes and some of them [9,11] were primarily suited for laboratory studies. On the other hand, Sensoria® (Sensoria Inc, Redmond, USA) has developed commercial instrumented socks for gait monitoring. The associated smartphone application running on iOS or Android is intended to help runners and provides real-time feedback on foot landing patterns, cadence and other important gait characteristics. Technical characteristics of the Sensoria product were not available at the time of this review.

Systems in [5,11,19,23] would need further human subject studies as they have not yet been fully tested. Additionally, it is important to note that none of the above-described systems have undergone a longitudinal free-living study, which is essential to understand the gait behavior of wearers in community living. Development and full-fledged validation of a socially acceptable, user friendly, and reliable footwear-based gait monitor well suited for longitudinal studies is still an open challenge in the field that needs to be addressed.

2.2.2 Plantar Pressure Measurement

Plantar pressure is the pressure distribution between the foot and the support surface during everyday locomotion activities. Foot plantar pressure measurement applications focus on measuring of the pressure distribution between the foot and the support surface. Figure 2-3a shows an illustration of a plantar pressure map during one stance phase (heel strike to heel off) of a healthy individual [26].

The foot and ankle provide the support and flexibility for weight bearing and weight shifting activities such as standing and walking. During such functional activities, plantar pressure measurement provides an indication of foot and ankle functions. Plantar pressure measurement has been recognized as an important area in the assessment of patients with diabetes [27]. The information derived from plantar pressure measurement can also assist in identification and treatments of the impairments associated with various musculoskeletal and neurological disorders [28]. Hence, plantar pressure measurement is important in the area of biomedical research for gait and posture analysis [13], [29], [30], sport biomechanics [31], [32], footwear and shoe insert design [33], and improving balance in the elderly [34], among other applications.

For all the above applications, there are solutions that utilize non-wearable systems, such as force plates and force mapping systems [35], but footwear is an ideal location for such measurements. Footwear-based platforms also offer much higher portability and can potentially enable monitoring outside of the laboratory, in uncontrolled, free-living applications. Almost all the footwear-based applications reviewed in this work have some form of plantar pressure sensing elements built in to them; however, in this section we place an emphasis on the footwear systems that deal explicitly with plantar pressure measurement. These systems are compared in Table 2-2. Figure 2-2b shows the F-scan® system by Tekscan, Inc. (Boston, MA, USA) [36].

As seen in the Table 2-2, the sensing nodes for plantar pressure measurement application are much denser compared to those used in gait monitoring or activity monitoring, with the F-scan® system using 960 sensing elements. This is because plantar pressure measurement applications demand the estimation of the absolute pressure that is exerted at different locations of the foot; while in activity and gait monitoring applications [7,30], it is more important to capture the relative changes in the pressure levels than the actual pressure values as previously discussed. F-scan® [29] can be used for the pressure ranges of 345 to 825 kPa, while Pedar® from Novel, gmbh (Munich, Germany) [31] can be used in the range of 15–600 kPa or 30–1200 kPa.

Since plantar pressure measurement applications are concerned more with the absolute pressure measurement and not the events, time resolution in the data from such systems do not play as vital a role as in gait monitoring. Sampling frequencies of as low as 13 Hz up to 750 Hz have been used in systems as shown in Table 2-2.

Table 2-2. Comparison of plantar pressure measurement systems

	Adin Ming et al. [37]	Lin Shu et al. [38]	Saito et al. [39]	TekScan F-Scan® [36]	Novel Pedar® [40]	Orpyx LogR® [41]
Sensing element	Piezo resistive material, total 75 nodes	Resistive fabric sensor array, six sensor array	Pressure sensitive conductive rubber	Fabricated resistive insole, 960 sensing elements	Capacitive sensing element, 256 nodes	The system has custom-built force sensor array of 8 sensors
Device usage	Academic research prototype	Academic research prototype	Academic research prototype	Commercial	Commercial	Commercial
Sampling frequency	13 Hz	100 Hz	50 Hz	Up to 750 Hz	78 Hz	100 Hz
Sensor data transmission method	Bluetooth	Bluetooth	Wired to PC	PC tethering, data logging, or Bluetooth	Bluetooth/SD card logging	Bluetooth
Visualization method	Real time visualization of plantar pressure distribution in PC	Real-time visualization of mean pressure, peak pressure, center of pressure (COP), and speed of COP, in PC and smartphone	Visualization of plantar pressure distribution in PC after data logging	Real-time visualization of plantar pressure distribution in PC	Real time visualization of plantar pressure distribution in PC	Real time visualization of plantar pressure distribution in iPhone
Validation	Validated against the standard force plate and the measured plantar forces showed R2 value of 0.981	Relative mean difference of 5% in plantar pressure against standard force plate	Validated against F-scan. difference in computed plantar pressure varied from −4% to 18%	Multiple validation studies as reported in [42]–[46] have validated the system	Multiple validation studies [45]–[47] have validated the system	A validation study in [48] reported r2 of 0.86 in plantar pressure measurement against (undisclosed) gold standard

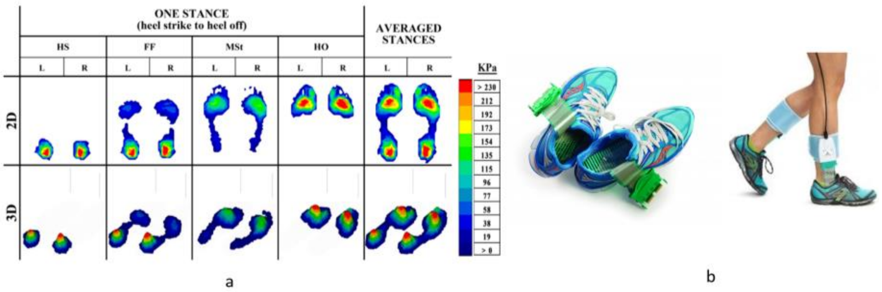

Figure 2-2. (a) Plantar pressure map during one stance [26]. HS—heel strike, FF—foot flat, MSt—mid stance, HO—heel off; and (b) F-Scan® System, courtesy of Tekscan, Inc.

A potential concern with the pressure sensing elements in the footwear is their drift over time, which will become important when the systems are used in real-life settings for long periods of time. A periodic recalibration would be needed to obtain repeatability as done for the case of F-scan® [45,50]. Studies [45], [46] have suggested that capacitive sensing based Novel Pedar® has higher repeatability and accuracy when compared to the resistive sensing based Tekscan F-scan® systems. However, out of all the systems reviewed, F-scan offers the highest spatial resolution with 960 sensing elements in the insole. The F-scan® system has a reported 2 h of battery life, which is low. The LogR® by Orpyx, Inc. (Calgary, AB, Canada) [41] has reported 8–12 h of battery life, long enough to last through a regular day of wear.

All of the systems listed in Table 2-2 have connectors on the insoles which need to be connected to the microcontroller unit (MCU) outside of the footwear. This can limit usability in free living conditions by causing the footwear to look unusual and feel uncomfortable. The system presented by Saito et.al [39] has a wired PC interface, which can limit use even in a controlled laboratory setup.

These above solutions measure the vertical force component of the ground reaction force (GRF), and Liu et al. [49] have presented a wearable force plate system for the continuous measurement of tri-axial ground reaction force in biomechanical applications. This system not only measures the vertical component of the GRF during ambulatory phase, but also measures transverse components of the GRF (anterior-posterior and medial-lateral). However, comfort levels wearing such systems made with tri-axial force sensors under the heel may be questionable, as the sensor itself is 5 mm tall and it would be rather uncomfortable under the heel. A better option for placing these sensors could be under the arch of the foot.

2.2.3 Posture and Activity Recognition, and Energy Expenditure (EE) Estimation

The ever increasing problem of obesity has brought immense importance to study in the field of posture and activity recognition and EE estimation. Weight gain is caused by a sustained positive energy balance; wherein daily energy intake is greater than daily energy expenditure. This is typically caused by living a sedentary lifestyle [50], [51]. In author [14] it was reported that obese individuals spend more time seated and less time ambulating than lean individuals. More than one third of U.S. adults are obese [1] and quantifying posture and activity allocation to help keep track of EE utilizing wearable sensors is quickly becoming a part of weight management programs. The applications extend beyond weight management programs, as posture and activity monitoring is an important aspect in the rehabilitation programs for post-stroke individuals [4]. Posture and activity classification is a large part of the consumer electronics industry's fitness segment. Fitness applications on smartphones, smart watches, and fitness trackers are becoming common parts of modern daily life [52]–[56]. Almost all of these solutions are based on accelerometry and there are many published studies on using accelerometer for posture and activity recognition [57]–[64]. There are also comparisons of commercially available accelerometry based activity and EE estimation monitors in [65]–[67]. In this chapter however, we focus only on footwear-based solutions used for posture and activity recognition, body weight, and EE estimation.

There are several footwear-based systems for posture and activity recognition purposes, and an example of these are the SmartShoe system developed by Sazonov et al. [68] which has been validated extensively for posture and activity monitoring. They have been used with healthy subject groups [29, 69, 70], people with stroke [4], [70] and children with cerebral palsy [71]. The most recent incarnation of the SmartShoe systems, named SmartStep by Hegde et al., has shown the capability to be accurate in posture and activity classification [20, 73, 74].

Chen et al. have designed a foot-wearable interface for locomotion mode recognition based on contact force distribution [74]. Kawsar et al. have developed a novel activity detection system using plantar pressure sensors and a smartphone [75]. Table 2-3 contains the comparison of these systems. Figure 2-3a shows a picture of SmartStep insole [76] and the associated Android application for daily activity monitoring.

All of the systems listed make use of various pressure sensors in order to determine the activity the user is undergoing. Pressure sensors can help to handle the ambiguity between weight bearing and non-weight bearing activities such as sitting and standing postures that cannot easily be determined using only accelerometry. An example of a pressure sensor signal located at heel for different daily living activities [72] (Figure 2-3b). All of the systems utilize motion sensors such as accelerometers and the systems in [77, 79] have a gyroscope as well.

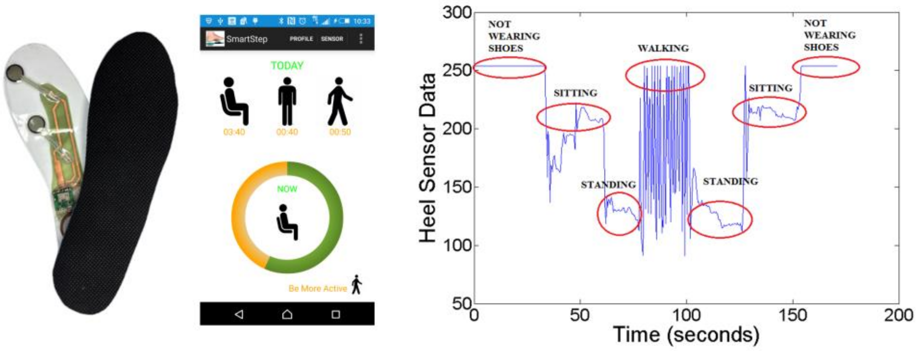

a b

Figure 2-3. (a) SmartStep system by Hegde et al. [76]; and (b) Heel pressure sensor signals for daily living activities [72].

Table 2-3. Comparison of footwear based posture and activity recognition systems

	Sazonov et al. [4], [68]–[70]	Hegde et al. [21], [72], [73]	Chen et al. [74]	Kawsar et al. [75]
Sensing element	Five Interlink force sensitive sensors FSR402 in the insole, accelerometer in the shoe clip on	Three Interlink force sensitive sensors FSR402, accelerometer, gyroscope all in the insole	Four FlexiForce A401 force sensor from Tekscan	Eight Fabric pressure sensors reported in [38]. Accelerometer and Gyroscope in the smartphone
Sampling frequency	25 Hz	25 Hz–75 Hz	100 Hz	37 Hz
Data transmission method	Bluetooth to smartphone	BLE to smartphone	RF module to PC	Bluetooth to smartphone
Data processing method	PC post processing for activity classification using neural network [6], decision trees [70], and support vector machines (SVM) [6]	PC post processing for activity classification utilizing multinomial logistic discrimination (MLD) [76]	PC post processing for activity classification using decision trees [74] and linear discriminant analysis [74]	Four different decision trees to classify activity from four sets of sensors (left shoe, right shoe, accelerometer, and gyroscope. Majority voting to decide the activity [75]
Activities classified	Sitting, standing, walking, upstairs, downstairs, cycling	Initial validation study classified sitting, standing, walking and cycling	Sitting, standing, level walking, obstacle clearance, upstairs, downstairs	Sitting, standing, walking, running
Real time activity feedback	Windows smartphone	Android smartphone	PC post processing and no real time feedback	Android smartphone
Clinical/Validation Study	Validated on stroke subjects [4], [77] and healthy subjects [6], [69]	Initial validation study on five healthy subjects [76]	Validated on five healthy subjects and one subject with amputee	NA
Accuracy	~99%	96%	98.4%	~99%

Similar to the gait monitoring systems, the pressure sensitive elements in the footwear for activity monitoring are used for marking the events. However, since changes in activity do not happen too often, a lower sampling frequency can also be used in activity classification to save battery power. In [78] it was shown that for accelerometer based daily activity classification, a 15 Hz sampling rate can provide a 85% classification accuracy. When it comes to footwear-based systems, as shown by works of Sazonov et al. even 1 Hz sampling rate can be used in monitoring of the daily activities with 93% accuracy [68], and as shown in [4], [68]–[70], a 25 Hz sampling frequency can provide a 99% accurate activity classification. Other described systems also have a very high accuracy (>96% across any system presented) in discriminating between the daily living activities of sitting, standing, walking, running, and cycling.

One of the limitations of footwear-based systems in activity monitoring is that they cannot be used in classifying upper-body activities. To monitor upper-body activities, additional sensors need to be worn on locations of the upper-body. An example of such a system is the one presented by Ryan et al., who have used a wrist worn accelerometer along with the footwear system to classify daily living activities of ascending stairs, descending stairs, doing the dishes, vacuuming, and folding laundry, along with many athletic activities [79].

A long battery life is very important for the usability of these systems. Reports [21,72,85] have discussed the battery life of the corresponding systems and the SmartStep system in [21], stands out among these, with more than four days of operations on single charge in certain modes. The other two systems had battery lives of approximately 5 h on a single charge.

None of the above systems have undergone longitudinal free living studies. There are many factors that need to be addressed to enable such studies in community living environments. Social acceptability, user friendly operation, comfort for wear and unobtrusiveness are some of the important challenges that need attention. SmartStep [21, 77] has tried to address many of these challenges in footwear-based systems, with its socially acceptable design, low power usage, and completely unobtrusive form.

In terms of data processing, as reported in [6], support vector machines (SVM), being computationally expensive, are not suitable for implementing in portable electronic devices, such as smartphones, for real-time activity classification purposes [6]. The study [6] also reported that activity prediction models based on multinomial logistic discrimination (MLD) is computationally less expensive in terms of required memory space and execution time, and performed equally well in terms of accuracy, as compared to SVM. Binary decision trees [74, 78, 79], being a light-weight classifier, can possibly enable the implementation of predictive models on the sensor itself. This can potentially reduce the power consumption at the sensor node that would occur during the wireless connection events for raw data transmission.

With respect to EE estimation, there are relatively few footwear-based systems that are targeted for such applications. The SmartShoe platforms have been extensively validated in EE (in controlled laboratory environments) [6], [80]. SmartShoes were compared against other accelerometry-based wearable devices and have proven to be equally, or more, accurate [81]. There are also several commercial footwear-based systems that can be used in EE, such as Lechal systems [82] and Lenovo SmartShoe [83], track their user's EE. The Lenovo ones have yet to enter the market.

In general, most of the present day solutions predict EE in terms of a steady state (sitting/standing/walking etc.). However, daily life is a mixture of both steady states and the continuous transitions between them. It is important to be able to quantify these in-between states in order to better estimate EE. Hence, we expect to see more and more research from a data processing perspective, to try to more accurately estimate EE in daily life. This may lead to the inclusion of several different sensors alongside activity predictors (heart rate, breathing rate and others) and novel data processing techniques, similar or better to the ones presented [84] in order to better estimate EE.

Excessive body weight is the factor which defines obesity and body weight is also one of the most significant factors in calculating EE. Self-reporting of body weight can be highly erroneous [85]; hence, objective and autonomous measurements of body weight can help in accurate EE estimation and obesity treatment programs. Footwear is an ideal location for automatic body weight estimation systems since all of the body's weight is placed upon the feet when standing. A few footwear-based systems have been used for body weight estimation [92,93]. One study [86] reported root-mean squared error of 10.52 kg in estimating body weight of nine study subjects, while the one study [87] reported an average overestimation error of 16.7 kg in estimating body weight of 10 study subjects. These studies validate the approach, but there is a room for improving the accuracy of the footwear-based systems in estimating body weight.

In all, footwear-based systems have yet to become matured in the field of daily energy expenditure estimation. The problem with measuring daily energy expenditure utilizing footwear systems is that people, on average, may wear footwear for 12 h of their day. This leaves a good 50% of the activities outside the purview of such sensor systems. Though one may argue that the majority of the remaining 12 h may be spent sleeping (6–8 h), to measure accurate daily living EE, one may have to use other sensor systems in conjunction with footwear-based ones. These may include smartphones or smart watches, which are generally used even when someone is not wearing footwear at home. Another potential concern with footwear-based wearable systems for use in daily living is that people usually tend to use multiple pairs of footwear. Insole based systems would be much more practical, as users can insert the insole into any of their shoes that they want to wear. However, the actions of taking out the insole from the shoe and inserting into another may not be a very comfortable act and future research work in this area needs to address this challenge.

2.2.4 Biofeedback

The sensing technologies embedded in the footwear in conjunction with real-time feedback mechanisms can be deployed in rehabilitation programs of many health conditions. For example, utilizing the real-time gait information retrieved from the footwear, post stroke individuals can be given feedback to improve the asymmetry in their walking. An example of real-time monitoring of stroke patient's gait and generation of active feedback to improve the asymmetry is depicted in Figure 2-4a. The feedback can be delivered in visual, auditory, or tactile manners. Several footwear-based systems have been presented in biofeedback applications and are presented in Table 2-4.

Orpyx® (Orpyx Inc, Calgary, Canada) have insole-based wearable systems that have been clinically validated [48] that give biofeedback to diabetic patients on a smartwatch, based on their plantar pressure profile [41]. This system makes use of a neurological rewiring phenomena in the brain, termed neuroplasticity. Khoo et al. [88] and, independently, Hegde et al. [89], and Bamberg et al. [90] (Figure 2-4b) have developed biofeedback devices for post-stroke patients to improve their gait asymmetry. Donovan et al. have worked on a shoe-based biofeedback device to assist people with chronic ankle instability [91].

Compared to gait and activity monitoring systems, biofeedback systems need to process the sensor data in real-time and also generate active feedback in real-time. Hence, these systems do not make use of elaborate sensing elements. All of them use only pressure sensing elements as seen in Table 2-4, with Donovan et al. [91] being the only exception which used EMG sensing along with pressure sensing. The sampling frequency can be as low as 20 Hz as shown by Hegde et al. [89], to save battery power. The computation methodologies need to be lightweight and cannot use a PC for providing real-time feedback.

Table 2-4. Comparison of footwear based biofeedback systems

	Orpyx [41], [48]	Khoo et al. [88]	Donovan et al. [91]	Hegde et al. [89]	Bamberg et al. [90]
Sensing element	Array of eight custom pressure sensors	Six FSR sensors	Pedar-x plantar pressure system and EMG	Two FSR sensors	Ten FSR sensors
Sampling frequency	Not reported	Not reported	100 Hz	20 Hz	114 Hz
Data transmission method	Wireless to smartwatch	Wired connection to MCU mounted on the lower back	Wired data logger	Wired connection to MCU mounted on the waist	Wireless to a portable PC
Feedback methodology	Smartwatch alerts when dangerous pressure levels are detected, so the user can modify behavior and avoid foot damage	Tactile and auditory feedback to correct the gait asymmetry	Auditory biofeedback to reduce the plantar pressure in the area of lateral forefoot	Tactile and auditory feedback to correct the gait asymmetry	Auditory feedback when the symmetry ratio is less than one
Computation method	Computation of plantar pressure levels for diabetic patients	Real-time computation of stance time difference; swing difference and generation of active feedback	Real-time computation of the lateral column plantar pressure and generation of active biofeedback	Real-time computation of stance time difference and generation of active feedback	Real-time Matlab program running on the PC that computes stance time and gait symmetry ratio
Clinical/Validation Study and results	NA	Validation on four healthy subjects and preliminary validation on post stroke patients. Gait parameters validated against gold standard (results not quantified)	Validated on nine subjects with chronic ankle instability. Pronounced reductions in peak pressure and pressure time integral of the lateral midfoot and lateral forefoot with the biofeedback	Validated on single stroke subject. Subject showed increased symmetry (step time differential improved by 48% standard deviation for the same increased by 88%)	Validated on three stroke patients. One subject reduced trunk sway by 85.5%, and the other subject reducing trunk sway by 16.0% and increasing symmetry ratio toward unity by 26.5%

All of the presented systems make use of auditory or tactile feedback mechanisms in order to communicate with the user. Accuracies of the systems seem comparable [94–96]. Additionally, all of these were externally wired systems (which could potentially get in the way of users). A full-fledged insole system would be much more attractive for real world use. In

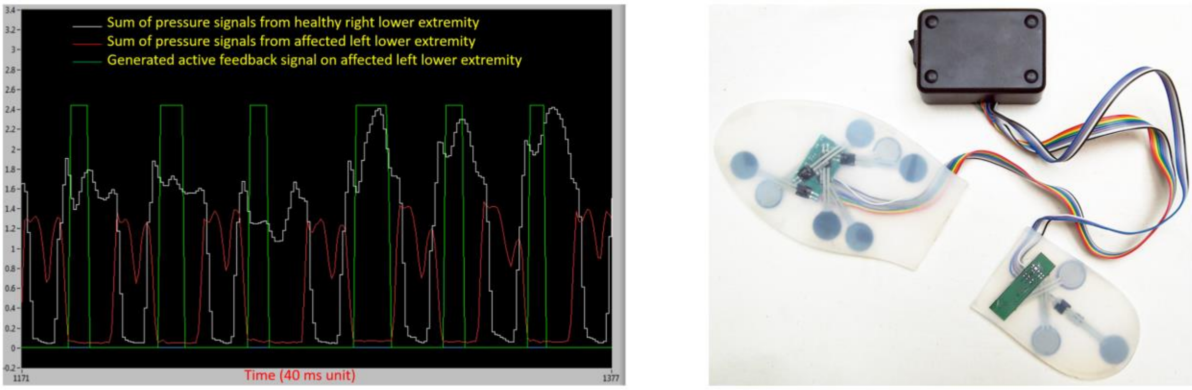

a b

Figure 2-4. (a) Pressure sensor signals for asymmetric walking of a post-stroke subject and generation of active feedback [89]; and (b) Biofeedback system presented by Bamberg et al. for stroke patients [90].

[91], during experiments, the device threshold was adjusted using a small screw driver to turn the trim pot’s dial. A more autonomous system than this would be attractive and make the device easier to use. Furthermore, all of these systems need further human subject validation.

Studies in [95–97] have showed significant improvements to the patients’ health conditions. These results indicate that footwear-based systems could indeed be of great use in rehabilitation and should be further pursued.

2.2.5 Fall Risk Assessment and Fall Detection Applications

One of the primary causes for the disorders referenced in the sections above is aging. By 2040, the number of elderly people in U.S. is projected to be 22% of the total population [3], and the risk of falling in older adults is an important social problem to be addressed [92]. Systems that monitor the individual’s gait over a long period of time and predict risk of falling are termed fall risk assessment systems [93]. On the other hand, a fall detection system is a real time assistive device which has a main objective of alerting when a fall event occurs. We review such footwear-based systems in Table 2-5.

Doukas et al. have developed an advanced fall detection system based upon movement and sound data [94]. “Wiisel” is an advanced insole-based system that is used for fall risk applications [22]. Otis et al. [95] have come up with an efficient home-based falling risk assessment test using a smartphone and instrumented insole. Sim et al. [96] have worked on a fall detection algorithm for the elderly using acceleration sensors on the shoes. Majumder et al. have implemented a real-time smartshoe and smartphone-based fall risk prediction and prevention system [97]. Figure 2-5a shows the Wiisel system that is used for fall risk applications.

a b

Figure 2-5. (a) Wiisel footwear system for fall risk application; and (b) Lechal system® for by Ducere Technologies pvt. ltd.

Table 2-5. Comparison of footwear based systems in fall risk applications.

	Doukas et al. [94]	Wiisel [22]	Otis et al. [95]	Sim et al. [96]	Majumder et al. [97]
Sensing element	Accelerometers and microphone	Textile based smart insole, 14 pressure sensors, accelerometer, gyroscope	FSR, accelerometer and bending sensor	Accelerometer	Piezo resistive sensors and inertial sensors from smartphone
Sampling frequency	NA	30 Hz	1000 Hz	225 Hz	25 Hz
Data transmission method	ZigBee to PC	BLE to smartphone	Bluetooth to Android	Bluetooth to PC	Wi-Fi to iPhone
Data analysis method	Short time Fourier transform and spectrogram analysis of the data to detect fall incidents. The classification of the sound and movement data is performed using Support Vector Machines	Data is transmitted from insoles to smartphone to back end server. Stand- alone program at the server analyses the gait and predicts fall risk	Proposed an automatic version of One-Leg Standing (OLS) score, based on COP measurements, for risk of falling assessment	Resultant acceleration signal is averaged and a threshold is used to predict the risk of falling	Tilt-invariant calculations on accelerometer and gyroscope data and usage of decision trees to classify high risk
Clinical/Validation Study	Three human subject validation while they performed walk, walk and fall, walk and run. 100% accuracy for fall detection and 96.72% for walk and run detection	Validated on 54 elderly participants [98], results NA	Twenty-three subject human subject study [99] including seven elderly and four PD subjects. Results suggest that the risk of falling depends on the type of ground	Six subject test. 81.5% sensitivity	Fifteen subject study. Subject dependent individual model has high accuracy but group model has accuracy of only 72%

Accelerometer is the common sensing element across all the systems used in this field as seen in Table 2-5. Otis et al. [95] and Sim et al. [96] have used relatively high sampling frequencies, with Otis et al. using 1000 Hz, though the reports did not substantiate the use.

Making the footwear systems comfortable for daily wear is a challenge and Wiisel insoles [22] have addressed this. These insoles are industrially built and with their built-in wireless charging, this solution may benefit the elderly. However, people need to remove the insoles from their shoes in order to charge them. This is due to a limitation of the current version of the wireless charging standard Qi, which allows a maximum of 1.5 cm distance between the wireless power transmitter and receiver. This might be increased to 4 or 5 cm in the future and will remove the need for taking out the insoles for charging purposes. Systems other than Wiisel in this section are all laboratory prototypes.

If the systems have some kind of real time feedback, such as to call for help, that would be beneficial. Only one study [97] has a real-time feedback implemented and adding this will be the next logical step for footwear systems used in fall risk applications.

Of the above mentioned systems, the one proposed by Doukas et al. [94] was the most accurate with 100% accuracy for fall detection. In that system, usage of microphone data along with accelerometer was novel. On the other hand, Sim et al. [96] system's 82% sensitivity is considerably low given the severity of misclassification.

2.2.6 Navigation and Pedestrian Tracking Systems

Another interesting area where footwear-based systems are being utilized is in the field of navigation assistive technologies and pedestrian tracking. These systems are aimed at providing assistance for the vision impaired, guiding emergency first responders, and work in augmented reality applications. In general, systems targeted for tracking utilize inertial sensors mounted on the footwear alongside GPS or radar; whereas navigation systems use actuators along with the sensors to guide the user in real-time. The key challenge for devices in this field is to be able to provide accurate location information without the need of a pre-installed infrastructure. In Table 2-6 several of these systems are reviewed.

All of the described systems in Table 2-6 make use of an accelerometer and gyroscope for computing the navigation path. These applications demand high temporal resolution in sensor sampling (as demonstrated by Foxlin [103] with 300 Hz), because of complex computation (such as Kalman filtering [103]) and integration that needs to be performed to accurately determine the path.

Schirmer et al. [100] and Lechal System [82] provide feedback for real-time navigation. In order to use the Schirmer et al. system [100], the user needs initial training to be able to understand the actuator patterns for front and back movement guidance, as they only use two actuators.

The Lechal® system by Ducere Technologies PVT. LTD (Secunderabad, Andhra Pradesh, India) [82], being a commercial system, is industrially built (Figure 2-5b). Though initially intended as an assistance for a blind subject population, it can also be used by all for navigating purposes. Footwear feedback levels in this system are user configurable and it also provides options for configuration using voice commands.

Table 2-6. Comparison of footwear based navigation systems.

	Schirmer et al. [100]	Bebek et al. [101]	Castaneda et al. [102]	Foxlin [103]	Lechal System® [82]
Sensors	Accelerometer, gyroscope, magnetometer, compass, smartphone GPS	Accelerometer, gyroscope, magnetometer heel of the shoe. capacitive pressure sensor at the heel	Accelerometer and gyroscope	Accelerometer, gyroscope, magnetometer	Insole pressure sensors not detailed. The electronics is mentioned to be having motion sensors
Actuators	Two vibration motors	No actuator	No actuator	No actuator	Haptic or vibratory feedback
Sensor sampling frequency	NA	NA	NA	300 Hz	NA
Data transmission method	BLE to iOS	Wired to laptop	Wired to laptop	RF to laptop	BLE to iOS or Android
Data analysis method	Phone computes walking path and turns, and communicates with the shoes to trigger the actuators	IMU bias compensation, and computing of position after zero velocity update (using the pressure sensor signals) and slope correction	Fuzzy logic procedure for better foot stance phase detection and an indirect Kalman filter for drift correction based on the zero-updating measurement	Zero velocity update of accelerometer and gyroscope, magnetometer calibration followed by Geomagnetic modeling and heading drift Correction	NA
Real time analysis	Different vibration patterns for different paths (front, back, left, right)	Future Work	Real time analysis in laptop	Future Work	Can provide turn-by-turn navigation feedback
Validation study	Twenty-one subject study showed that 99.7% of the time users correctly identified the path and turns as fed back by the shoes	Six walking experiments of half hour each, average relative error 0.35% in the final position tracked by the system	Three walking experiments, average relative error of 0.55% in the final position tracked by the system	Single user, 118 m walking indoor with 0.06% error and 741 m outdoor experiment with 0.3% error	NA

The wired connection to a laptop limits the use of systems in [109,110] for practical applications. Reported error in navigating a predefined path is very much comparable in all these systems and is less than 1% in the final position tracked by these systems.

2.2.7 Other Enabling Technologies

Energy harvesting from footwear is an area which has been of interest for a long time. As electronics are becoming smaller and smaller, the recent trend in wearable technology is to move towards smaller batteries or battery-less systems and to tap the energy needed from the human body or its motions. As early as 1995, Starner [41] reported that 67 watts of power are available in the heel movement of a 68 kg person who is walking at a pace of two steps per second. Even a fraction of that energy, if harvested, can easily power today's low power electronics. Many attempts are underway to tap the energy from body heat and the force produced during locomotive activities.

In Table 2-7 several footwear-based systems are compared that make use of energy harvesting methods. Shenck et al. have devised a methodology for energy scavenging with shoe-mounted piezoelectric [104]. Orecchini et al. have come up with an inkjet-printed RFID system for scavenging walking energy [105]. Zhao et al. have developed a shoe-embedded piezoelectric energy harvester for wearable sensors [106]. Kymissis et al. have tested three different energy harvesting elements in their work [107]. Meier et al. have presented a piezoelectric energy-harvesting shoe system for podiatric sensing [108].

Table 2-7. Comparison of footwear based energy harvesting systems.

	Shenck et al. [104]	Orecchini et al. [105]	Zhao et al. [106]	Kymissis et al. [107]	Meier et al. [108]
Energy harvesting element	Piezoelectric lead zirconate titanate (PZT)	Piezoelectric pushbutton	Polyvinylidene difluoride (PVDF)	PZT, PVDF, and rotary magnetic generator	Vibrational transducer and piezoelectric transducer
Placement of the energy harvesting element	Insole	Underneath the shoe heel	Insole	Insole for PZT and PVDF, under the shoe for rotary magnetic generator	Shoe heel
Validation application scenario	Shoe-powered RF tag system	Self-powered RFID shoe	NA	A self-powered RF Tag System	Self-powered gait data capture system
Salient features	One of the first practical systems demonstrating the feasibility of the approach	Emphasis was put on designing RF antenna, in the shape of a logo to make the system socially acceptable	Flexible and thin insole platform	Compared the efficiency and practicality of 3 different energy harvesting elements	Were able to run a data acquisition at 5 Hz from harvested energy
Reported harvested energy	8.4 mW in a 500-kohm load at 0.9 Hz walking pace	833µJ (test conditions not reported)	1 mW during a walk at a frequency of 1 Hz	From PZT 1.8 mW, from PVDF 1.1 mW, from rotary magnetic generator 0.23 W	10–20 uJ of energy per step

The energy can be harvested by vibration, compression, or bending produced in the footwear while the wearer performs locomotion activities such as walking. Piezoelectric lead zirconate titanate (PZT) and polyvinylidene difluoride (PVDF) are quite commonly used energy harvesting elements. PZT is a ceramic material, while PVDF is a plastic material.

From one study [107] it was concluded that, even though mechanical systems such as the rotary magnetic element generate two orders of magnitude more energy than other systems, they are difficult to integrate into footwear. PZT and PVDF are more compact elements and can be much more easily integrated. The combination of the harvesting element and the placement of the element determine the resultant harvested energy.

Among the described works, Nathan S. Shenck [104] seems to be the one with the highest-reported power generated, but the system appears to be a laboratory prototype. The Rich Meier et al. solution [108] involves alteration of the shoes, which would limit its usage in generic footwear systems.

Though the amount of power generated by these systems is quite low, many of these systems were able to provide enough energy to drive low power RFID systems. For the systems demanding higher power, the resulting power from energy harvesting can be utilized in supplementing the power provided by the battery, to extend its runtime.

2.3 Recent Trends and Future

2.3.1 Socially Acceptable and User Friendly Solutions

It is important that footwear-based systems are as discrete and user friendly as possible. Most of the systems discussed in this chapter require a wireless/wired MCU placed outside the footwear. For free living daily life studies this may be a concern, and we are seeing work being done to move towards full-fledged insole-based systems. Insoles are now being equipped with all of the sensing elements, battery, recharging circuitry, and wireless interfaces [22,77,88,91]. Some systems [49,88] have wireless charging capabilities which make them more user friendly.

The SmartStep [73] system has an over-the-air firmware upgrade feature, which can be used to easily configure the system for use in different applications. The concept of real-time data collection and offline transmission of SmartStep [73], can be attractive for the elderly population as they do not need to carry smartphones with them to use the system. In this scenario, the sensor data is logged in the system's flash memory during wear and later is transferred to the base station when the insoles are being charged. These trends will hopefully continue and can help researchers, as well as users, to better utilize such systems.

2.3.2 Footwear as Internet of Things (IoT) Devices and Big Data

IoT is a field that is redefining the way people interact with their environment in their daily lives. IoT can enable every object we interact with (for example: key chains, coffee mug, cloths, appliances, and many more) to be a sensor and a minicomputer connected to the internet [109]. We foresee that footwear is going to become a part of the IoT revolution soon and can help people become more connected and help them better manage their lives. The application scenarios such as gait and activity monitoring, fall risk/fall detection, and others, can take advantage of such infrastructure. An example use case can be that the individual with asymmetric walking (caused by a neurological disorder), wears IoT-enabled footwear, which sends the gait parameters to the physician in a distant place in real-time. The infrastructure can also allow the physician to give feedback to the individual based on the progress.

The next problem which arises after the systems are ready for daily usage and are a part of the IoT, is how to handle the enormous amount of data coming in from these systems. Novel data processing techniques, which do not only deal with the data from one set of sensors/systems, but from multiple sensors in a smart environment, will be gaining more and more traction from researchers. This greater expanse of data will help to make better informed decisions. We also foresee that footwear-based systems are going to play an important role in the remote monitoring of disabled and elderly people in the future.

2.3.3 Advanced Study Approaches for Footwear-Based Systems

From a research perspective, many of the footwear-based systems have not undergone longitudinal free-living studies. Footwear are subjected to enormous amounts of wear and tear, and the electronics built into them need to be able to withstand this for a long period of time. This may be one of the reasons why Nike and some other footwear manufacturers have stopped producing their SmartShoe product lines [110]. We foresee that, in the coming years, there will be more and more longitudinal studies in free-living conditions conducted, in each of the different application scenarios.

2.3.4 Affective Computing

Affective computing is a field of technology, in which systems can determine the users' mood and emotions, based upon his or her behavior sampled through different physiological factors, and adjust a smart environment to suit their mood. There are wearable systems that monitor users' joy, stress, frustration, and other moods/emotions utilizing heart rate monitoring sensors, electroencephalogram (EEG) sensors, electrodermal activity (EDA) sensors, and others [111].

From a footwear-based systems perspective, there was some initial work done with this by Lenovo with their Smartshoes [83], that display a person's mood on a small screen embedded directly on the footwear, though technical details were not available at the time of this review. Additionally, there is a Kickstarter campaign underway to make shoes that can change their entire appearance with a smartphone application [112]. Using affective computing, it would be possible to one day change the shoes color or display to reflect the user's mood.

2.4 Conclusions

In this chapter footwear-based wearable systems based on their target application were reviewed. Existing footwear-based solutions from academic research as well as commercial ones in the areas of gait monitoring, plantar pressure measurement, posture and activity classification, body weight and EE estimation, biofeedback, fall risk applications, navigation, along with footwear-based energy harvesting solutions were detailed. The chapter also discussed sensor technology, data acquisition, signal processing techniques of different footwear-based systems along with critical discussion on their merits and demerits.

CHAPTER 3 SMARTSTEP: A FULLY INTEGRATED, LOW-POWER INSOLE BASED MONITOR

Published: N. Hegde, E. Sazonov, “SmartStep: A Fully Integrated, Low-Power Insole Monitor” Electronics 2014, 3, 381-397

Design and development of the SmartStep insole is the first major contribution of this dissertation. This chapter describes the hardware and firmware design process to make SmartStep low power, fully integrated, user friendly and socially acceptable.

3.1 Introduction

Shoe-based activity and gait monitoring systems are gaining widespread popularity in research as well as in the market place. Shoe-based sensors are being used in applications ranging from studies of obesity to post-stroke rehabilitation, from energy expenditure studies to training activities in sports. One of the most popular applications for shoe-based sensors is gait analysis, and various analysis systems based on different sensor modalities have been proposed and applied both to healthy individuals and patients with neurological disorders [5,9, 15, 115–121]. In-shoe sensors have been applied for monitoring of plantar pressure [120], ground reaction forces [121], estimation of center of mass displacement during walking [122], pedestrian navigation [123] and pedestrian tracking [124]. A number of publications describe the use of shoe-based sensor systems for biofeedback in rehabilitation applications, such as PDShoe [125], a system that provides biofeedback to improve gait of Parkinson’s patients and that provides feedback on an Android smart phone [126]. Shoe sensors have also been applied in several different populations: children with cerebral palsy [127], Parkinson's patients [117, 127], post-stroke individuals [1, 78], and of course, healthy individuals [128].

Our laboratory developed various generations of a shoe-based platform named SmartShoe that incorporated pressure transducers and an accelerometer, and have been used in a number of different applications. SmartShoe has demonstrated accurate (98%) classification of the six major postures and activities [128] in healthy individuals and comparable recognition of postures and activities in post-stroke individuals [4]. The ability of SmartShoe to reliably recognize postures and differentiate between weight-bearing and non-weight-bearing activities enables accurate energy expenditure prediction [129]. SmartShoe was also used for estimation of the body weights of wearers [86] and to accurately capture temporal gait parameters of healthy and post-stroke individuals [114].

Most of the above mentioned shoe-based platforms, including the SmartShoes, have obvious limitations – mainly to accommodate the sensors and wireless electronics in the shoes – either there is a need to modify the shoe or attach additional hardware to the shoe. Such modifications are typically labor-intensive and may potentially diminish original functionality of the shoe (e.g. by creating holes and allowing moisture into the shoe), whereas attachments may not be reliable and can create trip hazards. Commercially available sensor-equipped shoes that minimized such issues appeared as early as 1986 (PUMA RS100 Computer Shoe [130]) and continue to be manufactured to this day (Adidas 1[131], Nike Lunar [132]). However, these commercially available shoe platforms do not offer all the rich features that the research platforms offer (e.g. easy access to sensor data), which can be used in multiple studies and target applications.

Other important issues that concern in-shoe systems are organization of low power operation and wireless delivery of the sensor data. The average current consumption with

SmartShoe platform was 40 mA [133], but to use SmartShoes for one day of wear (12 hours), battery with a capacity of more than 480 mAh was needed. In-shoe systems designed for long-term monitoring of gait or other parameters should present minimal burden in charging the shoe sensor batteries. In-shoe location is also problematic in terms of subject mobility, as the shoe data is typically delivered to a base station and the individuals cannot be always expected to be in the vicinity of the base station, such as a smart phone –used for data collection and logging. Finally, the monitoring system must be robust enough for long wear.

In an effort to concisely address all the above mentioned factors, we have developed SmartStep. SmartStep is a physical activity and gait monitor that is fully integrated into an insole, meets the low power requirements; addresses the issue of reliable data delivery in conditions of intermittent wireless connectivity; and maximizes the convenience, applicability, and social acceptance of the monitor. SmartStep is unobtrusive for the wearers, as the electronics, sensors, wireless module, and rechargeable battery are encapsulated inside the insole. This helps in making the wearers less conscious of wearing an activity monitor while they perform their daily activities in free living conditions. In addition, SmartStep does not require modification of the shoe, nor there is a need to attach additional hardware to the shoe. Compared to commercially available products, SmartStep offers rich features for the researchers interested in human subject studies of activity and gait. The device has the data retention capability, and the individuals wearing the SmartStep need not be in the constant vicinity of the smart phones. With the use of BLE along with all low power electronic components, SmartStep consumes less power. This article concentrates on addressing the following system design challenges:

- Managing low power in an ‘always ON’ wearable electronic system.
- Handling of the data retention scheme.

- Mechanical reliability of the wearable system for a prolonged wear.

In addressing these challenges, this article describes the SmartStep hardware, firmware, Android application, and specific experiments targeted at characterizing power consumption, flash buffering scheme, and reliability of the system.

3.2 Methods

3.2.1 SmartStep Hardware

We had reported a framework for the SmartStep development in our previous work [72]. This manuscript presents and characterizes the final prototype. The electronic printed circuit board (PCB) houses a low power 3D accelerometer - ADXL346, a low power 3D gyroscope - L3GD20, a low power flash memory - MX25L16 (16 M bit), and Blueradios BLE module - BR-LE4.0-S2A that is based on CC2540 SOC from Texas Instruments (TI). The PCB also has an on board power management circuitry and 3 pressure sensor interfaces. Accelerometer, Gyroscope and Flash are all interfaced to the CC2540 on the same Serial Peripheral Interface (SPI) bus with different chip select pins. Accelerometer and Gyroscope both have the provisions to interrupt the CC2540 core. The design utilizes 16 out of 17 available I/O pins from the BLE module. The PCB is 24 mm x 19 mm and weighs 4 g. A rechargeable lithium battery - ML2020 (3V, 45 mAh) powers the whole system.

The SmartStep insole system is assembled on a flexible 8 mil (0.2mm) thick FR4 PCB. Three Interlink FSR402 pressure sensors are located under biomechanically important support locations: the heel, the 1st metatarsal head, and the big toe. After placing the FSRs at the proper locations, the entire FR4 PCB is laminated to provide higher strength to the assembly. The electronic PCB is mounted on the FR4 PCB at the location of the arch of the foot (where forces developed during ambulation are minimal), and encapsulated in epoxy resin. The whole assembly is then encapsulated in urethane rubber for cushioning and protection. Individuals can wear additional cushioning materials based on need. The insole weighs 71g in total. Figure 3-1 demonstrates the block diagram of SmartStep, along with pictures of fully mounted PCB and fully encapsulated insole.

3.2.2 SmartStep Firmware

The firmware for the SmartStep is built around TI's BLE stack version 1.4.0 [134]. The algorithm for the application from the SmartStep point of view is completely reentrant. It is an 'always ON' system, which has no reset or power switch on board.

Below are the definitions of terms from the BLE perspective that are repeatedly referred in the article:

- Characteristic: A characteristic contains a single readable and/or writable value and descriptors that describe the characteristic's value. In case of SmartStep, there is a characteristic which is used for control and another for sensor data transmission.

Figure 3-1. SmartStep block diagram and fully encapsulated insole.

- Descriptor: Descriptor is a defined attribute that describes a characteristic value.

- Service: A service is a collection of characteristics.
- Server: A device which has defined characteristics in it. In the present context, SmartStep is the server.
- Client: A device which reads from or writes to server. The Android application is the client in the case of SmartStep system.
- Connection event: The event that takes place periodically when there is an established connection, where the server and the client can communicate the data.
- Connection Interval: The time interval that defines the connection events' period.
- Event timers: The timers provided by the BLE stack that are used to schedule events. In SmartStep, one event timer handles the sensor reading event and another timer handles the notification events. Normally, both timers operate at 25 Hz (a sampling frequency shown to be sufficient for accurate posture and activity recognition in an earlier study [21]).
- Notification: A method of data communication from the server to the client during the connection events, in which the client does not acknowledge the reception of the data from the server. As per the BLE standard, each notification data packet can have a maximum size of 20 bytes. SmartStep transmits sensor data to the smart phone using notifications, each containing sensor data acquired during a sensor read event along with a timestamp. Figure 3-2 shows the format of a notification packet when pressure sensors and accelerometer are being read during sensor read events, excluding gyroscope readings (the number of bytes for each field is shown in the brackets). As seen in Figure 3-2, when the gyroscope is not read, the notification packet contains 16 bytes of data.

Heel PS (2) MSB	3rd Meta PS (2)	Big Toe PS (2)	x- ACC (2)	y- ACC (2)	z- ACC (2)	Time Stamp (4)

Figure 3-2. Notification packet when the gyroscope is not used[1].

When the gyroscope is also being read during sensor read events, a notification packet contains 19 bytes of data as shown in Figure 3-3:

Heel PS (1) MSB	3rd Meta PS (1)	Big Toe PS (1)	x- ACC (2)	y- ACC (2)	z- ACC (2)	x- Gyroscope (2)	y- Gyroscope (2)	z- Gyroscope (2)	Time Stamp (4)

Figure 3-3. Notification packet when the gyroscope is used.

- Indication: A method of data communication from the server to the client during the connection events, in which the client acknowledges the reception of the data from the server.
- Advertising event: The event that takes place in SmartStep periodically when there is no established connection. During this event, SmartStep transmits the advertising packet, attempting to get connected with the client.
- Advertising interval: The time interval that defines period of advertising events. In case of SmartStep this is 1 s.
- Sleep State: A state of the SmartStep system, while all the electronic components are in sleep mode drawing minimal current from the battery.

During the firmware initialization action in SmartStep, the default connection interval is set to be at 160 ms. Automatic updating of the parameters defining the connection interval can take place on the fly, when the SmartStep intends to have it altered. The SPI module, ADC

[1] PS – Pressure Sensor, ACC – Accelerometer, MSB – Most Significant Bit.

module, event timers, accelerometer, gyroscope, and flash memory are initialized during initialization sequence, but become active only when they are enabled by the client. Actions from the smart phone's side will be discussed in the Section 2.5.

In a general usage scenario, the SmartStep advertises periodically so that any clients scanning for the server can find, and try to establish connection with, the SmartStep. Once there is a connection that is established between the SmartStep and client, the SmartStep waits for the control commands from the client. The client writes a characteristic value, communicating with the SmartStep about the initial setting needed for the particular data logging session. These settings define whether or not the gyroscope is read and whether or not the data retention scheme must be in place for the session. After this, the client starts the data logging session, and the SmartStep reads the sensors, forms a notification packet of the read data, and transmits the data to the client. This mode of operation is maintained until the client commands to stop the data streaming or there is a connection loss. If the client commands to stop the data streaming, the SmartStep still maintains the connection, but halts the sensor readings. At this stage, the client can choose to get disconnected from SmartStep or start another data logging session. While in the data logging session, if there is an unintended connection loss, the SmartStep may enter flash data retention scheme or halt the sensor readings based on the initial setting for the current session. If the data retention scheme is active, then SmartStep makes sure that all the flashed data contents are transmitted once the BLE connection gets reestablished again by entering the modified notification mode.

The state flow graph in Figure 3-4 describes the whole operation of the SmartStep, which can be operating in one of the below modes at any given point of time:

- Periodic advertisement mode: SmartStep remains in limited discoverable mode - which means advertising event takes place periodically and not indefinitely. The advertising period is 30 s (advertising state) followed by another period of 30 s with no advertising (sleep state). There is no connection with the client yet.

- Notification mode: SmartStep enters notification mode after establishing a connection with the client. The sensors are sampled at 25 Hz and the connection interval is 160 ms. The SmartStep can be in one of the following states in this mode: sleep state, sensor read event state, notification set event state or BLE connection event state.
- Flash buffering mode: SmartStep enters flash buffering mode when there is a loss in the established connection between SmartStep and the client. In this mode, SmartStep samples sensors at 25 Hz and writes the sensor readings to the flash memory. In an attempt to get reconnected with the client, SmartStep keeps advertising periodically. The SmartStep can be in any of the following states in this mode: sleep state, sensor read event state, advertising event state or flash buffer write event state (which is handled by notification set event).

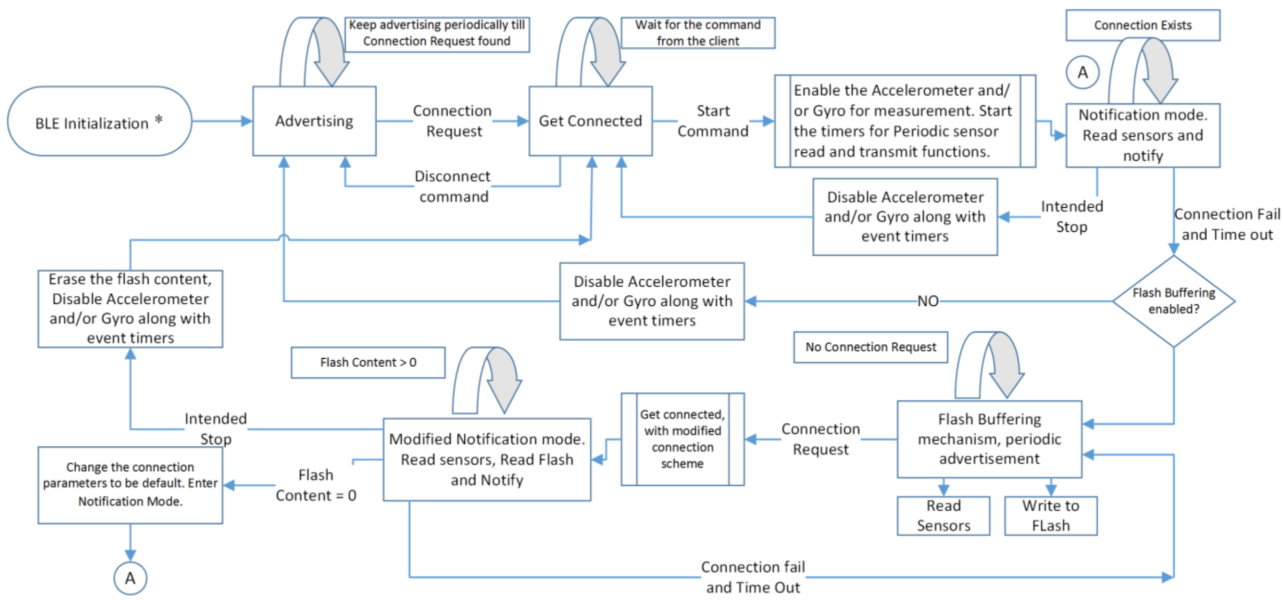

Figure 3-4. System operation and state flow graph.

- Modified notification mode: When the SmartStep is reconnected with the client from the flash buffering mode, SmartStep enters modified notification mode. In this mode, the connection interval is 80 ms (half that of normal notification mode), notification set event interval is 20 ms and sensors are sampled at 25 Hz. The SmartStep can be in one of the following states in this mode: sleep state, sensor read event state (which handles current sensor data as well as flash buffered data), notification set event state or BLE connection event state.

3.2.3 Low Power Schemes

This section describes the system design aspects utilized in SmartStep, which help in achieving low power functionality in an 'always-ON' SmartStep system:

- During advertising, the SmartStep remains in limited discoverable mode.
- For the sensor data transmission from the server to the client, notification methodology is used as opposed to indication methodology.
- Enabling/disabling of notification is carried out in two steps from the client side. In the first step, the client application writes to a characteristic variable in the server, before enabling or disabling notification. If the action from the client requests for enabling of the notification stream, the accelerometers and/or gyroscope are put into measurement mode (the mode in which the sensors sense and measure the motion/rotation), and the event timers are started. As a second step, notifications are turned on.
- The event timers are running and sensors are in measurement mode as long as the SmartStep is in notification/modified notification mode. Before stopping the notifications, the client again writes to the characteristic variable, after which, the whole system is put in a lower power mode.

- While in measurement mode, the ADXL346 operates in low power, with output data rate (ODR) set to 25 Hz. This low power mode is slightly noisier than the normal operating mode of ADXL346 [135], but consumes 50% less current than in the normal mode.
- Only during ADC reads, the resistive pressure sensors are supplied with current.
- BLE allows up to 80 bytes of user data to be transmitted in each connection event. Hence, SmartStep's connection interval is defined as 4 times that of notification set events, and this implies, in the place of 4 connection events – one for each notification packet, SmartStep has one connection event, saving the radio power consumption.

3.2.4 Flash Management Scheme

Flash memory is utilized to save the sensor data, when there is an unwanted connection loss. This unwanted loss of connection can happen when the wearer of SmartStep walks out of the range of the network (away from his phone), while the SmartStep is in notification or modified notification mode. When any such situation arises, SmartStep ensures that the sensor data is preserved by entering into flash buffering mode. In this mode, rather than communicating the data over BLE, SmartStep keeps writing the data to the flash memory in pages (256 Bytes). Flash buffering mode is automatically switched to modified notification mode when the SmartStep comes in the BLE range of the phone again. In the modified notification mode, the flashed data is read in pages, and this buffered data is notified along with the current sensor readings to the phone. Both the most recent (real-time) data and flash buffered data are transmitted in the case of reconnection after a connection loss, thus avoiding the potential lag due to tran smission of buffered data. Periodic housekeeping happens in the firmware, erasing the read pages in sectors (4K Bytes). The flash memory has the capacity of 16 M bit, and given that the sensors are read at 25Hz, and each notification packet is 16 bytes in width (in case there is no gyroscope reading), the flash memory can be used to buffer the data for maximum of 1.5 hrs. If the flash memory gets completely filled, then the sensor reading is halted until the SmartStep connects with the smart phone again. Figure 3-5a explains the operation of the flash buffering mechanism.

3.2.5 Android Implementation

The current implementation of the Android application (App) is based on Google's most recent Android version 4.4.2, which has native android support for BLE [136]. The App can scan for available SmartStep servers, connect to the server, search for the available services from the server, read/write characteristic variables in the server and enable/disable notifications from the server. The App user can select whether the data retention mechanism is needed for the data logging session and also whether the SmartStep needs to read the gyroscope or not. During the session, the sensor data notified by the SmartStep, can be displayed on the screen

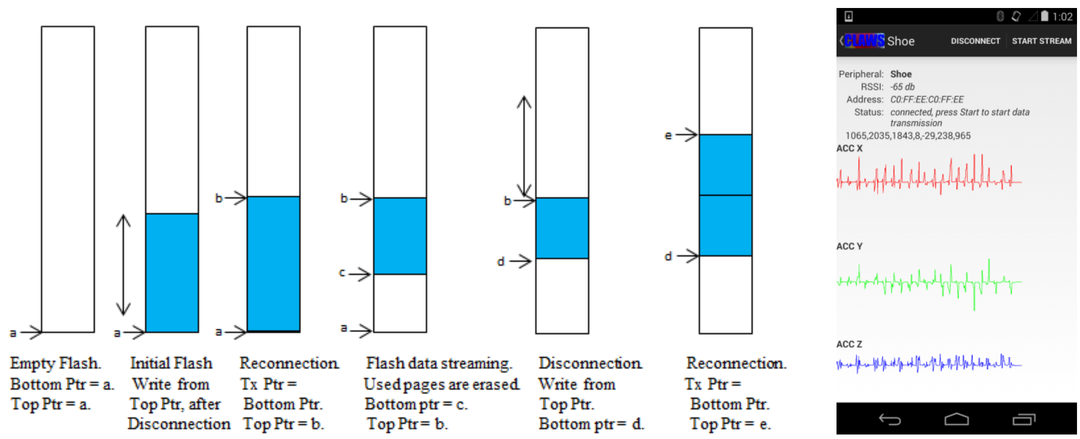

(a) **(b)**

Figure 3-5. (a) Flash management mechanism. (b) Screenshot of the android app.

in real time, and also can be written to a comma separated value (csv) file on the smart phone's storage. During the data logging session, if there is an accidental connection loss, the App immediately gets connected back in the same mode as it was operating. If a connected server goes outside the range and if there is a time out, the App starts periodic scanning – in an attempt to find the server. When the server comes back in the BLE range, the App reconnects with the server and re-enables the notifications stream.

When there is inconsistent network strength, reconnecting to the server is prone to constant disconnections, which may cause additional data loss in SmartStep. To avoid this, the application checks radio signal strength indicator (RSSI) during scanning and automatic reconnection takes place only when RSSI is higher than -75 dB, which is an empirically established threshold determined by the authors. Figure 3-5b shows a screen shot of the application while it is capturing a subject's walk – while wearing SmartStep.

3.3 Experimental Section

3.3.1 Data Retention Scheme Tests

3.3.1.1 Formal Test of Data Retention Scheme for Single Disconnection

20-minute experiment was conducted to test the functionality of the data retention scheme and frequency scaling for a single disconnection. The SmartStep was in connection with the smart phone App initially for a minute, after which the wearer went outside the range of BLE network (typically 50 m) for 5 minutes. At that time, the sensor data were logged into the flash memory, and once the wearer came back, the App automatically connected with the SmartStep. Following this, the SmartStep sent the flash buffered data along with current sensor readings. The entire experiment ran for 20 minutes and the data received from the experiment were stored in a csv file from the app. The presence of time stamps in the notification packets helped in sorting the received data and a quantitative measure on data received (DR) and data loss (DL) was calculated using a Matlab script as:

$$DR = \left(\frac{NTS}{LTS-FTS+1}\right) * 100 \qquad (1)$$

$$DL = \left(1 - \frac{NTS}{LTS-FTS+1}\right) * 100 \qquad (2)$$

where, NTS is the total number of timestamps received, LTS is the last timestamp received, and FTS is the first timestamp received.

3.3.1.2 Formal Test of Data Retention Scheme for Multiple Disconnections

An hour-long experiment, emulating multiple nested disconnects was conducted. First, the SmartStep was in connection with the App for 10 minutes. Following this, the wearer went outside the network range for 10 minutes. When the wearer came back in range, as per the connection scheme, it would take 10 minutes to get all the flashed data; however, the wearer went out of the network after 5 minutes of first reconnection, and came back into the network 5 minutes later. Following this, the wearer was in the network for the next 30 minutes. This is a very common usage scenario in which wearers of SmartStep could move in and out of the vicinity of the phone arbitrarily. A quantitative measure on DR and DL during the whole experiment session was calculated using the Matlab script as done in test 3.3.1.1.

3.3.2 Power Consumption Tests

Multiple power consumption tests were conducted to measure power consumption and to estimate expected battery life of the SmartStep in different modes of operations. The power consumption by the SmartStep depends on the types of sensors being read and state of the BLE stack. A 10 Ω resistor was placed in series with the battery supply and the voltage across the resistor was captured using an oscilloscope. The average current was calculated in the method explained previously [137]. To find conclusive data on power consumption vs. functionality trade off, all the possible modes of SmartStep were considered, namely:

- Periodic advertisement mode.
- Notification mode:
    - With pressure sensors and accelerometer.
    - With pressure sensors, accelerometer and gyroscope.
- Flash buffering mode.
- Modified notification mode.

In addition, the power consumption breakdown between different states of the system for a given mode of operation was calculated by considering all of the different states in which the system can be operating, at any given time, in the given mode of operation. Each individual state's contribution towards the total power consumption for a given particular mode was calculated. Equation 3 gives a quantitative measure of the contribution of a given event state in notification mode (CXX):

$$C_{XX} = \left(\frac{A_{XX}}{ANM}\right) * 100 \qquad (3)$$

where, AXX is the average current consumed by the state XX, and ANM is the average current consumption in notification mode.

3.3.3 Test for Functionality and Reliability of the Insole Monitor

3.3.3.1 Mechanical Reliability for Prolonged Wear

Characteristics and response of the pressure sensors after machine-generated cyclic loading experiments were reported in a previous study [28]. However, during dynamic human activities, the insole will be subjected to bend (which cannot be emulated with the available machine test frame) and this can affect the sensor behavior. Hence, to understand the behavior of the pressure sensors in the SmartStep over a prolonged human wear, the following experiment was conducted.

The responses of the pressure sensors at the heel and meta positions were recorded before the first wear with the help of a calibrated weight (36 Kg). The insole was worn by one healthy subject, with the shoe size equal to the size of the manufactured SmartStep insole (US M9)[2]. The subject was wearing the insole in free living condition and performing activities that included, but were not limited to walking, running, bicycling, etc. as per his daily schedule. Every week the responses of the pressure sensors were recorded using the same calibrated weight. The test ran for a total of 4 weeks.

3.3.3.2 Real Life Experiment to Understand the Achievable Battery Life on a Single Charge

Power consumption tests conducted in section 3.3.2 gave an estimate of expected battery life while using SmartStep, in different possible modes of operation, when considered individually. However, in real life, the actual power consumption by SmartStep depends on a mixture of different modes, in which the SmartStep can be operating at different times. Hence, to get an understanding of SmartStep's battery life in a real life use case, an experiment was

---

[2] For different shoe size, there will be different insoles, which are all based on a generic design.

conducted on a single healthy subject wearing SmartStep and the sensor data were logged in the smart phone over BLE.

Before starting the experiment, the SmartStep battery was fully charged to 3 V. The data were logged continuously until the battery depletion. During the experiment, the subject was in free living conditions and was performing various activities – which were not monitored. After the experiment, the logged data were processed, and using Equation (1) and (2), a quantitative measure on DR and DL was calculated. The timestamps in the received data were also used to get a conclusive assessment of the achievable battery life in a real life use case.

3.4 Results

3.4.1 Data Retention Scheme Tests

3.4.1.1 Formal Test of Data Retention Scheme for Single Disconnection

Figure 3-6a shows the scatter plot of the timestamps received for the data retention experiment. In the Figure, during time intervals A and D, the SmartStep was in normal notification mode, interval B was the disconnection period and during interval C SmartStep was in modified notification mode. In the interval C, the bottom blue line represents timestamps for the flash buffered data and the top blue line represents the timestamps for the data read in real time, indicating that both the buffered and the real time data were being transmitted. During this 20-minute test, 97.5% of the sensor data was received successfully.

3.4.1.2 Formal Test of Data Retention Scheme for Multiple Disconnections

Figure 3-6b shows the scatter plot of the timestamps received for the experiment with multiple nested disconnects. In the Figure, intervals A and F correspond to normal notification mode, interval C is the first modified notification interval, interval E is the second modified notification interval, and intervals B and D are the first and second disconnection intervals respectively. In the intervals C and E, the bottom blue lines represent timestamps for the flash buffered data and the top blue lines represent the timestamps for the data read in real time. In the one-hour experiment, 98.9% of the sensor data was received successfully.

3.4.2 Power Consumption Tests

Figure 3-7a shows the scope traces captured for the connection event. It can be seen from the trace that there were 4 transmissions of notification packets happening at the connection event, confirming the notification packet grouping methodology used. Similar to the traces in Figure 3-7a, scope traces for all the different states of activities of SmartStep in different modes were captured, and the average current consumption along with the expected battery life were calculated. The results (rounded to the nearest hundredth) are presented in Table 3-1. Table 3-2 presents power consumption breakdown among the possible states for notification mode - with and without gyroscope.

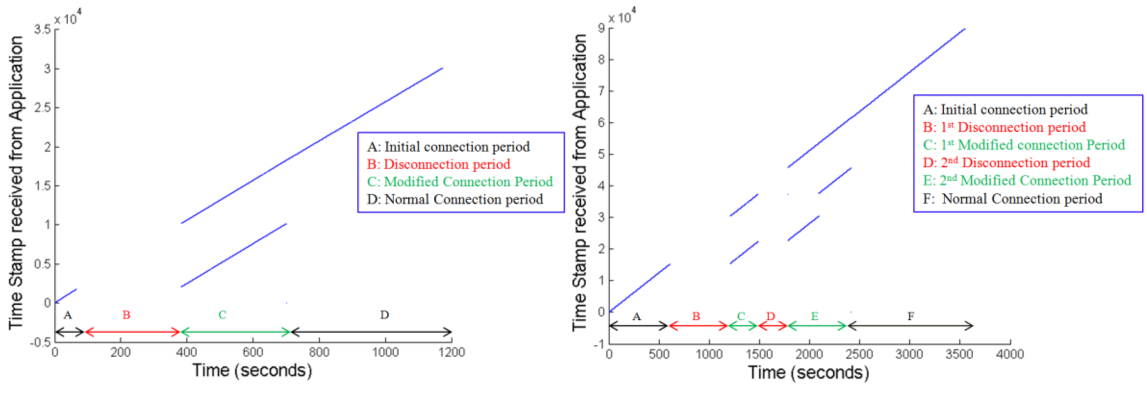

(a) **(b)**

Figure 3-6. Scatter plots for formal test of data retention scheme: (a) Single disconnection (b) Multiple disconnections

Table 3-1. Power consumption test results

Scheme used	Average current consumption (mA)		Expected battery life (Hours)	
	Without Gyro	With Gyro	Without Gyro	With Gyro
Periodic advertisement mode	0.05	0.05	900.00	900.00
Notification mode	1.45	1.65	31.03	27.27
Flash Buffering mode	1.00	1.20	45.00	37.50
Modified Notification mode	1.99	2.19	22.61	20.54

Table 3-2. Power consumption breakdown in the notification mode.

Event State	Notification mode (without Gyro)		Notification mode (with Gyro)	
	Average current consumption (mA)	Contribution (%)	Average current consumption (mA)	Contribution (%)
Sleep state	0.11	7.65	0.11	6.73
Sensor read	0.44	30.00	0.61	36.38
Notification Set	0.36	25.18	0.39	24.23
BLE connection	0.54	37.17	0.54	32.66
Total	1.45	100	1.65	100

3.4.3. Test for Functionality and Reliability of the Insole Monitor

3.4.3.1 Mechanical Reliability for a Prolonged Wear

Figure 3-7b shows the graph of pressure sensor readings plotted against time of wear. The meta sensor drifted a total of 10% over the span of 4 weeks of wear, while the heel sensor drifted 9% in the same period.

3.4.3.2 Real Life Experiment to Understand the Achievable Battery Life on a Single Charge

The SmartStep was able to continuously send sensor data to smart phone for 24.6 hours over BLE on a single charge. Two disconnections happened during the experiment, in which the SmartStep was able to preserve the sensor data. In this experiment 98.6% of the sensor data was received successfully.

3.5 Discussion

A low power fully integrated insole monitor – SmartStep was designed and developed in this study. This insole monitoring system was designed with pressure sensors, an accelerometer, gyroscope, BLE connectivity, and flash memory along with a rechargeable battery – which were integrated in the insole. The insole system was aimed at resolving the limitations of the existing shoe monitoring systems.

From the formal experiments on functionality of the data retention scheme, it was confirmed that the implementation of a flash buffering scheme was able to preserve the sensor data, whenever there was a loss of connection. The results for these experiments showed that the data retention scheme in SmartStep could handle multiple disconnection/reconnection

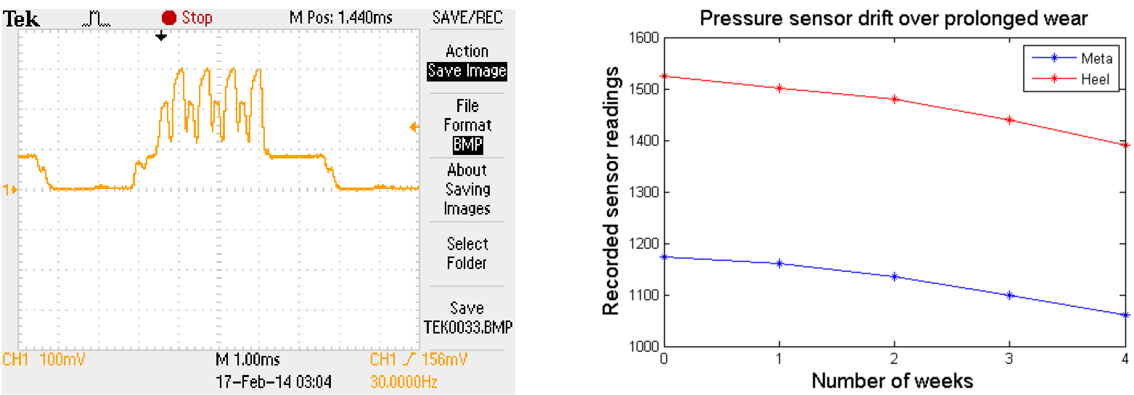

(a) (b)

Figure 3-7. (a) Scope trace for connection event. (b) Pressure Sensor readings plot displaying the drift.

events successfully, and retrieve a very high percentage of data (~99% during one-hour experiment). A portion of the lost data (~1%) can be accounted by the time difference between the connection loss and time out period (6 s in the case of SmartStep), only after which, the flash buffering mechanism gets activated, and the sensor data sampled during the timeout period are not buffered in the flash. Another reason can be that, as the wearer moves away from the smart phone, the BLE signal strength gets gradually reduced and not all the packets which are sent, are received. The design choice of implementing notification methodology as a means of data communication, in which there is no acknowledgement for the received data from the client to the server, can be contributing to the packet loss. However, choosing indication method over notification method, would have affected the power consumption figures by increasing the current consumption by BLE connection events.

Among all the modes tested for power consumption, the periodic advertisement had the least average current consumption, as sensors were inactive in that mode and radio was on for a short period during advertising events. Flash buffering mode was the next least in power consumption, since in this mode, SmartStep read the sensors, wrote the sensors' data to flash memory, and did not have an active BLE connection. Power consumption during notification mode was higher than the flash buffering mode, as in this mode the sensors were read and also radio was active because of active BLE connection. The modified notification mode was the highest power consuming amongst all, as in that particular mode the BLE connection frequency was doubled to that of the normal notification mode. During the normal notification mode (without gyroscope) the average current consumption was 1.45 mA and this is a significant improvement (~28 times) from that of the SmartShoes with 40 mA average current consumption.

Since the pressure sensors were placed right under the foot inside the shoe, which was quite a harsh environment in free living conditions, we expected that these sensors would wear out and also drift over time. It was encouraging to observe that the pressure sensors in SmartStep were able to tolerate prolonged human wear in free living conditions. This result indicates that, from the mechanical reliability aspect, the SmartStep can be used in prolonged human subject studies lasting a month; however, for studies longer than a month, it will be better to have a more reliable system, with less drift – which will be emphasized in the future research.

SmartStep had a battery life of 24.6 hours on a single charge. This battery life figure falls between the characterized operating hours for notification mode and modified notification mode, in which the SmartStep could be operating in real life. This shows that the SmartStep, indeed, is a low-power system. In terms of battery life, with a 500 mAh battery capacity, SmartShoes could operate for 12 hours; with a 2000 mAh battery [5] lasts for 20 hours; while with a 40 mAh battery capacity, SmartStep could operate for more than 24 hours. Considering 12 hours of wear per day, SmartStep could be used for more than 2 days on a single charge, providing a battery life suitable for use of SmartStep in research studies.

Table 3-2 results indicate that more than 50% of the total power consumption in notification mode was because of BLE activities (which include 'notification set event' and 'BLE connection event'). Hence, the battery life can be improved by reducing the number of 'BLE connection events' and 'notification set events' in the system, which will be dealt in the future research. By incorporating a higher capacity coin cell battery in the SmartStep assembly, such as with 100mAh capacity [138], SmartStep's battery life can be doubled. There is a plan to move to a CC2541-based BLE module, which is a lower power solution compared to CC2540. Using CC2541 along with a dc-dc convertor would save more than 30% of the power consumption when the radio is active [139]. Also, there is an ultra-low power variant to the ADXL346 accelerometer: ADXL362 [140], which consumes ~20 times less current than ADXL346. However, even after these improvements, the SmartStep can be used for 7-8 days only on a single charge, and has to be recharged after that. Implementing a simple recharging mechanism (such as 'wireless charging' as opposed to 'wired charging' in the present implementation) will also be the topic of future research.

3.6 Conclusion

This article described the solutions to the system design challenges identified during the development of SmartStep, a fully integrated, low power insole monitor. The conducted power tests demonstrated that average power consumption in SmartStep was ~28 times lower than that of the original SmartShoe monitor and the real life experiment conducted in this study suggested that the present implementation of SmartStep can be used for more than 2 days on a single charge. The present implementation of data retention scheme was functioning as it was intended and with minimal loss of data (<1.5%). The results from the mechanical reliability experiment suggested that the SmartStep pressure sensors tolerated prolonged human wear. These results, along with the proposed improvements, suggest that the SmartStep can be used in long-term monitoring of gait, physical activity or other parameters. Utilizing the SmartStep monitoring systems in the studies on physical activity and gait monitoring of human subjects in free living conditions, and processing the sensor data captured from SmartStep will be the topic of our future research.

CHAPTER 4 IMPLEMENTATION AND EVALUATION OF AN ANDROID BLUETOOTH LOW ENERGY APPLICATION METHODOLOGY FOR MULTI-SENSOR INTERFACE

This work has been submitted to the Pervasive and Mobile Computing Journal, Elsevier and is currently under review.

Ability to interface more than one Bluetooth low energy sensor to the Android smartphone for communication is a pre requisite to the human subject studies to be run on SmartStep. This chapter describes a novel methodology in achieving a robust and reliable Android application to interface multiple Bluetooth low energy sensors.

4.1 Introduction

Bluetooth Low Energy (BLE, v 4.0) is a wireless personal area network technology designed by the Bluetooth Special Interest Group. BLE is aimed at applications such as fitness, healthcare, security, and home entertainment control [141]. BLE is intended to provide significantly lower power consumption compared with the previous Bluetooth versions. In our previous work, we have achieved improvement of two orders of magnitude in lowered power consumption of a wireless sensor with BLE, compared to Bluetooth v 2.1 [21], [72].

Compared to other mobile operating systems (OS), The BLE support in the Android OS is relatively new [8]. The implementation of an Android application that deals with single BLE sensor system was addressed in our previous work [21], [72], but BLE multi sensor scenarios involving an Android device are not described in the literature. There are many applications that may benefit from the use of multiple wireless sensors, such as physiological monitoring [142], [143], biofeedback [90, 146 147], gait and activity monitoring [1, 148], body sensor networks [149,150] and others.

Consider a BLE body sensor network scenario, in which a number of wireless sensors are located on different body parts and there is a base station system (stationary or mobile) to collect the data from the sensors. The base station system interacts with all the sensors and is also connected to the internet cloud. Consider the scenario wherein a number of BLE sensors communicate with the base station simultaneously without manual intervention, during the course of operation. In such a situation where the sensors can come into range and go away from the base station at different times, there is a need for a systematic methodology to handle the communication between the sensors and the base station. This situation is different from the case wherein a smartphone user manually interacts with two or more BLE sensors. In general, BLE communication between a sensor and a base station offers the following challenges:

- The application running in the base station needs a reliable BLE connection establishment procedure with the sensor.
- The information exchange mechanism between the base station and the sensor should enable the sensor to reliably communicate with the smartphone application. Also, there should be minimal loss in the sensor data collected.
- The BLE disconnection process needs to be handled correctly, making sure that the necessary information is all conveyed from the base station to the sensor, and data transmission timers in the sensor are all halted before the actual disconnection event.

In a multi-sensor scenario with no manual intervention, the above challenges are compounded, as the actions of connection establishment, data exchange, and disconnection need to happen in a reliable manner with each of the sensors, while the sensors can enter or leave the network any time. In such scenarios, it was observed in our laboratory experiments that lack of a systematic design methodology results in many problems. These problems can lead to malfunctioning in some sensor nodes or throughout the whole network. One of the potential issues in the design methodology is that, in an Android activity or a service handling a particular sensor, BLE actions are initiated without waiting for the successful completion of the previous actions. Another example of a potential issue is that the Android services or activities, each handling different simultaneous BLE connections, are blind to each other (no inter-service communication). Different services/activities may initiate BLE actions independently of each other which may potentially mutually interfere. Adopting such methodologies in a multi-sensor network may result in some nodes failing to register the data writes from the smartphone application or others failing to be disconnected properly. This may also result in periodic data transmission timers to be unnecessarily active in some sensor nodes, draining the sensor's battery (whereas BLE is all about saving battery power).

Two challenges are addressed in this work. Firstly, in implementing a BLE multi-sensor application that functions without user intervention, we introduce, describe, and evaluate the 'Sequential Actions following Successful Callback (SASC)' methodology. The SASC methodology will be utilized for handling BLE connection, data collection, event notification, and disconnection processes in a BLE multi sensor scenario. Secondly, profiling tests were conducted to evaluate the SASC methodology in terms of percent data retrieval/throughput, CPU loading and power consumption for varying BLE connection intervals and number of sensors. In previously published research [149], there was some initial evaluation of the performance of BLE, in terms of throughput vs connection interval and simultaneous connections. To the best of our knowledge, the evaluation of BLE in a real world scenario involving multiple sensors and an Android smartphone is being described for the first time.

SmartStep [20, 73, 74] (a wearable monitor that is fully integrated into shoe-insoles with BLE connectivity) is used as an example platform for testing the multi-sensor BLE system. The following sections detail the application scenario under consideration, describe SASC methodology used to achieve Android multi sensor BLE application, and the profiling tests conducted to evaluate the performance of the methodology.

4.2 Methods

4.2.1 Application Scenario

An application scenario, wherein a number of BLE sensors are worn on body and there is a BaseStation (Android device) that is interacting with these sensors<< rewrite it is NOT a sentence now. The sensors come in and go out of the base station’s wireless range at different times, based on the application needs. When the sensors are worn on the body, they collect the data and whenever they are connected to the base station over BLE, they transfer the collected data to the base station. Implementation of actual events that trigger the sensors to stop data collection and start advertising over BLE is left up to the particular application. A possible scenario that can trigger this transition can be one in which sensors being put on recharging of their batteries when the user comes back home. Other possible scenarios may include use of the inertial sensors to capture the periods of static placement of sensors and periods of wear and decide on the required BLE actions accordingly.

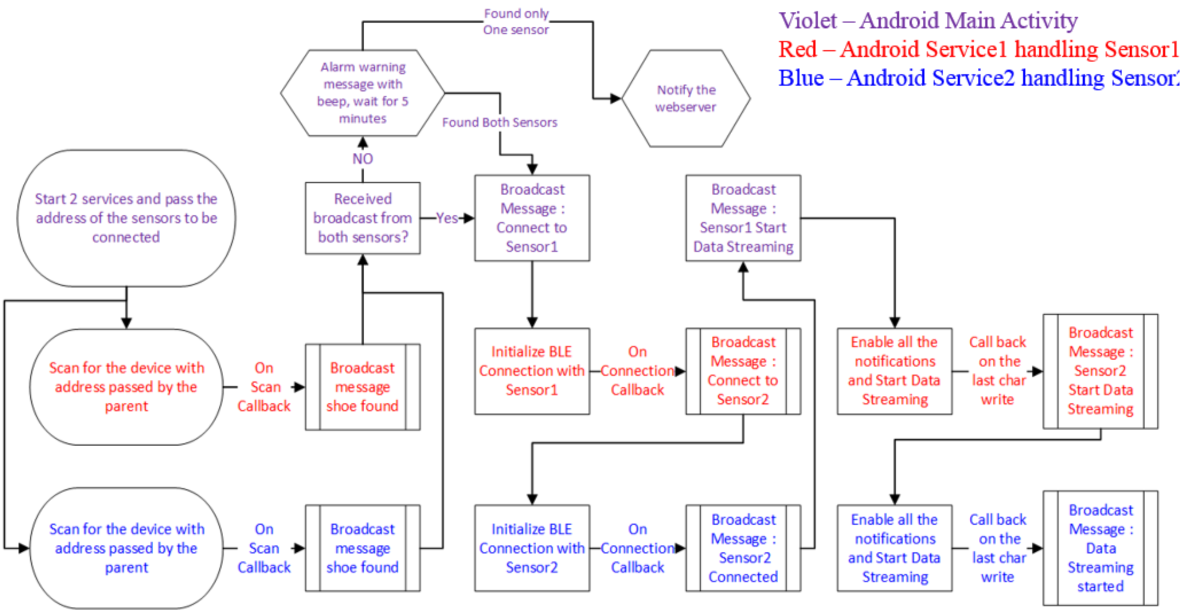

Figure 4-1: SASC multi sensor BLE Android methodology

4.2.2 SASC Methodology

The following description relies on BLE terminology that is described in detail elsewhere [21]. In the proposed SASC methodology, every BLE action by the BaseStation in a multi-sensor scenario is handled in a sequential manner, to make sure that BLE actions across different services or within a particular service would not mutually interfere. Before initiating another BLE action, the SASC methodology makes sure that the previous action completes successfully. Successful completion is verified by waiting for the success flag in the callback methods for the particular BLE action.

The implementation of user interface (UI) is left up to the particular application at hand. The Android activity handling the UI (called UI_Activity) is supposed to deal with the first time sensor selections (scan for sensors, give option to choose the desired ones etc.). SASC comes into play after the specific sensors are selected. The following sections explain the implementation of SASC.

4.2.3 Connection Establishment

For the sake of simplicity and clarity, assume a scenario involving two sensors, though in applications this can be up to 7 sensors, the upper limit in present day Android implementation [150].

After the desired sensors are selected, the UI_Activity initializes the Android services to handle each of the sensors, and passes them the BLE address of the particular sensor. In this case of two sensors, call the two services, Service1 and Service2, and the two sensors as Sensor1 and Sensor2. Once initiated, these services start to scan for the particular devices as shown in Figure 4-1. As the services find the appropriate sensors, they initiate a broadcast message that they have found the sensors. The connection establishment procedure would not start until all of the sensors are discovered by their respective services. Once all the sensors are discovered, the UI_Activity informs Service1 to connect to the Sensor1.

As shown in Figure 4-1, inside the callback function for the connection event for Sensor1 in Service1, the connection event for Sensor2 from Service2 is triggered. Since there are two sensors in this scenario, successful connection with Sensor2 triggers the broadcast message to enable characteristic writes from Service1 to Sensor1 (in case there are more sensors, actions of connection establishment are carried out with each of the sensors before the characteristic writes are attempted). Service1 starts writing the characteristics to Sensor1 and inside the callback method for the last characteristic write, the characteristic writes from Service2 to Sensor2 are triggered.

4.2.4 Information Exchange Mechanism between the Sensors and the BaseStation

The information exchange between the BaseStation and the sensors can happen via characteristic read/write or notification events:

A characteristic write is performed by the BaseStation to write a particular value to a characteristic on the sensor (e.g. timestamp). The BaseStation waits for successful completion of the particular characteristic write operation before proceeding with any further BLE operations. As per SASC, if for any reason, a particular characteristic write is not successfully completed, it is then performed again before attempting the next BLE action.

Special events occurring at sensors (e.g. charging disconnect or data streaming complete), and periodic data from the sensors are received via notifications. A descriptor write is performed by the BaseStation to enable or disable notification events. While enabling or disabling notifications from the characteristics on the sensors, each service waits for the successful completion of the descriptor write operation in the corresponding call back method. Once again, as per SASC, if a particular descriptor write is not successfully completed, then it is performed again before attempting the next BLE action.

In the SASC method, all of the special event notifications (which are not periodic in nature) are enabled first, before enabling the periodic data stream notification from any of the sensors. Also, all of the necessary characteristic and descriptor writes are completed across all the sensors before starting periodic data stream notification from any of the sensors.

4.2.5 Disconnection Process

The scenarios wherein the BaseStation and the sensors are ‘always ON’ systems are considered, which means that they need to be extremely robust. In this scenario, it’s the disconnection event that triggers the sensors to switch from BLE communication mode to sensor data collection mode. Implementation of the disconnection process plays an important role in achieving correct functionality of the BaseStation over a period of time.

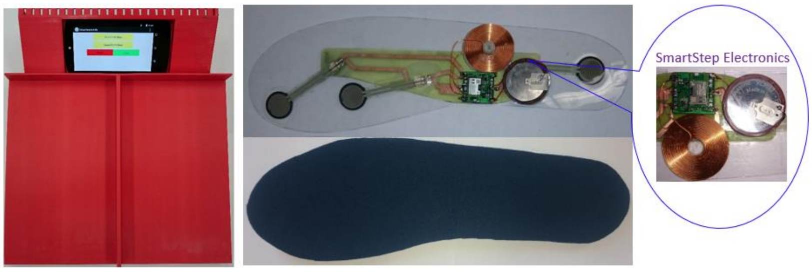

Figure 4-2. Base station and the SmartStep Sensor System

Implementation of the actual events that give raise to a disconnection event is left up to the particular application scenario. In any case, SASC methodology expects the sensors to notify about their wish to get disconnected from base station and the sensor's firmware needs to be implemented accordingly. Once the particular service handling a specific sensor receives the event notification, notifying the sensor's wish to get disconnected, the service lets the UI_Activity know about it. When the UI_Activity approves the disconnection event, the service initiates descriptor writes to disable all the event notifications from the particular sensor. These descriptor writes are carried out in the same way as described in B.2. After all of the notification events of the particular sensor are disabled successfully following the SASC method, then the particular service triggers disconnection events and after a successful disconnection event, the UI_Activity is informed about the same. The particular service then enters periodic scanning phase. When multiple disconnect notifications arrive at the same time, as per the SASC methodology, the disconnection events are handled in a sequential manner, and are sequenced by UI_Activity.

The method of disabling all notifying characteristics before a disconnection event with SASC, makes sure that the notification event timers are all halted, and would not drain the battery power during the sensor data collection period. When the sensors advertise the next time, the scanning services follow the same procedure of connection establishment and information exchange as shown in Figure 4-1.

4.2.6 Testing Scenarios

To test the SASC methodology for correct functionality in a BLE network without user intervention, it is applied in designing an Android BaseStation application that deals with two SmartStep devices that collect gait data. In a general usage scenario, at the start of the day the user takes the shoes from the base station and wears his/her shoes embedded with the SmartSteps, and performs all of their daily activities. During wear, the SmartSteps' sensors are sampled at 50 Hz and the sampled data is logged in the SmartStep's flash memory. The radio is turned off during this stage. At the end of the day, the user places the shoes on the base station to recharge the SmartSteps' battery. Radio communication is turned on utilizing the information provided by the wireless power reception system. The smartphone connects to the sensors over BLE and retrieves the sensor data collected in the SmartSteps (at 50 Hz). After data retrieval completion, the smartphone transfers the data to a web server for further processing. This methodology of real-time sensor data logging and offline data transmission is adopted to help users in the target application who may not be able to always carry the smartphone. To synchronize the data collected from the two SmartSteps for further signal processing, each SmartStep maintains a POSIX timestamp counter. The counter is corrected from the smartphone whenever there is a BLE connection event. The UI in this case is dovetailed for "always on" application scenarios and it allows the user to configure the BaseStation's settings for the first time. After the initial configuration the BaseStation works autonomously without user intervention. The UI displays relevant information and warning messages during operation. Figure 4-2 shows the different system components.

To profile the SASC methodology for different numbers of simultaneous connections and varying BLE connection intervals, SASC methodology is applied in designing a real time streaming version of the base station (RT_BaseStation). We want to evaluate the throughput from RT_BaseStation, its CPU loading, and its power consumption. The reason is that, even though modern Android devices are equipped with high end CPUs and gigabytes of RAM, their wireless network interfaces are subjected to limitations in the number of simultaneous connections that they can maintain, or the data rates that they can handle. Theoretically, there is no set upper limit to the number of simultaneous connections a master can serve in BLE network [149], but the present day Android OS allows only 7 [150]. Hence, we have carried out benchmarking tests that involve 1 to 7 sensors with connection intervals that range from 7.5 ms to 1000 ms. The choice for the upper end of the connection interval range has been derived from the fact that, in general, BLE is meant for low frequency data transmission, and 1 Hz is quite common in BLE applications (for example in a BLE heart rate monitor). The choice for the lower end of the connection interval is chosen since the lowest connection interval possible is 7.5 ms in BLE. The RT_BaseStation UI allows the user to select the desired number of sensors. Also, to help with running profiling tests for a particular amount of time, the UI in this case allows manual connect and disconnect functionalities.

A smartphone (Google Nexus 5 with Android version 6.0) was used for testing the SASC methodology under the above application scenarios. The smartphone has a chipset (Qualcomm Snapdragon 800) with quad-core CPU (2.3 GHz Krait 400).

4.2.7 Sensor Description

Each SmartStep sensor has an accelerometer and a gyroscope on board as well as flash memory for optional storage of sampled sensor data. These sensors use the BLE stack 1.4.0 (Texas Instruments) [134] and are programmed using the IAR integrated development environment. BLE connection parameters and sampling frequency are configurable for the sensor. SmartStep sensors can be used in real time data streaming or in real time data collection and offline data streaming as detailed in [73].

4.2.8 Experiments

a) Free Living Validation of SASC Methodology

The following experiment was conducted to verify the functionality of SASC methodology in handling multiple BLE sensors in a completely autonomous scenario, with no manual intervention. The SmartSteps were initialized from the BaseStation and were worn for one day by 3 human subjects (2 males with shoe size US M9 and one female with shoe size US W9). At the end of the day the shoes were placed on the BaseStation, after which the data collected by the SmartStep insoles during the whole day of wear were transferred to the smartphone. This procedure was repeated for seven days by each of the subjects. At the end of the experiment, the data retrieved by the BaseStation were analyzed to determine the percent data retrieval using the information from the POSIX timestamps in the SmartSteps. A quantitative measure of the percent data retrieved (DR) by the BaseStation was calculated for both sensors on each day using a Matlab script. The metric was quantified as follows:

$$\mathrm{DRi} = (\mathrm{NTSi} \,/\, (\mathrm{LTSi} - \mathrm{FTSi} + 1)) \times 100 \qquad (1)$$

where NTSi is the total number of timestamps received, LTSi is the last timestamp received and FTSi is the first timestamp received for the i^{th} sensor ($i \in$ {left, right})

b) Percent Data Retrieval/Throughput Evaluation of SASC Methodology

To evaluate the percent data retrieval/throughput of SASC, RT_BaseStation was used with different numbers of sensors and connection intervals. The connection interval was varied from 7.5 ms to 1000 ms and the number of sensors was varied from 1 to 7 (7 being the maximum number of sensors allowed in Android BLE) and the sensor data were recorded in the smartphone. The SmartStep sensors are used as standalone sensor modules and are loaded with real time streaming firmware [73]. Each sensor sampled the accelerometer and gyroscope data at the specified sampling rate, the same as connection frequency, and along with the 4-byte timestamp, each sensor communicated a 16-byte data notification packet to the smartphone during every connection interval. Each test case was run for 10 minutes. Figure 4-3 shows the laboratory set up of 7 sensors with an Android phone used for the tests.

The data received in each of the cases was saved as a comma separated value file in the smartphone and was later used to determine the % data retrieval metric (DRi (1<=i<=7)), with the help of a Matlab script. The presence of the timestamp allowed the metric to be quantified as described before in (1). Average DR for each case was obtained by averaging across DRi.

c) CPU Loading and Power Consumption Profiling of SASC Methodology

These experiments were conducted to evaluate the CPU loading and power consumption in the Android device, for different numbers of simultaneous BLE connections and varying BLE connection intervals. The power consumption by the BLE sensors themselves has been previously described [20, 74].

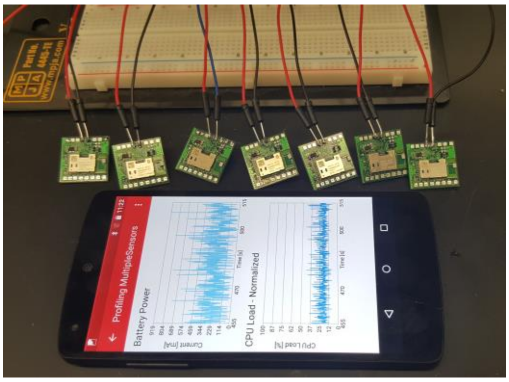

Figure 4-3. Laboratory set up for profiling

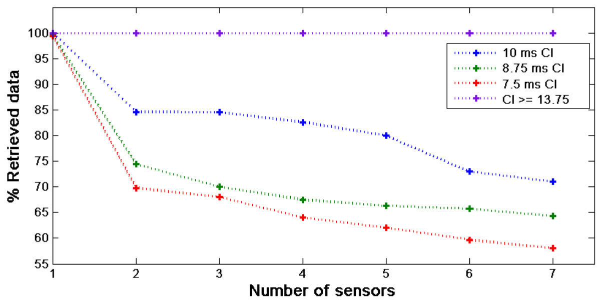

Figure 4-4. Results of data retrieval tests

The Trepn Profiler (Qualcomm®) [151] was used to profile both CPU loading and power consumption on the smartphone, while the smartphone was running the RT_BaseStation. The connection interval was varied from 7.5 ms to 1000 ms and the number of sensors was varied from 1 to 7. The CPU loading and the power consumption by the RT_BaseStation was recorded for each test case, which ran for 3 minutes (the time needed to obtain a stable CPU loading measure). During the profiling tests, it was made sure that no additional applications were running in the background which could potentially affect the results.

4.3 Results

4.3.1 Free Living Validation of SASC methodology

We had to exclude the data from two days of experiments from one of the subjects, as the left insole sensor had stopped functioning because of improper placement of the insole on the base station. This led to the battery failing to get charged. For the rest of the data (total 19 days) the timestamp analysis showed that 100% of the data collected by the SmartStep sensors from all 3 subjects was successfully retrieved by the BaseStation over BLE in this free living experiment.

4.3.2 Percent Data Retrieval/Throughput Evaluation of SASC Methodology

Average percent data retrieved for different number of simultaneous connections and varying connection intervals is reported in Figure 4-4. Connection intervals greater than or equal to 13.75 ms resulted in 100% of the data being retrieved from all the sensors by the application. The number of simultaneous sensor connections did not have an impact on the data retrieval for these connection intervals. However, for intervals less than 13.75 ms, there was a drop in the percent data retrieval.

4.3.3 CPU Loading and Power Consumption Profiling in a BLE Multi Sensor Scenario

Percent CPU loading for different number of simultaneous connections and varying connection intervals are reported in Figure 4-5. The results show that as the number of sensors increased or as the connection interval decreased, the CPU loading of the RT_BaseStation increased.

Power consumption of the multi sensor application for different number of simultaneous connections and varying connection intervals are reported in Figure 4-6. The results suggest that as the number of sensors increased or as the connection interval decreased, the power consumption from the RT_BaseStation increased.

4.4 Discussion

The human subject tests were run in real life environments and the BaseStation was able to retrieve all the data collected during a total of 19 days of experiments with 3 test subjects. The BaseStation also was able to act upon the special event notifications and sensor

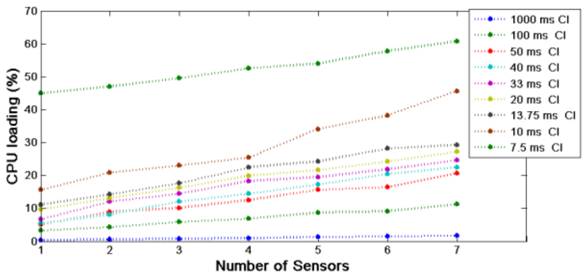

Figure 4-5. CPU loading test results.

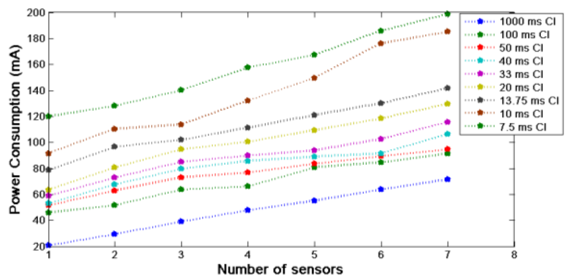

Figure 4-6. Power consumption test results.

status information correctly. These results suggest that the use of the proposed SASC methodology produces a reliable and robust multi-sensor Android application.

The results of the data retrieval tests (Figure 4-4) showed that in the cases with connection intervals less than 13.75 ms, for a single sensor the retrieval rate was 100% but dropped to 71% gradually as the number of simultaneous connections increased to 7 sensors. At these connection intervals, the BaseStation might be facing a resources overload to deal with multiple simultaneous connections. A closer look at the data received from each of the sensors revealed that for some of the sensors the retrieved data were close to 100% and for some others much less (sometimes around 30%) bringing the average down. Between a connection interval of 13.75 ms and a connection interval of 7.5 ms, there was a difference of 42% in the amount of retrieved data (for 7 sensor case). The data retrieval may be also dependent on the specific Android device (Google Nexus 5), or the BLE chipset used in the sensor (Texas Instruments CC2540). However, based on these results, it may be advisable to use connection interval of 13.75 ms or greater if the applications require retrieval of all the data.

As per the specifications of BLE v 4.0, the maximum data throughput is 270 kbps [152]. However, [149] reported 58.48 kbps in a realistic scenario involving the same CC2540 BLE solution from TI with 7.5 ms connection interval. On a similar line, but under Android OS framework, our tests demonstrated a maximum throughput of ~70 kbps (7 sensors, 7.5 ms connection interval), which is higher than the results presented elsewhere [149], but considerably less than the BLE specifications in [152]. The limitation may be because of the current implementation of BLE in the Android OS, or the particular Android device that was used, or as noted in [149], might be caused by the BLE chipset and the TI stack in the sensor.

In the test cases, the size of each periodic data notification packet was 16 bytes, while the maximum allowed size is 20 bytes per notification packet in BLE. A smaller or larger notification packet size would likely have an effect on the results of the profiling tests and this may be explored in future work. Also, in BLE, each connection interval can carry up to 80 bytes of data in total. While we tested using just one notification packet per connection interval, it may be interesting to test the cases with multiple notification packets in a single connection interval and measuring the throughput in such scenarios.

In the TI BLE solution that we used, given one notification packet per connection event, each connection event lasted approximately 3 ms [137]. Considering a case with 1000 ms connection interval and single sensor, there would be one connection event every second that the smartphone CPU needs to handle. In this case, smartphone CPU should be active for ~3ms in each second, resulting in 0.3% CPU loading. In support of this argument, the observed loading for this case was 0.3%. On a similar line, for 7.5 ms connection interval case, there would be 133 connection events in each second. If each connection event lasts ~3 ms, the CPU should be active for ~400 ms in one second (or ~40% loaded). The observed loading for this case was 45%, which is close. This explanation is valid for all the connection intervals tested, for one sensor connection case. However, for multiple sensors, this argument does not hold, and the reason can be that the Smartphone’s CPU is a multicore system and is managed by an OS. A more detailed analysis is required to identify how different processor cores handle different sensors in a BLE multi sensor scenario.

The results of the power consumption tests (Figure 4-5) suggest that a connection interval of 10 ms or 7.5 ms caused the BaseStation to consume considerably higher power. The power consumption for the 7.5 ms case was approximately 1.5 times that of the 13.75 ms case across any number of sensors. High power consumption at short connection intervals (less than

13.75 ms) may be attributed to BLE stack overhead. Based on these results, it may be advisable to use connection interval of 13.75 ms or greater to keep the power consumption low.

The OS of the smartphone device has a major impact on the testing and operation of the system. Present day Android OS's limitation of maximum 7 simultaneous BLE connections might be increased in future versions of the OS. Also the reported SASC methodology has been validated only for Android OS and may need modifications for iOS or Windows mobile. Other than SASC, there may be other multi sensor communication strategies that work equally well or better.

4.5 Conclusion

This research evaluated the performance of a multi-sensor Android BLE application and a new methodology - Sequential Actions following Successful Callback (SASC). Benchmarking tests and free living tests were conducted to validate the SASC implementation schemes. The benchmarking tests gave quantified results on metrics such as throughput, CPU loading on the smartphone and power consumption by the Android application for various numbers of sensors and varying connection intervals. The results of throughput evaluation suggest that the maximum achievable throughput in Android BLE multisensor scenario was ~1/4th of the theoretical maximum. The results of the CPU loading and power consumption tests suggest that CPU loading and power consumption figures can be kept low by using connection interval of 13.75 ms or greater. The proposed SASC methodology was also used in a real life use-case for gait data collection using SmartStep sensors, and a total of 19 days of human subject tests resulted in 100% data retrieval. These results suggest that the proposed methodology can serve as a foundation for applications requiring management of multiple BLE connections.

CHAPTER 5 THE PEDIATRIC SMARTSHOE: WEARABLE SENSOR SYSTEM FOR AMBULATORY MONITORING OF PHYSICAL ACTIVITY AND GAIT

This work has been submitted to the IEEE Transactions on Neural Systems & Rehabilitation Engineering and is currently under review.

As an example application of footwear based wearable system, this chapter describes human subject studies involving children with Cerebral palsy while they wore a SmartShoe which captured their activity and gait. The chapter details novel signal processing algorithms that dealt with orthotic effects on pressure sensor signals and describes machine learning models for activity and gait monitoring.

5.1 Introduction

Cerebral palsy is a group of neurological disorders that appear in early childhood or infancy, and permanently affect the muscle coordination, body movement, and balance in the patients [153]. One in three children per 1000 births are affected by CP [154]. CP affects the part of the brain that controls muscle movements, and the most common effects are stiff or tight muscles and exaggerated reflexes, a lack of muscle coordination when performing voluntary movements, walking with one foot or leg dragging, walking on the toes, a crouched gait, or muscle tone that is either too stiff or too relaxed. As a result, people with CP who are able to walk may have unsteady gait and problems with balance. Many affected children have progressive musculoskeletal pathology, including spasticity, muscle weakness and shortening, and bone deformity [157, 158]. Other neurological symptoms that commonly occur in individuals with CP include hearing loss, impaired vision, seizures and others.

CP is not a curable disease, but treatment will often improve a child's capabilities. In general, early treatments or rehabilitation programs can help such children to overcome developmental disabilities, learn new ways to accomplish the tasks that challenge them, or improve their muscle control. Treatment options for children with CP include physical therapy, orthoses, pharmacological agents, and surgery [157].

The early introduction of independent mobility in such children is also important because the ability to explore one's environment has been demonstrated to improve self-esteem in children [158]. Patients with CP usually have a very inefficient gait pattern, and there can be an energy expenditure gain of as much as 350% [158]. Hence, one of the important aspect in CP rehabilitation programs is to measure the activity levels of the children and their gait patterns.

Constraint-Induced Movement therapy (CI therapy) is a neurorehabilitation technique developed to improve use of the more affected upper or lower extremity after a stroke [159]. A number of studies have reported positive effects for this intervention in both adults and children [160], [161]. One of the goals of this treatment is to improve gait symmetry and functional independence in everyday living. Thus, measuring gait parameters is important for assessing impairment level and treatment outcome.

Traditional rehabilitation programs for CP children utilize commercially available stationary laboratory systems for gait monitoring [9]. However, measuring the effects of rehabilitation programs in a community living is more important. Under certain conditions, e.g., those that support the development of learned nonuse, performance in the laboratory will not accurately reflect behavior in the community [164, 165]. Self-report methods that are available for measuring behavior in the community are subject to several different types of bias. There are also published works utilizing a commercial sensor Kinect® (Microsoft Inc, Redmond, USA) for gait monitoring [7, 8], but these cannot be used in a free living environment.

Accurate activity monitoring in community living is a prerequisite to gait monitoring in community living, as the gait parameters are to be estimated from walking episodes [69]. Daily life is a mixture of different activities such as sitting, standing, walking and others, and unless these different activities are accurately distinguished, gait monitoring cannot be performed accurately in free living conditions.

Wearable systems for activity tracking are becoming a part of modern daily life. The majority of these are wrist worn and accelerometry based [56, 166]. Such systems suffer from low accuracies in distinguishing weight bearing and non-weight bearing activities, such as sitting and standing. Footwear based wearable systems have the advantage over these systems, since these can have plantar pressure sensors that can help to distinguish sitting and standing activities [68]. The footwear based systems may also incorporate inertial sensors such as accelerometers and gyroscopes to differentiate other daily living activities. For example, Chen et al. have designed a foot-wearable interface for locomotion mode recognition based on contact force distribution [74]. Kawsar et al. have developed a novel activity detection system using plantar pressure sensors and a smart phone [75]. Sazonov et al. have presented footwear based wearable systems for activity monitoring of healthy adults [68] and adult stroke subjects [1, 167].

Information from the pressure sensors in the footwear can also be used for estimation of temporal gait parameters such as cadence, stance time and others. Spatial gait parameters such as step length, stride length and others can be estimated utilizing the accelerometer and gyroscope. For example, Bamberg et al. presented a gait monitoring shoe system for Parkinson diseased subjects [12], as have, Mariani et al. [14]. Sazonov et al. reported a footwear based system for gait monitoring in adult stroke subjects [5]. Leunkeu et al. [15] worked on footwear based gait monitoring system for CP children but the system was not tested against criterion standards. Crea et al. [8] developed an insole based gait monitor which has yet to be validated fully. González et al. [19] worked on a gait monitoring footwear system that was validated on healthy adults. Footwear based gait monitoring systems have also been utilized for human identification as reported by Huang et al. [16].

This research evaluated a wearable sensor system for combined activity and gait monitoring in CP children. The CP children wear orthotics that affect the pressure sensor signals. Hence, the methodologies and models developed for activity and gait monitoring of adult subjects [2, 167, 168] could not be applied directly to gather sensor data from CP children. This application offered newer challenges and demanded new signal processing methodologies for accurate activity and gait monitoring. Specifically, the following challenges are addressed in this work:

- Development of novel signal processing algorithms that can deal with the pressure sensor signals from children with varying weights and CP children wearing orthotics.
- Development of machine learning models for accurate activity classification.
- Development of gait computation methodology dealing with CP children with orthotics.
- Estimation of stance asymmetry ratios from SmartShoe and validation against GaitRite.

5.2 Methodology

5.2.1 Pediatric SmartShoe System

The underlying hardware of the Pediatric SmartShoe system is the same as those utilized in adult version of the SmartShoes [79]. However, the target population in this application has a much smaller shoe size (US children's size 12 to youth size 2). Each SmartShoe carries five FSR< spell out sensors (Interlink, Inc), and a 3-D accelerometer ADXL326 (Analog Devices, Boston, USA). The FSR sensors were located at the heel, the heads of the metatarsal bones, and the big toe, and are soldered on a flexible printed circuit board. A plastic enclosure, hosting the accelerometer, rechargeable battery and Bluetooth 2.1 wireless interface was mounted on the heel at the back of the shoe. (Figure 5-1). Data were sampled from the pressure sensors and accelerometer at 400Hz with a 12-bit ADC, down sampled to 25 Hz and sent to a Microsoft Windows® mobile application and stored as a comma separated value file. Further details of the hardware can be found elsewhere [79].

5.2.2 Subjects and protocols

Twenty-one subjects (11 healthy children, 6 males, 5 females; 10 CP children, 6 males, 4 females) were recruited to participate in this study. The protocol was approved by the University of Alabama at Birmingham and the University of Alabama Institutional Review

Figure 5-1. Pediatric SmartShoe

boards. The parents of the children signed the informed consent. The subjects' demography is as shown in Table 5-1.

Table 5-1. Anthropometric characteristics of participants

	Healthy n= 11	CP n=10
Age (years) (mean ± std)	6.6 ± 1.5	6.2 ± 1.5
Height (m) (mean ± std)	1.2 ± 0.1	1.2 ± 0.1
Weight (kg) (mean ± std)	24.4 ± 4.4	22.3 ± 4.6
Weight (kg) (range)	17 - 33	16 - 31
Shoe Size (range)	US children's 12 – Youth 2	US children's 12 – Youth 2

The children were instrumented with the pediatric SmartShoe of appropriate size, and performed a structured protocol (Table 5-2) that included variants of sitting, standing and walking.

Table 5-2. Activities in the protocol

Activity	Description	Time (minutes)	Class Label
Sitting	On child chair	2	Sit
	On adult chair	2	
	On parent's lap	2	
	On the floor playing toys	2	
Standing	Standing still	2	Stand
	Standing while playing toys	2	
	Standing while being dressed	2	
Walking on the ground	Slow walk	2	Walk
	Fast walk	2	
	Run	2	
Walking on the GaitRite	Slow walk	Span of GaitRite mat, 3.6 m	Walk
	Fast walk		
	Run		

For validation of the temporal gait parameters, some of the walking episodes were performed over the GaitRite mat, (CIR Systems, Inc. Franklin, NJ, USA) consisting of an electronic walkway with a useful area of 61 × 366 cm (24 × 144 in) connected to a Windows®-based PC. SmartShoe data from each experiment were manually annotated, labeling the type, start and end of each activity. The annotated data were later used for developing machine learning models for activity classification and automatic gait parameter estimation.

5.2.3 Time Series Representation of the Sensor Data

A single sample of data from a SmartShoe is represented by vector $S = \{PH, P1M, P3M, P5M, PHx, AAP, AML, ASI\}$, where PH is heel pressure, $P1M$, $P3M$, $P5M$ are pressures from first, third, and fifth metatarsal head sensors, respectively; PHx is pressure from the hallux sensor, AAP is anterior–posterior acceleration, AML is medial–lateral acceleration, and ASI is superior–inferior acceleration. Data from both the shoes are synchronized utilizing the timestamp information available in the SmartShoe sensor data [79]. The time series data from both of the shoes were combined as $D_i = \{SL, SR\}_i$, $i = \{1,2\ldots\ldots M\}$, where SL, SR are the data samples from the left and right shoe, respectively, and M is the length of the time series.

5.2.4 Signal Pre-Processing

In our previous studies on adults, the signals from the pressure sensors were the determining factor for achieving the high accuracy of discrimination between sitting and standing [69, 167]. However, most of our adult participants did not wear orthotics, the use of which is prevalent in children with CP. The orthotics create a residual pressure reading in the insole pressure sensors that impacts both activity recognition and gait parameter estimation. When not addressed, this can mean that pressure sensor data for a sitting activity of a CP child with orthotics, can be very similar to the standing activity of a child without orthotics. To remove this variation in the pressure signals in different children for the same activities, while minimizing the orthotics effect on the signals in CP children, a novel signal preprocessing methodology is proposed here. The presented methodology also helps in taking out the pressure sensor signal variation because of the variation in children's weight (Table 5-1). The signal pre-processing involved the following steps:

- Initial 2 seconds of the data in D_i^k were discarded to get the data in steady state of activity in k, where k= {1 for sitting, 2 for standing, 3 for walking}.
- All of the activities' data for each subject were grouped together.
- Sum of all five pressure sensors (P_Sum_i), for each shoe data was computed for the entire time series data set, comprising all the activities.

$$P\_Sum_i = PH_i + P1M_i + P3M_i + P5M_i + PHx_i \qquad (1)$$

- The offset in P_Sum_i time series data was removed by seeking the local minima using [167] in P_Sum_i, and subtracting the waveform by the average value of the local minima. This makes the P_Sum_i waveform to be shifted to a near zero starting value (if there was no orthotics effect, then the offset would be close to 0). Figure 5-2 shows an example of a time series waveform prior to and after the preprocessing methodology for a CP child wearing orthotics.
- P_Sum_i was scaled to be in the range of [0,1].

5.2.5 Machine Learning Models for Activity Classification

The pressure sensor signals and accelerometer signals from SmartShoes were used in developing the machine learning models. Statistical features were computed from the sum of five pressure sensor signals (P_Sum_i) and resultant acceleration (RA_i). RA_i is defined as

$$RA_i = \sqrt{(AAP_i)^2 + (AML_i)^2 + (ASI_i)^2} \qquad (2)$$

Features were computed in every 2 s interval (epoch) of the time series data in line with our previous work [1, 69], for both shoes. Table 5-3 shows the features extracted.

Table 5-3. Features extracted from the SmartShoe sensor data

#	Description	#	Description
1	mean of P_Sum_j* from left lower extremity (LE)	7	mean of P_Sum_j from right lower extremity (RE)
2	standard deviation of P_Sum_j from LE	8	standard deviation of P_Sum_j from RE
3	mean of RA_j from LE	9	mean of RA_j from RE
4	standard deviation RA_j from LE	10	standard deviation RA_j from RE
5	number of mean crossings of P_Sum_j from LE	11	number of mean crossings of P_Sum_j from RE
6	number of mean crossings of RA_j from LE	12	number of mean crossings of RA_j from RE

** j is the time index of the sensor data in each 2 s epoch and j = {1,2,..50}*

In developing an activity prediction model, Multinomial Logistic Discrimination (MLD) was used as a supervised classification algorithm. This specific methodology was used because we have previously shown [6] that MLD can result in comparable accuracy with Support Vector Machine (SVM) or Artificial Neural Network (ANN), while consuming less memory and is faster for real time computation.

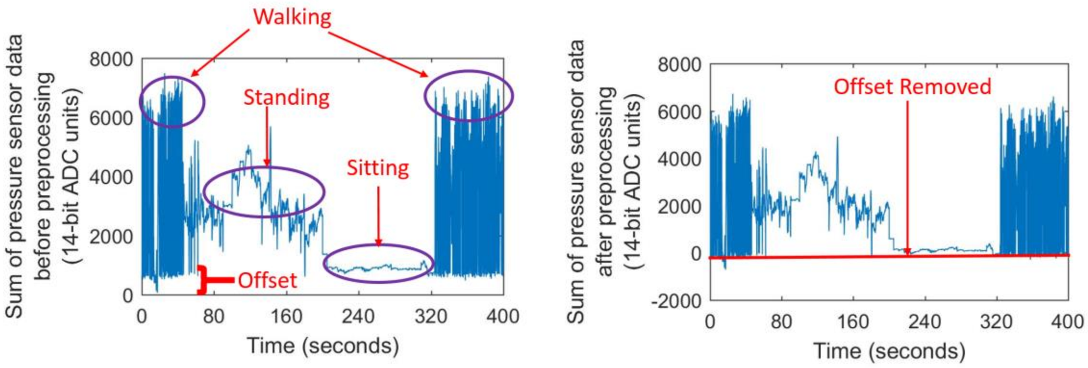

Figure 5-2. Sum of pressure sensor data from SmartShoe for a CP child wearing orthotics

A total of 5620 epochs were utilized in the activity classification model development, corresponding to ~190 minutes of data. The pairs of feature vectors and class labels were presented to the MLD for training and validation of the models. A leave-one-out cross validation strategy was used in the model development, meaning that sensor data from 20 subjects was utilized in model training phase and the resulting model was tested on the 21st subject. The process was carried over iteratively, covering each of the subject's data as the test set. Healthy and CP children data were together used for training the activity classification model and there was no need for separate models for CP children. A confusion matrix was computed for each of the runs of leave-one-out cross validation and the average accuracy of classification was computed from the cumulative confusion matrix.

5.2.6 Computation of Temporal Gait Parameters

SmartShoe pressure sensor data from the experiments that were conducted on GaitRite were considered for gait analysis. From each extremity SmartShoe data, sum of the 5 pressure sensors (P_Sum_i) was used in the computation of temporal gait parameters. Temporal gait parameters were computed from the time instances of heel strike (HS) and toe-off (TO). The procedure had the following steps, which were applied to the SmartShoe data from left lower extremity and right lower extremity separately:

1. Local maxima and minima vectors were computed on P_Sumi utilizing the Matlab functions for computing the local extrema [167], represented as

$$maximaVector = \{maxima_1, maxima_2, \ldots., maxima_P\};$$

$$minimaVector = \{minima_1, minima_2, \ldots., minima_Q\};$$

where P and Q are the number of local maxima and minima in P_Sum_i *respectively.*

2. The range of P_Sumi was calculated utilizing maximaVector and minimaVector as follows.

$$Range = mean(maximaVector) - mean\ (minimaVector)\ (3)$$

3. To make the detection of HS and TO points adaptive to variation in P_Sumi across different subjects, an adaptive threshold value for marking HS and TO in the P_Sumi was defined. The threshold is dependent on the computed minima and the range for the particular P_Sumi waveform, similar to the described methodology in [5]:

$$Threshold = mean\ (minimaVector) + (0.2 * Range) \quad (4)$$

4. Time instances of HS and TO were calculated as below:

Traverse through P_Sum_i *from i=0 to i=M*

Mark time instance 'i' as HS

"if ((P_Sum_i *< Threshold) and (*P_Sum_i *+1> Threshold))"*

Mark time instance 'i' as TO

"if ((P_Sum_i *> Threshold) and (*P_Sum_i *+1 < Threshold))"*

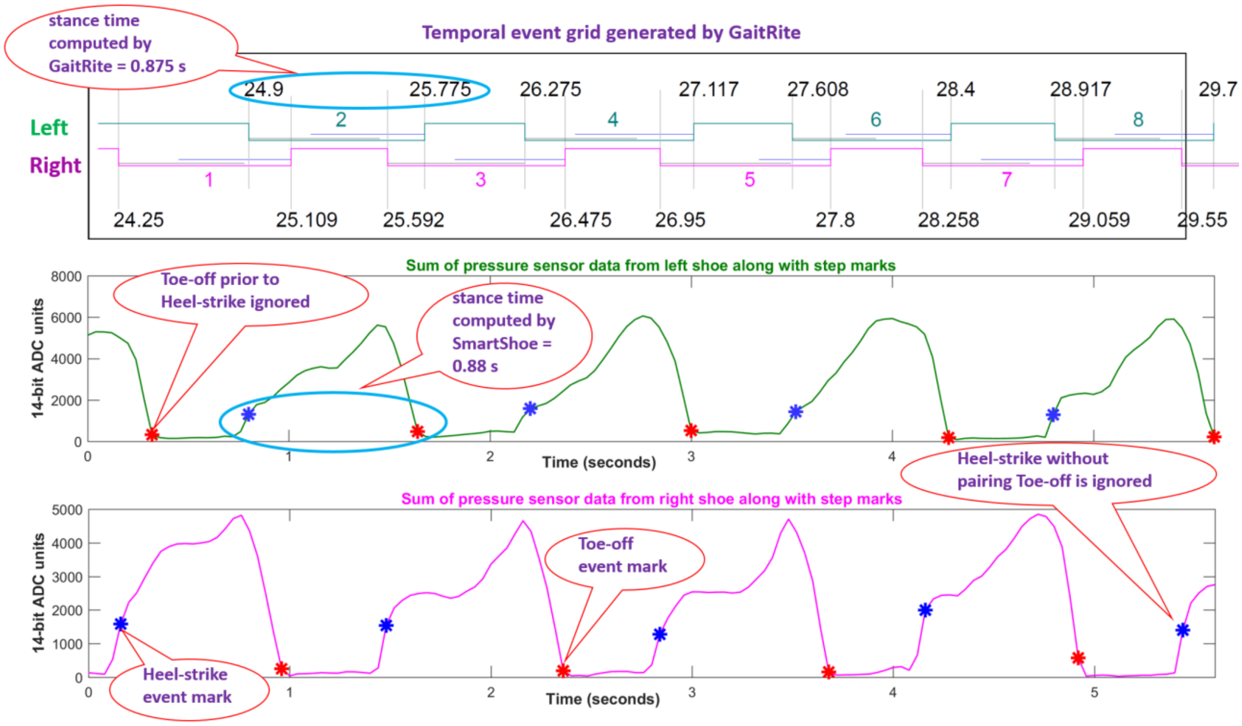

Figure 5-3. Temporal events as recorded by GaitRite and the Pediatric SmartShoe

Figure 5-3 shows an example HS and TO extraction scenario for an experiment during slow walk, as captured by the GaitRite and from the Smartshoe sensor data. TO time instances detected prior to the first HS was ignored and so was the final HS point without a pairing TO as shown in Figure 5-3. The methodology resulted in HS and TO vectors (HS_v and TO_v) of equal length represented as:

$HS_v = \{HS_1, HS_2..,HS_N\}$, $TO_v=\{TO_1,TO_2...,TO_N\}$, where N is the total number of HS or TO considered.

We had to deal with very short walking periods on the GaitRite, and from the SmartShoe data we observed that in many instances the children did not stop walking right after completing the walking on GaitRite, and the SmartShoes captured a few additional steps after the walking on GaitRite. This would affect the comparison of gait parameters computed from the shoe sensor to that of GaitRite; hence we had to match the exact steps taken on

GaitRite to those from Shoe data (in real life use cases this process would not be necessary). For this purpose, a quantitative relationship between number of steps as computed by GaitRite (NS) with the number of HS-TO pairs (N_{pair}) were established as follows:

```
if (NS is odd)
    Npair for the first landing extremity on GaitRite = (NS+1)/2;
    Npair for the second landing extremity on GaitRite= (NS+1)/2;
else
    Npair for the first landing extremity on GaitRite = (NS/2) +1;
    Npair for the second landing extremity on GaitRite = NS/2;
end
```

Information about the first landing extremity on GaitRite was obtained from the GaitRite data from each of the experiments for all the subjects. For all the experiments, HS-TO pair in the P_Sum_i time series which fell outside the boundary of N_{pair} were all ignored in gait parameter estimation. The cadence parameter was estimated as follows:

```
if (NS is odd)
    cadence = (NS/ (F(HSN) – F(HS1));
else
    cadence= (NS/ (S(HSN) – F(HS1));
end
```

where $F(HS_N)$ and $F(HS_1)$ are the last and first heel strike time instances of the first landing extremity on GaitRite, and $S(HS_N)$ is the last heel strike time instance of the second landing extremity on GaitRite.

Other temporal gait parameters such as gait cycle time, swing time, stance time, step time and single support time for both the lower extremities were computed in the same way as performed in [5]. Gait asymmetry ratio was computed for each child (healthy and CP) for slow walk, fast walk and running episodes utilizing the SmartShoe sensor data and from the GaitRite, and was computed as:

$$Asymmetry\ ratio = \frac{stance\ time\ of\ MALE}{stance\ time\ of\ LALE} \qquad (5)$$

wherein, MALE – most affected lower extremity and LALE – least affected lower extremity. For CP children MALE and LALE were identified from the information provided by the parents. For healthy children, non-dominant lower extremity was used as MALE.

5.2.7 Data Analysis

The accuracy of activity classification by the SmartShoe system was evaluated by comparing the SmartShoe predicted activity to the actual activity that children performed, during the structured protocol. The gait analysis was carried out for CP and healthy children separately, and among them for slow walk, fast walk and run separately. The accuracy of the SmartShoe system's gait parameter estimates was evaluated by computing their relative error. The deviation of each SmartShoe computed gait parameter from the corresponding estimate by GaitRite were calculated and expressed as percent of the GaitRite estimate value:

$$M_{RE} = ((M_{GR} - M_{SS})/M_{GR}) * 100)\ ) \qquad (6)$$

where in M_{GR} is the gait parameter M as computed by GaitRite, M_{SS} is the gait parameter M as computed by SmartShoe and M_{RE} is the percent relative error in the computation of gait parameter M.

The validity of the stance asymmetry ratio was evaluated by calculating the root mean square error (RMSE) between the asymmetry ratio computed from the GaitRite results and the ratio computed from the SmartShoe. Bland-Altman plots were utilized to see if there is any significant bias present in the results. Wilcoxon signed-rank test for paired observation was carried out at 95% significance level to determine if there are significant differences between the asymmetry ratios computed by SmartShoe and GaitRite.

5.3 Results

5.3.1 Activity Classification

Table 5-4 shows the cumulative confusion matrix of leave-one-out cross validation for CP children, resulting in average accuracy of 95.3%. Table 5-5 shows the cumulative confusion matrix of leave-one-out cross validation for healthy children, resulting in average accuracy of 96.2%.

Table 5-4. Activity classification results for CP children

		Predicted class			
		Sitting	**Standing**	**Walking**	**Class-specific recall**
Actual class	**Sitting**	**634**	**23**	**10**	**0.95**
	Standing	**6**	**567**	**42**	**0.92**
	Walking	**1**	**23**	**909**	**0.97**
	Class-specific precision	**0.99**	**0.93**	**0.95**	**0.95**

Table 5-5. Activity classification results for healthy children

		Predicted class			
		Sitting	Standing	Walking	Class-specific recall
Actual class	Sitting	997	8	3	0.99
	Standing	51	951	57	0.90
	Walking	2	8	1328	0.99
	Class-specific precision	0.95	0.98	0.95	0.96

5.3.2 Gait Parameter Computation

Table 5-6, Table 5-7 and Table 5-8 show the average estimated gait parameters during for different cases. In these tables, GTL is the gait cycle time of left extremity, GTR is the gait cycle time of right extremity, StanceL is the stance % of GTL, StanceR is the stance % of GTR, SwingL is the swing % of GTL, SwingR is the swing % of GTR, StepL is step time of left extremity, StepR is the step time of right extremity, SingleSuppL is the single support % of GTL, and SingleSuppR is the single support % of GTR (terminologies as presented by GaitRite). Table 5-9 shows the average of percent relative error and Table 5-10 shows the standard deviation in the percent relative error for all the cases. Here, H refers to healthy children, CP to CP children, S to slow walk, F to fast walk and R to run. Table 5-11 shows the asymmetry ratios of the CP children and Table 5-12 shows the same for the healthy children.

Table 5-6. Gait parameters for children during slow walk

	Healthy slow walk, n=11		CP slow walk, n=10	
	GaitRite	**Computed**	**GaitRite**	**Computed**
Cadence (per min)	125.40	122.09	120.45	120.8
GTL (s)	0.96	1.01	1	1.02
GTR (s)	0.96	1	1.01	1.03
StanceL (%)	60.12	59.79	61.64	59.27
StanceR (%)	60.17	59.63	60.46	59.39
SwingL (%)	39.86	40.21	38.37	40.73
SwingR (%)	39.80	40.37	39.51	40.61
StepL (s)	0.48	0.50	0.50	0.50
StepR (s)	0.48	0.50	0.51	0.52
SingleSuppL (%)	39.62	40.28	39.79	41.06
SingleSuppR (%)	40.06	40.41	38.09	40.51

Table 5-7. Gait parameters for children in fast walk

	Healthy slow walk, n=11		CP fast walk, n=10	
	GaitRite	**Computed**	**GaitRite**	**Computed**
Cadence (per min)	166.42	165.93	168.91	167
GTL (s)	0.73	0.75	0.73	0.75
GTR (s)	0.73	0.76	0.73	0.75
StanceL (%)	57.9	57.69	57.51	56.47
StanceR (%)	57.81	56.89	56.60	54.70
SwingL (%)	42.12	42.31	42.51	43.53
SwingR (%)	42.22	43.11	43.41	45.30
StepL (s)	0.37	0.38	0.36	0.37
StepR (s)	0.36	0.38	0.37	0.38
SingleSuppL (%)	42.4	43.66	43.24	45.74
SingleSuppR (%)	41.93	41.96	42.860	43.53

Table 5-8. Gait parameters for children during run

	Healthy run, n=11		CP run, n=10	
	GaitRite	**Computed**	**GaitRite**	**Computed**
Cadence (per min)	212.52	210.13	213.92	205.08
GTL (s)	0.57	0.59	0.57	0.60
GTR (s)	0.57	0.60	0.57	0.61
StanceL (%)	37.72	38.70	45.22	46.98
StanceR (%)	37.85	39.06	44.13	43.37
SwingL (%)	62.30	61.30	54.76	53.02
SwingR (%)	62.14	60.94	55.85	56.63
StepL (s)	0.29	0.30	0.28	0.31
StepR (s)	0.28	0.29	0.29	0.29
SingleSuppL (%)	62.11	62.48	56.05	57.41
SingleSuppR (%)	62.34	60.17	54.57	52.65

Table 5-9. Average relative error for all cases (%)

	H-S	**H-F**	**H-R**	**CP-S**	**CP-F**	**CP-R**
Cadence	2.46	0.26	1.13	0.30	1.24	1.84
GTL	-3.79	-3.32	-3.84	-2.36	-2.17	-3.18
GTR	-3.68	-4	-5.99	-2.05	-3.12	-4.56
StanceL	0.52	0.25	-2.32	3.16	1.34	-2.06
StanceR	0.84	1.56	-2.98	1.52	2.67	-1.50
SwingL	-0.95	-0.67	1.55	-5.7	-1.63	1.38
SwingR	-1.55	-2.18	1.78	-3.44	-3.64	0.42
StepL	-3.30	-4.27	-5.61	-5.06	-2.56	-2.24
StepR	-3.91	-3.85	-1.63	1.29	-2.97	-2.52
SingleSuppL	-1.81	-3.04	-0.49	-3.05	-4.45	-1.06
SingleSuppR	-0.95	-0.37	3.08	-6.44	-1.82	2.41

Table 5-10. Standard deviation of relative error all cases (%)

	H-S	H-F	H-R	CP-S	CP-F	CP-R
Cadence	3.38	5.34	5.91	4.05	4.78	4.31
GTL	2.79	4.44	5.52	2.26	4.15	5.40
GTR	3.67	3.57	4.67	2.97	3.13	6.27
StanceL	2.14	4.75	2.09	5.86	4.17	7.79
StanceR	2.15	4.01	4.77	6.57	6.07	8.74
SwingL	3.19	6.43	1.40	9.44	5.61	6.51
SwingR	3.38	5.23	3.18	9.20	7.71	8.38
StepL	2.89	5.47	5.36	2.16	5.94	7.54
StepR	5.53	5.99	5.08	5.48	6.01	7.44
SingleSuppL	3.89	6.85	4.68	9.59	9.20	7.28
SingleSuppR	4.53	7	6.43	9.86	6.99	8.79

Table 5-11. Asymmetry ratios of CP children

Child ID	**Slow Walk**		**Fast Walk**		**Run**	
	Shoe	**GaitRite**	**Shoe**	**GaitRite**	**Shoe**	**GaitRite**
1	1.01	1.01	1.03	0.98	1.08	1.07
2	0.87	0.89	0.89	0.93	0.87	0.90
3	0.93	0.97	0.96	0.94	0.99	1.03
4	1.05	1.1	1.09	1.08	1.08	1.12
5	1	0.99	0.99	0.99	0.93	0.90
6	0.95	0.95	1	0.97	0.95	0.90
7	1.01	0.98	0.96	0.87	0.82	0.91
8	0.97	0.96	0.82	0.98	0.86	0.96
9	0.91	0.94	0.89	0.95	0.86	1.01
10	0.99	0.96	1.02	0.97	1.05	1.09
RMSE	**2.7%**		**6.7%**		**7%**	

Table 5-12. Asymmetry ratios of healthy children

Child ID	Slow Walk		Fast Walk		Run	
	Shoe	**GaitRite**	**Shoe**	**GaitRite**	**Shoe**	**GaitRite**
1	0.98	0.98	0.99	0.99	1.06	1.03
2	1	0.98	1.01	0.95	1.04	1.02
3	1.03	1	1.04	1.03	0.96	1
4	1.01	1	1.07	1.01	1.07	1.08
5	0.99	0.99	1.03	1	0.98	0.98
6	1.01	1.01	0.96	0.98	1.02	0.99
7	1.01	1	1.09	1	0.91	0.99
8	1.01	1.02	0.99	1.02	0.81	0.86
9	1.02	1.01	0.99	1.01	0.98	0.99
10	1	1.01	1.02	1.01	1.04	0.99
RMSE	**1.3%**		**3.9%**		**4.4%**	

Figures 5-4 and 5-5 show the Bland-Altman plots for the asymmetry ratios of CP and healthy children respectively, computed from the average ratios for each child, across different walking speeds. These plots demonstrate that the errors between SmartShoe and GaitRite computed metrics do not follow any specific pattern, and are not biased to either side (under- or over-prediction) with average bias being negligibly small (0.016 for CP children and -0.005 for healthy children). Wilcoxon signed-rank test for paired observations for all the cases in Table 5-11 and 5-12 resulted in $p>>0.05$, suggesting that there are no significant differences between the asymmetry ratios computed by SmartShoe and GaitRite.

5.4 Discussion

In this study, we have proposed and validated the Pediatric SmartShoe: a wearable sensor system for ambulatory monitoring of physical activity and gait. Validation of this wearable system was conducted on healthy children and children with CP. The use of orthotics by the children with CP and the large variation in stature among all of the children, affected the SmartShoe pressure sensor response. A novel signal processing methodology for pressure sensor data pre-processing was developed in this work to address this challenge, as described in section II.D.

The activity classification results showed high accuracies of 96.2% for healthy children, and 95.3% for CP children, in classifying daily living activities of sitting, standing and walking. Using a similar methodology, our previous work demonstrated the accuracy of activity classification for the adult version of the SmartShoe in healthy and post-stroke adults [24], [35]. In this study, we validated the methodology in healthy children and those that have CP. The presented results suggest that our approach of utilizing sensorized footwear for activity classification performs well on children of different ages and weight.

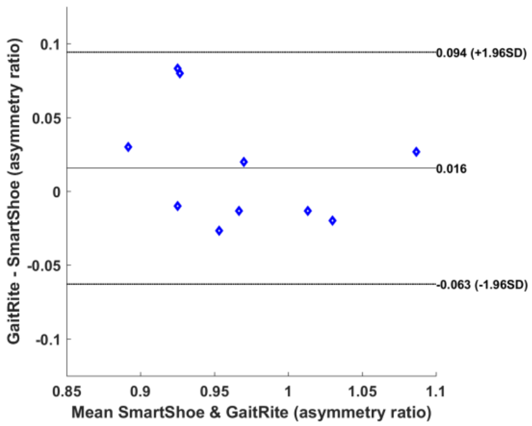

Figure 5-4. Bland-Altman plot CP

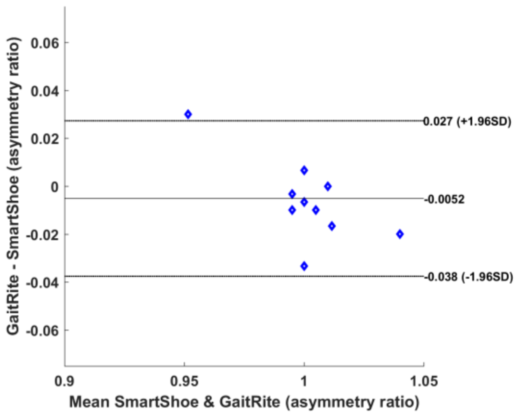

Figure 5-5. Bland-Altman plot for healthy

For the activity classification, we used 2 s intervals in line with our previous work [37]; this approach also seems to be valid for children. With regard to sampling frequency, as suggested by the high accuracy in the activity classification results, 25Hz implemented by SmartShoe electronics seems to be sufficient. However, a limitation of the 25Hz sampling was that it did not allow for computation of double support time as the resolution in the time series data was not sufficient to capture this parameter. The future implementation of the SmartShoe will use a higher frequency (e.g. 75Hz [25]), which should be sufficient for measurement of double support time.

Only temporal gait parameters were computed in this study. Computation of spatial gait parameters would usually involve systems with a gyroscope [25], which was not present in the SmartShoe that we used in this study. Recent development of our hardware has resulted in a SmartStep insole based activity and gait monitoring system [38], [39] that has a gyroscope and can be used for estimation of spatial parameters.

The previous published work reported gait estimation errors up to 18% [27], while this work has improved upon that significantly, with the highest average error for CP children being 6.4%. The improvements result from the method we employed in computing parameters, such as cadence, which matches more closely with the definition of cadence; while the previous work ignored the heel strike and toe off instances, and relied on the maxima and minima in the time series. In real life use cases there will be larger episodes of walking than the few seconds we had in the laboratory conditions. The short length of the GaitRite imposed a limitation on the data; we had to match the number of steps to GaitRite for precise comparison purposes, which will not be required in real life use cases.

Table 5-11 and 5-12 illustrate that the CP children have a more asymmetric gait (ratio was less than 1 or more than 1 in many instances), while for healthy children the ratio is very close to 1 in most instances. The low RMSE values between the asymmetry ratios computed from SmartShoes and GaitRite (minimum of 1.3% for healthy children during slow walking and maximum of 7% for CP children during running) suggest that the Pediatric SmartShoes can be utilized in monitoring gait of CP children in the community. The RMSE values increased as the walking speed of the children increased, which can be potentially reduced by utilizing higher sensor sampling frequencies. We had previously conducted small case studies on the use of SmartShoes in computation of gait asymmetry ratio of CP children in community living [40], and this study validates the approach in the laboratory, and supports the conduct of larger studies in community living in the future. Also, the SmartShoes could potentially be modified to provide feedback to CP children to improve their gait asymmetry, in a manner similar to the procedures employed in [41], [42].

5.5 Conclusion

Theory and data suggest that it is important to monitor gait of CP children in the community, in addition to assessing their gait in the treatment setting. Since daily life is a mixture of multiple activities, accurate classification of daily living activities is a pre-requisite for gait monitoring in community living. In this work we have proposed and validated a footwear-based activity and gait monitoring system for children with CP. Activity classification resulted in 95.3% accuracy for CP children and 96.2% for healthy children. Average relative error for gait parameter computation across 6 different sets of experiments (for healthy and CP children, and for slow walk, fast walk and running for each group) ranged from 0.2% to 6.4%. These results suggest that the presented footwear-based wearable system may potentially be used for the accurate monitoring of activity and gait of children with CP in community living.

CHAPTER 6 MONITORING ACTIVITIES OF DAILY LIVING WITH UPPER AND LOWER BODY-WORN SENSORS

This work is submitted to the IEEE Journal of Biomedical and Health Informatics and is under review.

Monitoring activities of daily living is important in treatment of many health conditions. This chapter throws light on accuracies of lower and upper-body sensors in recognizing a broad set of activities of daily living. The chapter describes the human subject study conducted in a controlled environment as well as in free living to assess the recognition abilities of the sensor system.

6.1 Introduction

Monitoring activities of daily living (ADL) is an important component in the treatment of health conditions such as obesity [168], [169]. Accurate monitoring of ADL is a prerequisite for estimating energy expenditure (EE) in daily life [80]. Monitoring of ADL also plays important role in rehabilitation programs for neurological disorders such as stroke, cerebral palsy, and Parkinson's disease [4], [77], [133]. Monitoring of ADL has also been proposed as a means of evaluating the quality of life in elderly [170], [171].

There are multiple approaches for monitoring of ADL. They can be broadly classified into non-wearable and wearable systems. Non-wearable systems include self-report instruments and the devices installed in the home (e.g., cameras, thermal sensors, infra-red sensors) to visually classify different activities [172]–[179]. However, self-reporting is subjective and prone to bias [180], whereas devices installed in the home only assess ADL in a limited space.

Wearable sensor systems have been proposed for monitoring of ADL since long time [181], [182]. Many of the present day activity trackers are wrist-worn or waist worn, often, based on accelerometry [57], [59], [61], [64], [183]. Wrist-worn devices may perform poorly at distinguishing lower body activities and postures. For example, sitting and standing are generally grouped together when utilizing wrist-worn accelerometers [184], [185]. Waist worn accelerometry based devices, placed at the center of mass of the body, are best suited for energy expenditure prediction for ambulatory activities. However, upper body activities can go undetected and also these devices may not be accurate in people with central obesity [183]. Accelerometry based devices also face challenges in recognizing activities such as cycling and walking on stairs.

There are many other types of activities that people perform commonly in their everyday lives such as driving and household activities. An average adult American spends 101 minutes every day driving [186], making it a significant portion of their day. Household activities can also comprise a significant portion of the day in some individuals. These activities are particularly challenging to classify. They are predominantly upper body activities, and activities such as vacuuming/sweeping and washing dishes involve continuous transitions between standing and walking. There are efforts being made to recognize such activities recently; for example, researchers have presented a methodology to classify ADL inside a smart home using a range of different wearable and non-wearable sensor systems in [187]. Another study in [188] attempted to classify 13 household activities including vacuuming, sweeping and stretching, and reported 57% accuracy using inertial sensors and 72% using visual sensors.

An alternative approach is to use a footwear based system that encapsulates pressure sensors under the foot. We and others have shown that this approach classifies ADLs with a high degree of accuracy [4], [68]–[70], [77], [189]–[191]. Our group has shown [69] that a footwear system can result in very high accuracy (>99%) in classifying the major activities of daily living such as sitting, standing, walking, ascending stairs, descending stairs and cycling. However, whether this approach is more accurate than wrist-based approaches, for a broader set of ADL, has not previously been considered.

In this study we compared the accuracy of recognition of a broad set of ADL by the wrist-worn sensors, insole-based sensors (SmartStep) and the combination of these sensors, both in the laboratory and the community. In the laboratory study, participants performed different ADL under controlled environments. In the free-living part, the same participants wore the sensors during a normal day. The ActivPAL accelerometer (PAL Technologies Ltd, Glasgow, Scotland), which has been shown to provide highly accurate classification of sitting, standing and stepping activities [192], [193], was used as the criterion standard in the free-living experiments. We also evaluated the perceived comfort of each of these sensors using an online questionnaire.

6.2 Methods

6.2.1 Sensor System

6.2.1.1 SmartStep and Wrist Sensor

The SmartStep (Figure 6-1) is an insole-based sensor system designed in our laboratory [21], [72], [73], [76]. The electronics were assembled on a flexible FR4 printed circuit board providing connections for force sensitive resistor sensors (FSR402, Interlink Inc.) positioned at the heel, the 1st metatarsal head and the big toe. A rigid FR4 printed circuit board attached to the flexible substrate by epoxy contains a 3D accelerometer (ADXL 362, Analog Devices Inc.), a gyroscope (L3GD20, ST Micro Electronics), 512 Mb flash memory (MX66L51235F, Macronix Inc.), a BLE module (PAN1720, Panasonic Inc.), and a Qi charging circuit. The rigid FR4 and a 45mAh Lithium Polymer battery were encapsulated in epoxy resin under the arch of the foot, where forces during ambulation are minimal. Orthotic foam placed on top of the electronics provided cushioning. The same SmartStep electronics were also used in the wrist sensor (Figure 6-2). Gyroscope data from the insoles were not used in this study as the gyroscope had an average current consumption of 5 mA, and thus limited the time of operation to less than 5-6 hours. However, the wrist sensor hosted a much larger 350mAh battery, allowing to collect data from the gyroscope and other sensors for over 24 hours. All sensors were sampled at 50 Hz with 12-bit precision for pressure sensors and 16-bit precision for the accelerometer and gyroscope. The data were wirelessly delivered over a BLE connection in real time to a smartphone that stored the data for off-line processing [73].

6.2.1.2 Criterion Measure

The ActivPAL accelerometer (AP), a commercially available positional sensor module that is worn on the thigh (Figure 3), served as a criterion measure during the free-living study. The AP classifies an individual's activities into time periods spent sitting or lying down,

Figure 6-1. SmartStep insole monitor

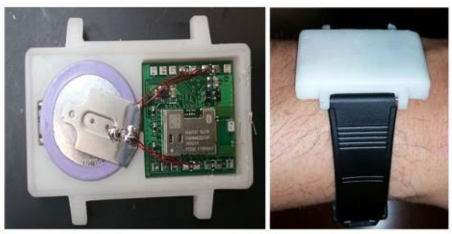

Figure 6-2. Wrist Sensor

Figure 6-3. activPAL

standing and stepping. Previous studies have shown the accuracy of AP to be more than 97% in controlled laboratory environments [192].

6.2.2 Study Population

15 healthy adults participated in the study (Table 6-1). Participants provided informed written consent prior to participation, and met the following inclusion/exclusion criteria.

Inclusion Criteria:

- Body mass index (BMI) 20-35.0 kg/m2
- Age 19-45 years
- No self-report of acute or chronic disease (diabetes, heart diseases, and joint problems in particular)
- Possessing valid driving license and car.

Exclusion Criteria

- Orthopedic, psychologic or neurologic impairments that prevent physical activity
- Need for orthotics
- For females: pregnant
- Acute or chronic disease: diabetes, heart diseases, and joint problems in particular

The study was approved by the University of Alabama institutional review board.

Table 6-1. Anthropometric characteristics of participants

	Male, n = 8	**Female, n = 7**
Age (years) (Mean +/- SD)	26.6 ± 3.4	23.3 ± 5
Height (m) (Mean +/- SD)	1.80 ± 0.05	1.65 ± 0.08
Weight (kg) (Mean +/- SD)	81.9 ± 17.2	66.7 ± 9.9
Weight (kg) range	65.3 – 118.8	54.4 – 85.3
BMI (kg/m^2) (Mean +/- SD)	25.2 ± 4.5	24.7 ± 5.4
Shoe size:	US M8 – M11	W6 – W9

6.2.3 Study Procedure

The participant's own shoes were instrumented with SmartStep sensors of appropriate sizes by replacing both of the original insoles with the SmartStep. The wrist sensor was worn on the wrist of the dominant hand like a wrist watch, and the AP was secured on the thigh of dominant leg utilizing adhesive tape.

During the laboratory part of the study, participants performed the activities listed in Table 6-2. Participants were allowed to rest at any time if needed. The duration of a lab visit was approximately 2 hours, resulting in approximately 1 hour of sensor data. A total of 16.7 hours of data were collected in the laboratory. For the free-living part of the study, participants were instructed to wear the devices from the time they arose (8 AM – 12 PM) until 9 PM. Sensor data were logged in the SmartStep and wrist sensor, and later transferred to the smartphone over BLE [73]. Participants were not limited in the range of activities performed during the free-living part.

Table 6-2. Activities in the protocol

Description of activities	Duration
Lie in comfortable way, on either of the sides or on the back, usage of smartphone allowed	5 min
Sit in comfortable way, with fidgeting or without fidgeting, usage of smartphone allowed	5 min
Stand in comfortable way, with fidgeting or without fidgeting, usage of smartphone allowed	5 min
Walking slow speed on a treadmill (self-chosen 1-2 mph)	5 min
Walking higher speed on a treadmill (self-chosen 3-4 mph)	5 min
Ascend stairs (2 trials)	1 min
Descend stairs (2 trials)	1 min
Ergometer cycling self-chosen rpm	5 min
Household activities: vacuuming, shelving items, washing dishes, sweeping the floor, 3 minutes per trial	15 min
Walking on the concrete floor with changing directions	5 min
Walking on grass with changing directions	5 min
Driving automatic shift car	10 min
Remove the shoes and wrist sensor and leave them in a self-chosen way	5 min

6.2.4 Data Processing

Data from the controlled laboratory part of the experiments were utilized in developing machine learning models for activity classification. The initial 4 seconds of data were discarded from each of the activities to obtain to ensure that steady state conditions were captured. No other preprocessing methodologies were used in the activity classification method.

Feature computation and activity classification were carried out in 4 second epochs to ensure accurate time resolution for transient activities. A total of 14,983 epochs were utilized in the leave-one-out cross validation, corresponding to ~1000 minutes of data. The MRMR algorithm (Max Relevance, Min Redundancy) [194] was used to derive the effective feature set from a group of features in each of the sensor system modalities. Many of the features that were chosen from MRMR selection were from sum of pressure sensor readings (*P_Sum(i)*) and resultant acceleration (*RA(i)*) for SmartSteps, and resultant acceleration and resultant rotation (*RG(i)*) from wrist sensor, which are defined as follows:

$$P_{SUM}(i) = PH(i) + P1M(i) + PHx(i) \qquad (1)$$

$$RA(i) = \sqrt{(AAP(i))^2 + (AML(i))^2 + (ASI(i))^2} \qquad (2)$$

$$RG(i) = \sqrt{(GX(i))^2 + (GY(i))^2 + (GZ(i))^2} \qquad (3)$$

where *PH* is heel pressure, *P1M,* is the first metatarsal head pressure, *PHx* is the hallux pressure, *AAP* is anterior–posterior acceleration, *AML* is medial–lateral acceleration, and *ASI* is superior–inferior acceleration, *GX, GY, GZ* are the rotation data from the gyroscope along the x,y,z axes respectively, i is the index of the time series data and i = {1,2…….*M*}, M being the length of the time series data. Table 6-3 describes the final set of features in all system modalities.

Multinomial Logistic Discrimination was used as a classifier for classifying the activities, so that the models could be eventually implemented on a smartphone for real time activity classification [6]. Three different classifiers were developed that dealt with each of the sensor configurations:

- SmartStep alone
- Wrist sensor alone
- SmartStep and Wrist sensor

A 15-fold leave-one-out cross validation methodology was used to develop the models for 13-class classifier, meaning that data from 14 participants were used in model development and tested on 15th one, and the process was carried out iteratively. To test how the lower and upper body sensor systems performed when all the household activities were considered as one group, a separate set of 10-class classifiers were developed, with all the household activities (activity number 9 in Table II) grouped together. Average accuracy in each case was determined utilizing the aggregate confusion matrix.

The AP was used in the laboratory study to determine the level of agreement with the other sensors in a controlled environment. Activities were grouped into sitting, standing, walking as shown in Table 6-4. The household activities were not considered for comparison as they were a mix of standing and walking activities. AP's accuracy was evaluated utilizing the manual labels for each of these activities.

Table 6-3. Final feature set

Sensor Modality	Feature Set
SmartStep alone	mean, standard deviation, number of mean crossings and entropy of sum of pressure and resultant acceleration, average maximum value of superior-inferior acceleration
Wrist sensor alone	mean, standard deviation, number of mean crossings and entropy of resultant acceleration and resultant rotation
Combined	mean, standard deviation, number of mean crossings and entropy of sum of pressure and resultant acceleration from SmartStep, average maximum value of superior-inferior acceleration from SmartStep, mean, standard deviation, number of mean crossings and entropy on resultant acceleration and resultant rotation from wrist

Leave-one-out machine learning models for activity recognition developed from the laboratory study were used as a predictive model on the sensor data collected from the SmartStep and the wrist sensor in the free-living study. These results are presented as percentage of time spent in predicted activities relative to the total time of wear. To compare the results of predicted activities from free-living with that of AP, activities were grouped as done in the laboratory study. Agreement between the two for each participant was established as follows:

$$Agreement = 1 - \left(\frac{\sum abs(TAP_K - TSEN_K)}{TTot}\right) \qquad (4)$$

where TAP_K is the time captured in activity K from AP, K = {sitting, standing, walking}, $TSEN_K$ is the time captured in activity K from sensor system (grouped labels for sensor system) and *TTot* is the total time captured as sitting, standing and walking. Average agreement across 15 participants is reported.

Table 6-4. Grouping of activities for comparison with AP

Description	**Sensor Label**	**AP Label**	**Grouped label**
laying down	1	0	0
sitting	2	0	0
standing	3	1	1
walking	4	2	2
driving	5	0	0
down stairs	6	2	2
up stairs	7	2	2
cycling	8	2	2

6.2.5 Online Questionnaire

To understand the perceived comfort of wearing AP, SmartStep and a wrist sensor in daily living, participants completed an online questionnaire (Table 6-5), developed on the basis of work by Knight and Baber [195]. Comfort was measured along three dimensions: emotion, perceived anxiety of wearing an activity monitor, and ease of the sensor attachment to and detachment from the body. The questionnaire designed for this study presented a set of 3 comfort statements for each of the sensors (total 9). Participants were asked to rank their perceptions on a linear scale of 1 to 10.

Table 6-5. Comfort statements created for each dimension

Dimension	**Statement**	**Scale**
Emotion	Perceived acceptability in terms of looks, while wearing the sensor	1 – least acceptable 10 – most acceptable
Anxiety	Perceived anxiety about being monitored while wearing the sensor	1 – least anxious 10 – most anxious
Attachment	Perceived ease in terms of attaching and detaching the sensor from the body	1 – very easy 10 – not so easy

6.3 Results

6.3.1 Controlled Laboratory Experiments

6.3.1.1 13 – Class Classification

Table 6-6 shows the confusion matrix for the SmartStep alone, with the overall classification accuracy of 81%. Table 6-7 shows the same for the wrist alone, with an accuracy of 69%. Table 6-8 shows the same for the combined SmartStep and Wrist sensors, with an accuracy of 89%.

Table 6-6. Confusion matrix for the SmartStep alone for 13- activity classification

	LD	***SI***	***ST***	***WA***	***DR***	***DS***	***US***	***CY***	***VA***	***SH***	***DW***	***SW***	***NW***
Laying down (LD)	0.93	0	0	0	0.04	0	0	0	0	0	0	0	0.13
Sitting (SI)	0	0.83	0.04	0	0.01	0	0	0	0	0.03	0.01	0	0.05
Standing (ST)	0	0.05	0.86	0	0	0	0.01	0	0.03	0.06	0.44	0.01	0
Walking (WA)	0	0	0	0.96	0.01	0.48	0.23	0	0.04	0.02	0	0.05	0
Driving (DR)	0.01	0	0	0	0.92	0.03	0	0.01	0	0	0	0	0
Downstairs(DS)	0	0	0	0.02	0	0.38	0.08	0	0	0	0	0	0
Upstairs (US)	0	0	0	0	0	0.11	0.67	0	0	0	0	0	0
Cycling (CY)	0	0	0	0	0	0	0	0.99	0	0	0	0	0
Vacuuming (VA)	0	0	0	0	0	0	0	0	0.23	0.12	0.02	0.3	0
Shelving items (SH)	0	0	0	0	0.01	0	0.02	0	0.24	0.39	0.04	0.25	0
Dish wash (DW)	0	0.01	0.09	0	0	0	0.01	0	0.05	0.13	0.48	0.03	0
Sweeping (SW)	0	0	0	0.01	0	0	0	0	0.41	0.25	0.01	0.35	0
Not wearing (NW)	0.06	0.11	0	0	0	0	0	0	0	0	0	0	0.82

overall accuracy = 81%

Table 6-7. Confusion matrix for the wrist sensor alone for 13- activity classification

	LD	***SI***	***ST***	***WA***	***DR***	***DS***	***US***	***CY***	***VA***	***SH***	***DW***	***SW***	***NW***
Laying down (LD)	0.69	0.17	0.01	0	0.04	0	0	0.01	0	0	0	0	0.07
Sitting (SI)	0.18	0.55	0.13	0	0.05	0	0	0.03	0	0	0.01	0	0
Standing (ST)	0.01	0.08	0.66	0	0.03	0	0.03	0.04	0.01	0.01	0.01	0.01	0.06
Walking (WA)	0	0	0	0.87	0.03	0.72	0.54	0.03	0.47	0.14	0.04	0.24	0.01
Driving (DR)	0.04	0.16	0.12	0.04	0.73	0	0.02	0.22	0.03	0.19	0.16	0.05	0
Downstairs(DS)	0	0	0	0	0	0.04	0.02	0	0	0	0.01	0.02	0
Upstairs (US)	0	0	0	0	0	0.1	0.3	0	0	0.01	0	0.01	0
Cycling (CY)	0.03	0.02	0.06	0.02	0.03	0	0	0.66	0.03	0	0.02	0	0
Vacuuming (VA)	0	0	0	0.01	0.01	0	0	0	0.28	0.06	0.03	0.06	0
Shelving items (SH)	0	0	0	0.03	0.03	0.03	0.02	0.01	0.05	0.4	0.09	0.09	0
Dish wash (DW)	0	0.01	0	0.01	0.03	0	0.01	0	0.03	0.13	0.6	0.02	0
Sweeping (SW)	0	0	0	0.01	0.01	0.11	0.07	0	0.11	0.06	0.03	0.51	0
Not wearing sensor(NW)	0.04	0.01	0	0	0.01	0	0	0	0	0	0	0	0.86

overall accuracy = 69%

Table 6-8. Confusion matrix for the combined SmartStep and wrist sensor for 13-activity classification

	LD	***SI***	***ST***	***WA***	***DR***	***DS***	***US***	***CY***	***VA***	***SH***	***DW***	***SW***	***NW***
Laying down (LD)	0.98	0	0	0	0.03	0.01	0	0	0	0	0	0	0.06
Sitting (SI)	0	0.88	0.05	0	0.01	0	0	0	0	0.02	0.01	0	0.01
Standing (ST)	0	0.05	0.92	0	0	0	0.01	0	0	0.01	0.06	0.01	0
Walking (WA)	0	0	0	0.96	0.01	0.4	0.18	0	0.03	0.01	0	0.02	0
Driving (DR)	0.01	0	0	0	0.92	0.05	0.01	0	0	0	0	0	0
Downstairs(DS)	0	0	0	0.01	0.01	0.41	0.11	0	0	0	0	0	0
Upstairs (US)	0	0	0	0	0	0.11	0.67	0	0	0	0	0	0
Cycling (CY)	0	0	0	0	0	0	0	0.99	0	0	0	0	0
Vacuuming (VA)	0	0	0.01	0.01	0	0	0.01	0	0.63	0.11	0.02	0.15	0
Shelving items (SH)	0	0	0	0.01	0.02	0	0	0	0.14	0.65	0.04	0.12	0
Dish wash (DW)	0	0	0.02	0	0	0	0	0	0.03	0.11	0.83	0.01	0
Sweeping (SW)	0	0	0	0	0.01	0.02	0.01	0	0.17	0.08	0.03	0.69	0
Not wearing sensors(NW)	0.02	0.06	0	0	0	0	0	0	0	0	0	0	0.94

overall accuracy = 89%

6.3.1.2 10 – Class Classification with Grouped Household Activities

When all household activities were grouped as one class, SmartStep's overall accuracy increased to 90%, with 87% accuracy for grouped household activities. The wrist sensor resulted in an accuracy of 73%, with 73% accuracy for grouped household activities. Combined SmartStep and wrist sensor resulted in an accuracy of 94%, with 96% accuracy for grouped household activities.

6.3.1.3 Accuracy of AP

Table 6-9 shows the confusion matrix for AP compared with manual labels from grouped activities (Table IV). The accuracy was found to be 98.7%. Computation as per equation 4 resulted in 97% agreement between AP and combination of SmartStep and wrist sensor system in controlled environment.

Table 6-9. Confusion matrix for AP

	Sitting	**Standing**	**Walking**
Sitting	1	0.06	0.01
Standing	0	0.91	0
Walking	0	0.03	0.99

6.3.1.5 Effect of Gyroscope in Wrist Sensor

When the gyroscope data from the wrist sensor were excluded from the model training phase in the 13 activity classifier of the combined sensor model, the accuracy of recognition for vacuuming was reduced from 63% to 57%, for shelving was reduced from 65% to 47%, sweeping was reduced from 69% to 54%, while for dish washing the accuracy was not affected (82% vs 83%). When the household activities were all grouped in 10-class classification, there was no difference in results with, or without, gyroscope data.

6.3.2 Free-living Tests Results

6.3.2.1 Activity Recognition from the Sensor System

Figure 6-4 shows a box plot of participants' various activities in free-living. The results are shown as a percent time spent in each activity as determined by the combined SmartStep and wrist sensor system, with respect to the total wear time (detailed in Table 6-10). Since the detected stair walking and cycling were less than 1% of the total time across subjects, they are not depicted in the Figure 4.

6.3.2.2 Agreement Between AP and The Sensor System

Table 6-11 shows the results of AP compared with SmartStep and wrist sensors from grouped activities, with an average agreement of 82.5%.

Table 6-10. Agreement between AP and sensor system in free living

Sub ID	Time of wear (min)	AP			SmartStep and Wrist Sensor		
		Sit	Stand	Walk	Sit	Stand	Walk
1	427	335.1	39.0	23.9	364.2	14.8	19
2	540	413.8	45.8	21.0	429.8	7.40	43.5
3	548	467.4	14.9	26	427	34.4	46.9
4	539	240.0	70.0	27.7	254.1	46.4	37.2
5	539	327.3	10	25.3	306.3	16.6	39.7
6	522	248.2	63.2	17.4	246.6	40.8	41.4
7	540	333.8	81.4	33.1	366.6	28	53.8
8	537	193.8	74.4	56	241.4	38.2	44.4
9	539	240.1	94.4	45.7	290.0	40.4	49.8
10	540	465.4	21.3	12.9	474.4	2.60	22.6
11	539	484.3	19.8	12.7	488.6	13.5	14.7
12	540	304.6	43.4	17.2	252.2	81.4	31.6
13	485	195.0	107.9	32.4	232.1	49.3	53.9
14	536	360.2	19.8	27.3	373.6	9.13	24.6
15	539	294.8	36.2	24.0	305.4	11.7	37.9

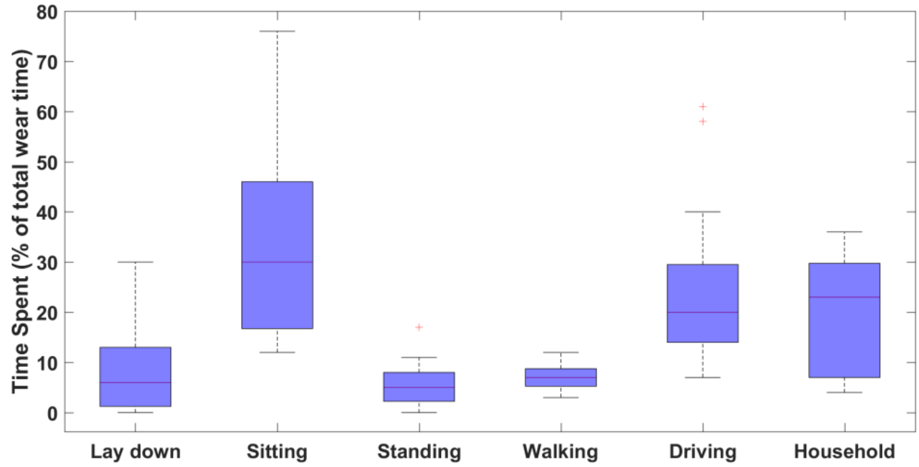

Figure 6-4. Time spent in each activity by participants in free living study. Ascend stairs, descend stairs and cycling were less than 1% of the total wear time across subjects, and are not depicted

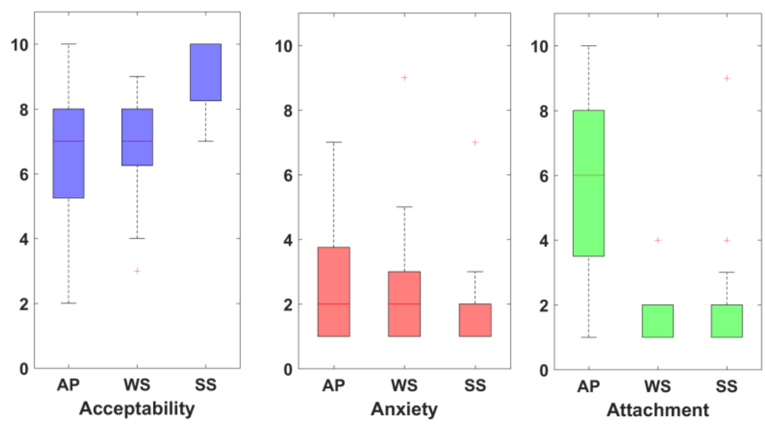

Figure 6-5. Results of questionnaire for perceived comfort, acceptability - higher score better, anxiety and attachment – lower score better. AP- ActivPAL, WS – Wrist sensor, SS- SmartStep

6.3.2.3 Results of the Online Questionnaire

The scores provided by the participants for each comfort dimension and for each of the sensors were averaged across all participants. The results are presented in Figure 6-5.

6.4 Discussion

The goal of this work was to compare the effectiveness of lower and upper body sensors, and their combination, in their abilities to monitor a broader set of activities of daily living (ADL). This was determined under controlled laboratory and free-living environments, while the participants wore a lower body sensor (SmartStep insoles) and a wrist-worn sensor. Machine learning models for automatic recognition of ADL in different sensor modalities were presented along with their corresponding results.

When the SmartStep system was considered alone for 13-activities classification (Table VI), the overall classification accuracy was 81%. SmartStep had very high accuracy rates for laying down (93%), walking (96%), driving (92%) and cycling (99%) activities. Sitting was misclassified with not wearing shoes 11% of the time, and standing was misclassified with dishwashing 9% of the time, which are reasonable given the similarities between those activities from the perspective of shoe insoles. Also, the SmartStep was prone to misclassify household activities, for example between vacuuming and sweeping, as shown in the results, which is also reasonable, given that these activities predominantly involve upper body movements. When these household activities were all grouped together in one class, the accuracy of SmartStep system alone was similar to the combined SmartStep and wrist sensor system (90% vs 94%). Given that the study consisted of participants with wide range of anthropometric characteristics (Table I), these results suggest that SmartStep can be utilized accurately to monitor ADL in many different populations.

When we considered the wrist sensor alone, the accuracy for 13 class classification was 69% (Table VII) while for 10 class classification (household activities grouped together) it was 73%. This result is better than previously reported [188], which had 57% accuracy for a wrist-worn sensor in classifying 13 activities. The improvement might be due to the presence of gyroscope in the wrist sensor. As the results suggest, presence of the gyroscope in the wrist sensor helped to improve the recognition of household activities (an increase of 10% across 4 household activities). This finding may help to decide a power consumption vs desired accuracy trade off, as the present day gyroscopes are not low power systems liming the battery life of the sensor. The inability to accurately discriminate laying down, sitting, and standing from the wrist sensor was expected, as evident from the other wrist-worn activity trackers [184], [185]. Walking and driving activities comparatively had higher classification rates, but could be misclassified with household activities. The wrist-worn device, is also not reliable for recognition of stair walking. Furthermore, even though household activities are predominantly upper body movements, the results show that, wrist sensor alone did not perform as well as the combined wrist and SmartStep system. As the results suggest, the SmartStep system outperformed the wrist sensor in classifying household activities when they are all grouped as one class (87% vs 73%).

When we considered a combination of lower and upper body worn sensors, the models were able to accurately classify activities such as driving, vacuuming, shelving items, cycling, washing vessels, walking on stairs and sweeping which are not addressed in traditional activity trackers. For the 13-activity classifier, cross validation accuracy using the SmartStep and the wrist sensor was ~90%. This is better than the 73% accuracy reported previously [188], which utilized visual sensors for classifying a similar set of activities. Another strength of this study is that, in an attempt to capture the realistic scenarios, the participants were asked to perform the activities in whichever way that's most comfortable to them. In terms of recognizing the driving activity, SmartStep alone did that with 92% accuracy, which did not improve when the wrist sensor was introduced. To the best of our knowledge, this is the first study where the driving activity was recognized by a footwear worn sensor.

The walking activities on the stairs had relatively less accuracies from the sensor system. One of the reasons for this might be the relatively smaller experiment times for these activities (>3 min for the rest of the activities, 30 s for the stairs activity), which could have affected the model training. This along with the fact that 20% of the stairs activity included walking on flat surface led to the stairs activity being mostly confused with walking.

Another encouraging result was the high accuracies of the sensor systems in recognizing period of not being worn (82% for SmartStep alone, 86% for wrist sensor alone, 94% for combined). This will prove useful when we utilize the sensors in longitudinal studies, as the time periods of sensor no wear can be automatically extracted from the sensor data. In contrast, AP for example, classifies the no wear periods as sitting/laying down or standing based on the orientation of the sensor module placed.

From the controlled laboratory experiments, AP's accuracy in classifying sitting, standing and walking was determined to be 98.7%, supporting previous works [192]. While this is impressive, the drawback is that many different activities such as cycling, walking stairs and others get grouped into the same group as walking; sitting is grouped with laying down; while physiologically they result in very different EE figures.

The free-living experiments demonstrated 82.5% agreement between our sensor system (SmartStep and wrist sensor) and the AP vs 97% in controlled environment. The sitting/laying down activities had better agreements (>94%). Since there was no direct observation for the free-living study, there was no way for us to validate the accuracies of AP vs our sensor system in free-living conditions. The important thing to consider is that while AP could recognize only 3 activities, the SmartStep alone can recognize up to 10. Recognition rate of household activities, due to their continuous transition nature, could not be included in the comparison between the sensors and the AP, and that's a limitation of the presented study.

In terms of perceived comfort, SmartStep had the highest score in terms of acceptability in looks and had the lowest score in anxiety of being monitored. Given that SmartStep is completely unobtrusive and is used like any other insole inside a shoe, this result was expected. The wrist sensor had the best score in terms of attachment, which can be explained due to the fact that it had a form factor of a wrist watch. As expected, AP had a lower score in terms of attachment and detachment, and comfort along the looks as the sensor was secured to the thigh using adhesive tape. However, the merit of the AP and wrist sensor is that they can be worn during the entire day (and night), while shoes are generally not worn during the entire day and night. Dealing with the missing data from wearable systems that are not worn will be an interesting topic for the future research.

6.5 Conclusion

In this work, we compared the accuracy of lower and upper body-worn sensors in classifying a broad set of activities of daily living (ADL). The SmartStep insole system (comprising of pressure sensors and accelerometer) was used as a lower body-worn sensor and a wrist sensor (comprising of accelerometer and gyroscope) was used as an upper body worn sensor. A leave-one-out cross validation of the data from the laboratory study resulted in 89% accuracy for the combined shoe system and wrist sensor, 81% for the shoe system alone, and 69% for the wrist sensor alone. In the laboratory study component, the agreement between AP and our sensor system was 97% and in the free-living it was 82.5%. Results suggest that a combined lower body and upper body sensor system can help better classify the ADL involving household activities better, but when the household activities are all grouped together, the SmartStep system alone can be sufficient for monitoring of ADL.

CHAPTER 7 ESTIMATION OF ENERGY EXPENDITURE ASSOCIATED WITH ACTIVITIES OF DAILY LIVING USING INSOLE BASED WEARABLE SYSTEM

The validation part of this study is not complete yet and the manuscript will be submitted after the study

Monitoring the daily energy expenditure associated with physical activities is important aspect of obesity management programs. This study introduces and validates an approach of utilizing insole-based wearable system for energy expenditure estimation. Two different branching methodologies were explored attempting to improve the estimation of energy expenditure by adding energy cost of activity transitions.

7.1 Introduction

Obesity has become an epidemic in the modern times with more than two-thirds of the adult population in the USA being overweight or obese [1], [169]. The modern sedentary lifestyle, resulting in a positive difference between energy intake and energy expenditure (EE) in daily living, has been recognized as a cause of obesity [168], [169]. Studies show that increasing the activity levels can help in obesity management programs [169]. Hence, objective and accurate monitoring of EE associated with activities of daily living (ADL) is an important aspect of obesity control [169].

Methodologies to monitor EE can be broadly classified into 4 categories: direct calorimetry, indirect calorimetry, doubly labeled water and wearable sensor approach. Direct calorimetry is performed by measuring the amount of heat produced by a person's body in a completely enclosed chamber [196]. In indirect calorimetry, the volume of oxygen (VO2) consumed during the breathing and production of carbon dioxide (VCO2) are measured to compute the EE [196]. The doubly-labeled water technique is performed by administering a dose of isotope-labeled hydrogen and oxygen water, and measuring the elimination rates of both isotopes during a specific amount of time [197]. Though these solutions are valid, direct calorimetry is confined to an enclosed chamber, indirect calorimetry is either performed in an enclosed chamber or requires people to wear face masks, while doubly labeled water experiments are expensive to conduct and labor intensive.

Many wearable solutions have been proposed to monitor ADL and to estimate the associated EE. The existing systems can be categorized in a number of different ways. The categorization may be based on the sensing elements used to estimate EE. Single-accelerometer-based devices have been widely explored for the purpose of EE estimation [81], [198]–[201]. Though widely used in research as well as commercial applications, accelerometer-based devices have limitations in recognizing activities such as cycling, walking on stairs and household work [185]. Many accelerometry devices perform poorly in differentiating static postures such as sitting vs standing, and these activities are grouped in the same class [184], [185], while metabolic costs of these two activities are different [202]. Some accelerometry based activity trackers are also prone to be recording false walking, during the periods of sitting or standing [203]. One of the strategies to overcome the limitation of single accelerometry-based devices has been to utilize multiple sensors, such as multiple accelerometers [204], or combining heart rate measurement along with accelerometry [205], [206]. There are also approaches that utilize heart rate alone to estimate EE [207].

Wearable systems for EE estimation can also be categorized based on the location of wear. Wrist worn sensors are very popular [55]; however, the existing research utilizing wrist worn sensors reported under-prediction of EE in light physical activities, and over-prediction of EE in vigorous activities [208]. Waist-worn sensors [209], [210] are popular in research; because these sensors are placed near the center of mass of the body, they tend to predict EE accurately for ambulatory activities. However, the waist-worn sensors perform poorly in populations with central obesity [183]. There are sensor systems that use chest straps [67], [211], ankle straps [212], along with those that are glued to the thigh [192].

The wearable systems can also be categorized based on the algorithms they use to estimate EE. One of the oldest methodologies to estimate EE is based on utilizing 'accelerometer counts' [198]. With the improvements in sensing and memory capabilities of wearable sensors, methodologies that utilize raw accelerometer data are prevalent today. There are clustering-based methodologies, which utilize the accelerometer data to cluster different activity types based on the EE cost of the activities being performed [213]. There are other methodologies that use the physical activity as a context in which EE is estimated, and EE of a given time period is evaluated based on the corresponding activity in that period (referred to as activity branched EE models) [6], [80], [214]. A pre-requisite of such activity branching methodology is accurate recognition of different postures and activities. Our previous work in the area have shown that footwear-based systems can get as high as 99% accuracy in classifying common ADL such as sitting, standing, walking, cycling and walking on stairs [69]. Under the branching methodologies, there are multi–context ensemble methodologies that have recently being explored [84] as well.

The human body has mass; lifting that mass (lying to standing for example) or accelerating that mass (sitting to walking for example) cost energy. Energy costs of such transition activities add to the steady state EE in the daily living. However, capturing and modeling such transitions is not well explored in research. There are studies that have transition-specific EE models between static activity (lying/sit/stand) to dynamic activity (walking) [215], but the transition between the static postures are ignored, as the ability of such systems to distinguish between static postures is limited. There is one recent study that aimed at computing sit-to-stand transition EE costs in individuals [202]. Although this study did not utilize any wearable sensor-based methods for EE estimation, the results suggested that EE among steady-state sitting, steady-state standing, and a sit-to-stand transition were all different.

In our previous work, we utilized pressure sensors in the footwear along with a shoe-mounted sensor hosting an accelerometer [6], [80]. This solution required a shoe clip-on, or required alteration of the shoes, limiting the usability; while being less socially acceptable. Our recent work in the area of footwear-based wearable technologies have resulted in the 'SmartStep' insole. SmartStep is a fully integrated wearable system [21], [72], [73], [76] (Figure 1), more discrete and socially acceptable than a shoe-mounted sensor.

One of the primary goals of the present work was to develop EE estimation models from the SmartStep insole, which has an embedded accelerometer and pressure sensors. Also, in the earlier research, we proposed a 4-branched EE models for the activities of sitting, standing, walking and cycling [80]. However, people perform many other activities in daily living such as household activities, lying down, walking on stairs and others. The second goal of this work was to explore if adding further branches would improve daily EE estimation. Our previous results suggested that the sensor system under-predicted the total EE by 4% [80]. This error might increase if the models were utilized in a whole-day EE estimation, compared to a few hours of lab visit. We hypothesized that failure to account for transition EE costs would result in significant under-prediction of EE in daily living. Hence, the third goal of this work was to test whether adding EE cost of activity transitions would improve the total error in the EE estimation. The fourth goal of this work was to validate the EE models in an experiment, independent from the one in which the models were developed (unlike leave-one-out validation methodologies utilized previously). In achieving these goals, the study included a human study in a controlled laboratory environment to develop EE estimation models from SmartStep and an independent study in a room calorimeter for validation of the EE models.

7.2 Methods

7.2.1 SmartStep Sensor System

A prototype of the SmartStep insole [21], [72], [73], [76] is shown in Figure 1. The SmartStep is built on a flexible FR4 printed circuit board and houses three force sensitive resistor sensors (FSR402, Interlink Inc) which are located at the heel, the 1st metatarsal head, and the big toe. A rigid printed circuit board integrating a 3D accelerometer (ADXL362, Analog Devices Inc.), 3D gyroscope (L3GD20, ST Micro Electronics), 512 Mb flash memory (MX66L51235F, Macronix Inc.), PAN1720 Bluetooth low energy (BLE) module (Panasonic Inc.) and wireless battery charging circuit is encapsulated in epoxy resin under the arch of the foot, where forces during ambulation are minimal. Orthotic foam provides the cushioning on top of the insole. The sensors are sampled at 50 Hz with 12-bit precision for pressure sensors and 16-bit precision for the accelerometer. SmartStep can be used in real-time data streaming mode or data logging mode based on the application needs [73]. The controlled laboratory part of this study utilized real time streaming and the chamber validation study utilized data logging feature.

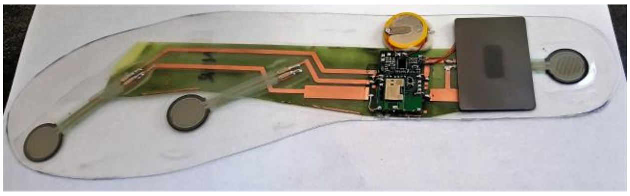

Figure 7-1. SmartStep Sensor System

7.2.2 Cosmed K4B2 Mask

A portable system for pulmonary gas exchange measurement (Cosmed K4B2 (CM), Cosmed Inc., Rome, Italy) [216], was used for indirect calorimetry in controlled experiments. EE was derived from the breath-by-breath data.

7.2.3 Participant Population

A total of 15 healthy adult participants, 8 males, and 7 females participated in the controlled study. Three adult participants, one male, and two females, participated in the chamber study. The participants signed an informed consent form, and the study was approved by the University of Alabama and the University of Colorado institutional review boards. Table 7-1 shows the participants' anthropometric characteristics.

7.2.4 Controlled Study Procedure

In the controlled study, participants were instructed prior to the study visit to wear comfortable shoes with removable insoles and come in exercise attire. The study required a single visit from each of the participant and the complete duration of the lab visit was approximately 2 hours. Original insoles from the participants' shoes were replaced by SmartStep insoles. CM was used to record the breath-by-breath EE under study protocol.

Table 7-1. Participants' anthropometric details

	Controlled Study		**Chamber Study**	
	Male, n=8	Female, n = 7	Male, n =1	Female, n = 2
Age (yrs.) (Mean ± SD)	26.6 ± 3.4	23.3 ± 5	63 ± 0	56 ± 9.9
Height (m) (Mean ± SD)	1.80 ± 0.05	1.65±0.08	1.57 ± 0	1.62 ± 0.07
Weight (kg) (Mean ± SD)	81.9 ± 17.2	66.7 ± 9.9	70.8 ± 0	63 ± 19.8
Weight (kg) range	65.3 – 118.8	54.4 – 85.3	70.8-70.8	48-76
BMI (kg/m2) (Mean ± SD)	25.2 ± 4.5	24.7 ± 5.4	22.9 ± 0	23.5±5.4
Shoe size:	US M8 – M11	W6 – W9	US M9	US M7 – M9

Table 7-2 describes the activities in the protocol. In an attempt to model the EE cost for transition activities, one-minute experiments which included transitions were designed. In these experiments, participants performed an activity for 30 seconds, transitioned to another activity, and performed that activity for 30 seconds, in line with previous research [202]. Figure 7-2 shows one of the participants performing some of the activities in the protocol.

Figure 7-2. One of the participants performing various activities

Table 7-2. Activities in the controlled study

Description	Duration
Lie in a comfortable way, on either side or on the back, usage of smartphone allowed	5 min
Sit comfortably, with fidgeting or without fidgeting, usage of smartphone allowed	5 min
Stand comfortably, with fidgeting or without fidgeting, usage of smartphone allowed, shifting weight from one leg to the other is allowed	5 min
Walking slow speed on a treadmill (self-chosen 1-2 mph)	5 min
Walking higher speed on a treadmill (self-chosen 3-4 mph)	5 min
Ascend stairs (2 trials)	1 min
Descend stairs (2 trials)	1 min
Ergometer cycling self-chosen rpm	5 min
Household activities: vacuuming, shelving items, sweeping the floor, 3 minutes per activity	15 min
Walking on a concrete floor with changing directions	5 min
Walking on grass with changing directions	5 min
Transition activities: lying-to-sitting, stand-to-sit, walk-to-sit, sit-to-lying down, standing-to lying down, walking-to-lying down, lying down-to-standing, sit to stand, walk to stand; all 1 min per trial, 2 trials per participant.	40 min

SmartSteps' and CM's clocks were synchronized prior to each participant's trial. Participants were allowed to rest at any time during the trial if needed. Data from the SmartSteps were collected for every activity in real time. A separate data sheet was maintained along with the time stamps for each of the activities, for the purpose of extracting the EE data from CM. A total of ~21 hours of data were collected in the laboratory study.

7.2.5 Chamber Study Procedure

The chamber study was conducted in a whole-room indirect calorimeter (type, mfg., location) [217]. The Participants stayed in the metabolic chamber for two 24-hour periods (two consecutive days or different days based on the participant's convenience).

As in the controlled study above, original insoles from the participants' shoes were replaced by SmartStep insoles. The room calorimeter recorded per minute EE. Out of two 24-hour periods of stay, one stay consisted of light household activities comprised of sweeping the floor, dusting, vacuuming, and cleaning the windows for 5 minutes each (a total of 20 minutes). The other stay consisted of moderate physical activities consisting of 30 minutes on a stationary bike, 30 minutes on a treadmill, and 20 minutes of light weight-lifting activities (shoulder press, dumbbell curls, bench step-ups, and push-ups). Participants started wearing the SmartSteps between 8 AM – 12 PM and wore them until 8 PM to 10 PM. Participants self-selected the intensity of the physical activity but were advised to work hard enough to sweat.

The data were logged in the SmartSteps during the time of wear [73]. During the night, the SmartSteps were placed on the Qi charging base station to recharge the SmartStep's battery. During the period of battery recharge, the logged data in the SmartSteps were transferred to the Android smartphone housed in the base station, which were later retrieved for offline processing. Three subjects underwent the chamber study. One of the subjects had a right extremity sensor failure during the experiments. Since both the insole's data are needed to accurately track the activity transitions, this participant's data were not included for validating the activity transition trials.

7.2.6 Activity Classification

Controlled laboratory experiments' data were utilized in developing EE models. The initial 4 seconds of data were discarded from each of the trials, to obtain the data in a steady-state of activities being performed. No other preprocessing methodologies were used in the classification of activities. Feature computation and activity classification were carried out in 4-second epochs. A total of 11227 epochs were utilized in the model training (corresponding to 748.5 minutes). A total of 96 features were computed as detailed in Table 7-3. Features were computed from individual sensor data and also from the sum of pressure sensor readings (PSum(i)), and resultant acceleration (RA(i)), defined as follows.

$$PSum(i) = PH(i) + P1M(i) + PHx(i) \quad (1)$$

$$RA(i) = \sqrt{(AAP(i))^2 + (AML(i))^2 + (ASI(i))^2} \quad (2)$$

MRMR algorithms (Max-Relevance, Min-Redundancy) [194] were used to derive the effective feature set. Multinomial logistic discrimination, which is a computationally lightweight classifier, was used for classifying the activities. From the set of activities, 8 steady state activities were derived: lying down, sitting, standing, walking, cycling, walking downstairs, walking upstairs and household activities. Walking activity included the slow walk and fast walk on the treadmill, walking on the concrete floor, and walking on the grass.

Table 7-3. Complete feature set

Feature Computed from SmartSteps	
Mean of ACC*, RA(i)	Entropy of ACC, RA(i)
Standard deviation of ACC, RA(i)	Entropy of PS, PSum(i)
Mean of PS*, PSum(i)	NOMC of ACC, RA(i)
Standard deviation of PS, PSum(i)	NOMC** of PS, PSum(i)
Median of ACC, RA(i)	Maximum value of ACC, RA(i)
Median of PS, PSum(i)	Maximum value of PS, PSum(i)

*ACC – 3 axis accelerometer signals, PS – 3 pressure sensor signals ** NOMC – Number of mean crossings

Vacuuming, sweeping and shelving items were all grouped as household activities. The grouping of household activities was carried out after verifying that the associated EE for each of these activities were not significantly different. Analysis of variance test on the energy costs of sweeping, vacuuming and shelving of the items across 15 subjects suggested that there were no significantly differences ($p>.05$) between the energy costs of these activities. A 15-fold leave-one-out cross-validation methodology was used to develop the models for 4-class classifier and 8-class classifier, meaning that data from 14 participants were used in the model development and tested on the 15th one, and the process was carried out iteratively. Average accuracy in each case was determined utilizing the aggregate confusion matrix.

7.2.7 Steady State EE Models

In our previous work on shoe-mounted sensors for EE estimation, we reported 4-branched models for EE estimation [21]. In this study, we tested whether adding further branches for other ADL would result in better performance. Hence, two separate sets of branching methodologies were developed: a 4-branched model and an 8-branched model. In the 4-branched model, there were branches for sitting, standing, walking and cycling; stair-walking and household activities were grouped into the walking branch as was done previously [21]. In the 8-branch model, there were separate branches for lying down, sitting, standing, walking, cycling, descending stairs, ascending stairs and household activities. The null hypothesis for the branching methodology was,

Ho: There would be no difference between performance of 4-branched and 8-branched models in EE estimation

Each of the branched models for EE estimation was trained using the same methodology. One-minute sensor data were used to derive the activity branch for that minute. A linear regression model for each of the activity branches was derived using ordinary least squares. Based on previous research [19], the following set of features were computed from 3 pressure sensors (PS) and 3-axis accelerometer (ACC): maximum value of the PS, number of median crossings of the PS and ACC, frequency of PS and ACC, standard deviation of the PS and ACC, and entropy of the PS and ACC. The features from the PS were combined by computing the medians of appropriate values: thus, the 3 maximum features for PS resulted in PSmax, 3 median crossing features resulted in PSmc, 3 frequency features resulted in PSfreq, 3 standard deviation and 3 entropy features resulted in PSstd and PSent, respectively. ACC features are denoted as Amc, Afreq, Astd and Aent where 'A' can be X, Y or Z, representing the 3-axis accelerometer signals. Anthropometric characteristics of weight, BMI, and age were also included as features.

To select the best predictors among the above set of features, a forward selection procedure was utilized with the following criteria: the best model had to have a high adjusted coefficient of determination, a low root-mean-squared error (RMSE) and a low value for the Akaike Information Criterion (AIC). Leave-one-out cross-validation was used, meaning that regression models were developed utilizing the feature set from 14 participants and the developed model was tested on the 15th. The accuracy of EE prediction from the 15th participant was assessed through comparison with the EE measurements from CM. The estimated EE was expressed in kcal/min. The following metrics were used to quantify the error in the prediction models:

Total error of prediction (signed), computed as the average total error of prediction in each activity branch for the subject being tested:

$$totERR = \sum_{i=1}^{N} \frac{totEE_i^{PRED} - totEE_i}{totEE_i} \qquad (3)$$

where, N is the number branches, $totEE_i$ is total EE measured by CM for branch 'i', and $totEE_i^{PRED}$ is the total EE predicted by a model for the same branch.

Per-minute RMSE: $RMSE = \sqrt{\frac{1}{T}\sum_{t=1}^{T}(EE_t - EE_t^{pred})^2}$ (4)

where, EE_t is the EE measured by CM for a given 1-minute interval; EE_t^{pred} is EE estimated by a model for the same 1-minute interval. Paired t-tests (two-tailed) were used to test the hypothesis posed earlier for the performance of branching methodology. Normality of the paired differences was tested utilizing the Matlab function available as used previously [218].

7.2.8 Transition-Specific EE Models

Our previous research showed that the shoe mounted sensors under-predicted total EE [80]. The hypothesis being tested in this study was, whether adding EE cost of activity transitions would improve the under-prediction. The null hypothesis for this was

H_o: Adding the transition EE cost does not improve the under-prediction in total EE.

The transitions activities were detected using the classification models described above. Transition-specific regression models were developed from the experiments that involved transitions between sitting, standing, walking and lying down. The transition EE cost was computed as follows:

$$EXY = AEY - SEY \qquad (5)$$

where, SEY is the steady state EE (kcal/min) for activity y, for a particular participant, AEY is the average EE (kcal/min) for activity y after a transition from activity x, EXY is the EE cost of the particular transition from x to y, for that participant. In terms of physics, these EE costs are the results of lifting or accelerating the body mass against the gravitational force; hence anthropometric details of the participants (height, weight, and BMI) were used to model the EE costs of transitions. Ordinary least squares regression models were developed as follows:

$$EXY \sim Intercept + a*Weight + b*BMI + c*Weight*BMI + d*height \qquad (6)$$

7.2.9 Validation of Models in Chamber Study

The activity classification and EE models built from the controlled experiments were tested on the data from the SmartStep in the chamber study. In both 4-branched and 8-branched cases, the models were tested based on total error and RMSE as defined in equations 3 and 4.

7.3 Results

7.3.1 Activity Classification Results

A total of 18 features were selected (Table 7-4), during the feature selection phase for activity classification. Table 7-5 shows the confusion matrix for the 4-class classification performed from the controlled laboratory experiments. Table 7-6 shows the confusion matrix for the 8-class classification. The weighted average accuracy for leave-one-out cross validation was 97% and 93.8% for 4-class and 8-class classifiers respectively.

Table 7-4. Final feature set

Final Features Set from SmartSteps for Activity Classification	
Mean of RA(i)	Entropy of RA(i)
Standard deviation RA(i)	Entropy of PSum(i)
Mean of PSum(i)	NOMC of RA(i)
Standard deviation of PSum(i)	NOMC of PSum(i)
Maximum value of superior-inferior acceleration	

Table 7-5. Confusion matrix for 4-class classification

	Sitting	**Standing**	**Walking**	**Cycling**
Sitting	0.95	0.04	0	0.01
Standing	0.05	0.91	0.02	0
Walking	0	0.06	0.98	0
Cycling	0	0	0	0.99

Overall accuracy = 97%

Table 7-6. Confusion matrix for 8-class classification

	LD	SI	ST	WA	US	DS	CY	HD
LD*	1	0	0	0	0	0	0	0
SI	0	0.94	0.02	0	0	0	0	0.01
ST	0	0.05	0.92	0	0	0.01	0	0.05
WA	0	0	0	0.96	0.48	0.22	0	0.02
US	0	0	0	0.02	0.4	0.1	0	0
DS	0	0	0	0	0.12	0.65	0	0
CY	0	0	0	0	0	0	1	0
HD	0	0	0.06	0.02	0	0.02	0	0.92

*LD – Lying down, SI – Sitting, ST – Standing, WA – walking, US – upstairs, DS – downstairs, CY – cycling, HD – Household, Overall accuracy = 94%

7.3.2 Steady State EE Models

The comparison of the accuracy of EE estimation by branched EE models is shown in Table 7-7. Table 7-8 shows the best set of predictors and equations for the 8-branched EE prediction model. Figure 7-3 shows the correlations and the Bland-Altman plot, from all 1-min measurements, from all 15 participants, for the 8-branch EE prediction model. These figures demonstrate the high correlation of predicted EE to actual EE (R^2=0.89) and negligibly small average bias (0.013 kcal/min) in estimating steady state EE. The paired t-test on the total error in the EE estimation of each of the 15 participants, between the 4-branched model and 8-branched model resulted in p = 0.016 (normality of the paired differences were ensured). At α = 0.05, the null hypothesis was rejected in favor of the alternative, suggesting that the

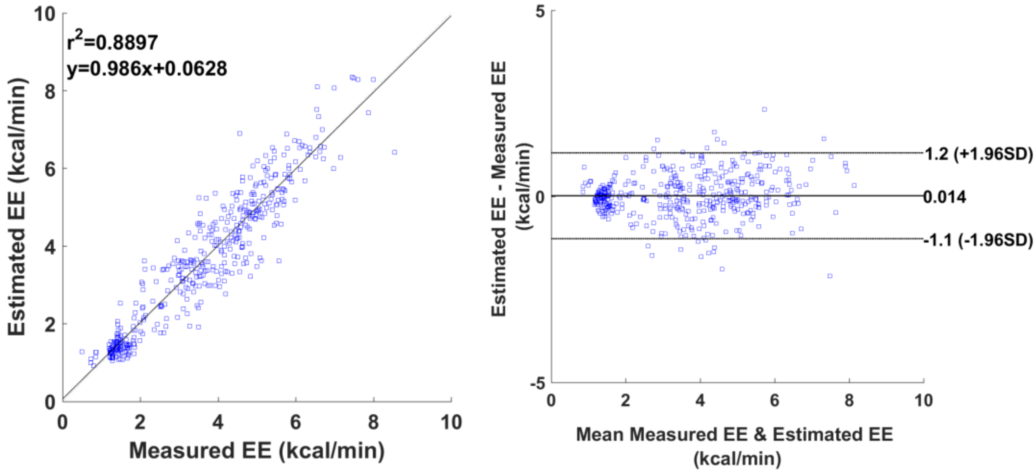

Figure 7-3. Correlation and Bland-Altman plots for the 8-branch EE models

performance of 4-branched and 8-branched models was statistically different. The average total error was ~2% less in the 8-branched model.

Table 7-7. Comparison of EE prediction performance

Branching Method	Total Error, %	RMSE, kcal/min	Limits of agreement, kcal/min	Goodness of Fit (R^2) and average bias
4-branched model	**7.0**	Sit model: 0.26 Stand model: 0.38 Walk/Jog model: 0.81 Cycle model: 0.55 **Weighted average: 0.67**	(-0.52,0.53) (-0.80,0.73) (-1.62,1.65) (-1.13,1.11)	$R^2 = 83\%$ Bias (kcal/min) = -0.004
8 branched model	**5.25**	Lying down model: 0.35 Sit model: 0.26 Stand model: 0.38 Walk/Jog model: 0.62 Cycle model: 0.55 Downstairs model: 0.79 Upstairs model: 0.74 Household model: 0.86 **Weighted average: 0.58**	(-0.76,0.64) (-0.52,0.53) (-0.80,0.73) (-1.27,1.23) (-1.13,1.11) (-1.66,1.64) (-1.48,1.57) (-1.75,1.73)	$R^2 = 89\%$ Bias (kcal/min) = 0.013

Table 7-8. EE regression equations

Branch	EE regression equations (kcal/min)
Lying down	$EE = 0.52 + 0.02*Weight+0.029*BMI + 0.003*Xstd$
Sit	$EE = -1.03 +7.5*10^{-3} *Weight +0.56*BMI +0.03*Ystd + 123*PSstd$
Stand	$EE = -1.66+1.8\cdot 10^{-2}*Weight - 0.45* BMI + 0.02*Xstd + 0.38*10^{-3}*PSmax - 1.24*Ymc+19.55* PSstd$
Walk/ Jog	$EE = -4.89 + 6.1*10^{-2}*Weight - 1.83 *BMI + 0.68* Yent +2.8* 10^{-3}* PSmax - 1.84* Xmc + 4.99* Zmc - 2.47* Ymc +0.4 *Xent$
Descend	$EE = 12.48 +0.01*Weight - 1.97*BMI+14.99* Zmc - 4.3*10^{-3}* Ystd - 1.7* Yent$
Ascend	$EE = 0.83 +0.05*Weight - 2.62\cdot BMI+0.01*Zstd++13.59 *Zmc + 1.04* Zent - 4.9* Ymc$
Household	$EE = 4.5 +6.5*10-3 *Weight - 0.12*BMI+0.03* Ystd - 0.73* Xent - + 2.2*10^{-3}* PSfreq - 0.03*Zstd - 1.71* Zmc$
Cycle	$EE = -3.15 + 3.7*10-2*Weight -0.3*BMI + 136.9* Zmc + 5.06* PSstd$

7.3.3 Transition Models

The goodness of fit (R^2) and the RMSE for each of the transition cases are shown in Table 7-9. R^2 values ranged from 49% to 74% across different models and RMSE ranged from 0.16 kcal/min to 0.5 kcal/min.

Table 7-9. Transition specific model results

	Sit to Lie	Stand to Lie	Walk to Lie	Lie to Sit	Stand to Sit	Walk to Sit	Lie to Stand	Sit to Stand	Walk to Stand
R2	74%	56%	53%	79%	49%	71%	57%	54%	72%
RMSE Kcal/min	0.48	0.41	0.50	0.2	0.36	0.28	0.24	0.29	0.16

7.3.4 Chamber Study Results

Table 7-10 shows the results of the 4-branched and the 8-branched models when applied to the chamber data. The 8-branched model resulted in 6% total error (weighted average), and 0.81 kcal/min average RMSE. The 4-branched model, when tested in the chamber data, resulted in 9% total error, 0.9 kcal/min average RMSE.

Transition-specific EE costs were added on the 8 branch model. For subject ID 1, transition models were not applied, since only one insole was operating. Table 7-11 shows the results.

Table 7-10. Results of chamber validation study for steady state models

SubID	Total minutes of sensor wear	Total EE by Chamber (kcal)	Total Predicted EE 8 branched model (kcal)	RMSE 8 branched model (kcal/min)	Total error 8 branched model (%)	Total Predicted EE 4 branched model (kcal)	RMSE 4 branched model (kcal/min)	Total error 4 branched model %
1 LID*	521	691	749	0.54	7.5	719	0.55	4
1 MID*	390	679	728	1.16	5.2	671	1.03	-1.1
2 LID	664	1093	1045	0.92	-4.4	1525	1.21	39
2 MID	344	741	650	0.8	-12	857	1	15.6
3 LID	599	1155	994	0.57	-13.8	1093	0.71	-5.4
3 MID	599	1266	1056	0.98	-16	1229	1.1	-2.9

*LID – Light intensity activities day, MID – Moderate intensity activities day

Table 7-11. Chamber results for the 8-branched models with transitions

Sub ID	Total minutes of sensor wear	Total Error before introducing transitions %	Total Error after introducing transitions %
2 LID	664	-4.4	4.3
2 MID	344	-12	-8.6
3 LID	599	-13.8	-6.3
3 MID	599	-16	-3.9
Weighted average		-11.28	-5.05

7.4 Discussion

The goal of this work was to develop energy expenditure (EE) estimation models utilizing a novel insole based wearable system – SmartStep, which is socially acceptable footwear-based solution and would need no alteration of the shoes. A controlled laboratory study was used in developing two sets of activity-branched EE models, transition specific models, and an indirect calorimeter chamber study to validate these models.

The 4-branched activity classification model resulted in 97% accuracy while recognizing sitting, standing, walking and cycling. The 8-branched model resulted in accuracy of 94% while recognizing a broader set of activities of daily living such as lying down, sitting, standing, walking, cycling, ascend stairs, descend stairs and household activities. Walking on the stairs had relatively lower accuracies in the 8-branched model, and one of the reasons might be the shorter walking episodes on stairs in experiments. Also, 20% of the ascend/descend stairs activity included walking on flat surface, resulting in these activities being mostly confused with walking.

The study explored whether adding more than 4 branches to EE model would help in EE estimation. The 8-branched EE model resulted in a goodness of fit (R2) value of 89% in the model development phase with 5.25% total error in the EE estimation and 0.59 kcal/min average RMSE. The 4-branched model resulted in a goodness of fit (R2) value of 83% in the model development phase with 7% total error in the EE estimation and 0.67 kcal/min average RMSE. Results from the model development phase suggested that increasing the number of branches from 4 to 8 slightly improved the goodness of fit, reducing the total error and RMSE.

When tested on the chamber data, the 8-branched model resulted in 6% total error and 0.83 kcal/min average RMSE. The 4-branched model resulted in 9% total error and 0.9 kcal/min average RMSE. Preliminary data from the chamber study indicated that the performance of 8-branched model is superior compared to the 4-branch models. We expect to distinguish the models better with more chamber study data, which is in progress.

Another hypothesis that was tested was that the under-prediction in total estimated EE could be improved by adding the EE cost of activity transitions. The goodness of fit (R2) values for the transition specific models varied from 49% to 75%. When the transition costs were added to the total EE in the chamber study, results show that there is 6% improvement in the total error of EE. The chamber study is still under way, and initial results are presented here.

This was the first study wherein the SmartStep's capabilities in the estimation of EE were studied, and the results suggest that the SmartStep can be used to accurately monitor EE in daily living. One of the strengths of this study was that, even though the models were validated in a completely independent environment, with different protocol and population, the results of the validation study were comparable to the results obtained during model development phase (6% total error vs 5.25% total error for the 8-branched model). Larger studies are underway to validate the device in completely free-living conditions.

What was not explored in this study is what is the optimum number of branches for estimating daily EE. We compared 4-branched vs 8-branched models; however, a more systematic study, specifically targeted at finding the optimum number of branches is needed to answer this question. This future study can test a gradual increase in branches from 2 to N (N being the upper limit after which there will be no improvement in performance of EE models) to determine the optimum number of branching needed. The choice of sensor technologies, sensor placement and processing algorithms may all play an important role in determining the answer for the above question. Another limitation of the current work is that the study did not consider the speed of transition to model the EE cost for the activity transitions. Inclusion of the speed of transition information can potentially help in better explaining the EE cost of transitions.

7.5 Conclusion

Accurate monitoring of EE is an important aspect of obesity management programs. In this study we validated the insole based wearable system SmartStep for estimation of EE in daily living. The study used two branching methodologies (4-branched and 8-branched) for capturing daily EE along with models for the transition between the steady state activities. As part of a broader validation study, the derived EE models were tested on the participants staying in an indirect calorimetry chamber. The results of both the controlled study and the chamber study suggested that the 8-branched model performed better in EE estimation than the 4-branched model. The addition of the transition-specific EE models improved the total prediction error in the chamber study. The results suggested that SmartStep can be used to accurately monitor EE of the wearers in their daily living.

CHAPTER 8 CONCLUSION AND FUTURE WORK

8.1 Conclusion

This dissertation contributes to the work on the design, development and validation of insole based wearable system for physical activity monitoring and energy expenditure estimation. The main contribution of this work is the development and testing of the hardware, firmware, and Android application for a wearable insole monitor; as well as development of methodologies for signal processing and machine learning algorithms for objective, automatic and accurate monitoring of gait, physical activity and energy expenditure. These contributions were achieved through a series of studies that investigated various aspects of sensor-based monitoring of gait and physical activity.

The dissertation starts with a review of the research in the footwear-based wearable systems. Different application scenarios such as gait monitoring, plantar pressure measurement, activity and energy expenditure monitoring, biofeedback applications and energy harvesting from the footwear were explored from the academia as well as commercial space.

A low power, fully integrated insole based wearable system – SmartStep was designed and developed. The dissertation describes design approaches that helped in making the SmartStep low power, user friendly and fully wireless. Compared with the earlier versions of the footwear based devices the power consumption of SmartStep was lower than 2 orders of magnitude.

For the gait and activity monitoring applications utilizing SmartStep, it's necessary to interface multiple SmartSteps (and potentially some other sensors, like a wrist sensor, as described in Chapter 6) to a smartphone. However, the existing research lacks systematic methodologies for the same. The dissertation details a novel methodology in interfacing many Bluetooth low energy based sensors to an Android smartphone. The implementation is first of its kind in the research, and explores the trade-offs between power consumption, throughput, CPU loading and number of sensors and BLE transmission frequencies. The implementation aims at developing a reliable connection establishment, information exchange and disconnection processes between the sensors and the smartphone in a multi sensor environment. The presented results can help a designer to choose an optimum combination of the number of sensors and transmission frequency based on the application requirements.

As an example application of the footwear based devices for activity and gait monitoring, a human subject study was conducted on healthy and children with cerebral palsy. This work utilized the SmartShoes, and the main contribution was in the development of new signal processing algorithms that dealt with the orthotics effect on the pressure sensor signals in CP children. Highly accurate activity classification results were obtained in this study in classifying a child's sitting, standing and walking. The gait parameter estimation accurately compared with the measures by the criterion measurement device.

SmartStep was validated as an activity monitoring device in monitoring a broad set of activities of daily living such as lying down, sitting, standing, walking, cycling, driving and household activities. The human subject study was conducted in the laboratory and free living conditions to test the accuracy of the SmartStep in recognizing these activities. The major contribution of the work is in comparison of lower and upper-body worn sensors, and their combination, in their ability to recognize these activities. The free living part of the study validated the machine learning models developed from the data in controlled environments. High accuracy of 90% was obtained for ADL monitoring with SmartStep.

SmartStep was also validated for its usage as a monitor for daily energy expenditure. Two sets of activity branched energy expenditure models were developed from the controlled environments. The EE models were validated on the data from a room calorimeter. The results of the chamber study suggested that while root mean square error among the 8-branched and 4-branched were comparable (0.8 kcal/min vs 0.9 kcal/min), total error was 3% less in the 8-branched model (6% vs 9%). The results also suggested that adding of transition specific models helped to reduce the total error in energy expenditure estimation.

8.2 Future Work

The SmartStep can be mainly used for 3 varieties of applications in its current form: gait monitoring, posture and activity recognition, and energy expenditure estimation. The hardware, firmware and the Android applications were developed from the perspective of running longitudinal studies in free living. In the future, there are innumerable opportunities to run larger human subject studies for gait, activity and energy expenditure monitoring of people who are disabled, post stroke subjects or obesity patients.

From the perspective of posture and activity recognition, and energy expenditure estimation, this dissertation validated the SmartStep under controlled conditions or short free living conditions, spanning across a day. However, a larger free living study with participants being tested under multiple other sensors and also doubly labeled water is under way, validating the approach in a weeklong free living conditions.

From the perspective of using SmartStep for gait parameter monitoring, the presented version of the device includes a gyroscope, which was not present in the older generations of

SmartShoe. Gyroscope, when utilized along with accelerometer, can help compute the spatial gait parameters such as step length and stride length. Also, the SmartStep insole can be embedded with a tactile feedback device, to provide biofeedback in real time to the disabled subjects to improve their gait patterns.

Going forward, an internet of things (IoT) framework can be built to provide the users a real time feedback from their physicians on their progress in their daily life. The infrastructure between SmartStep and Smartphone is already described in the dissertation, and building an internet interface between the physician's computer and SmartStep needs to be addressed in the future. The signal processing of the sensor data coming from SmartStep was handled offline in this dissertation. However, for real time feedback, all the processing need to be moved to Smartphone or IoT framework. All the machine learning algorithms detailed in this dissertation are developed with the foreseeable future requirements. Also, the processing of the sensor data (at least in parts), can be performed on the sensor itself to bring the power cost of wireless transmission lower, while increasing the battery life. Further work is needed to develop these new methodologies, for improving the value of SmartStep as a reliable wearable system for longitudinal usage.

As chapter 2 of the dissertation detailed, affective computing is a new area for wearable systems. Different footwear based applications under affective computing can be explored for SmartStep in future. Also, advancement in energy harvesting technologies can help either extend the battery life of SmartStep, or completely eliminate the battery subsystem from the SmartStep. That can be one of the interesting future directions where footwear based wearable systems, along with SmartStep, can take to take the technology forward.

REFERENCES

[1] "Adult Obesity Facts | Data | Adult | Obesity | DNPAO | CDC." [Online]. Available: http://www.cdc.gov/obesity/data/adult.html. [Accessed: 02-Dec-2015].

[2] "Stroke Facts | cdc.gov." [Online]. Available: http://www.cdc.gov/stroke/facts.htm. [Accessed: 07-May-2015].

[3] "Aging Statistics." [Online]. Available: http://www.aoa.acl.gov/Aging_Statistics/index.aspx. [Accessed: 07-May-2015].

[4] G. D. Fulk and E. Sazonov, "Using sensors to measure activity in people with stroke," *Top Stroke Rehabil*, vol. 18, no. 6, pp. 746–757, Dec. 2011.

[5] P. Lopez-Meyer, G. D. Fulk, and E. S. Sazonov, "Automatic detection of temporal gait parameters in poststroke individuals," *IEEE Trans Inf Technol Biomed*, vol. 15, no. 4, pp. 594–601, Jul. 2011.

[6] E. Sazonov, N. Hegde, R. C. Browning, E. L. Melanson, and N. A. Sazonova, "Posture and activity recognition and energy expenditure estimation in a wearable platform," *IEEE J Biomed Health Inform*, vol. 19, no. 4, pp. 1339–1346, Jul. 2015.

[7] J. Perry, *Gait Analysis: Normal and Pathological Function*. SLACK, 1992.

[8] S. Crea, M. Donati, S. M. M. De Rossi, C. M. Oddo, and N. Vitiello, "A Wireless Flexible Sensorized Insole for Gait Analysis," *Sensors*, vol. 14, no. 1, pp. 1073–1093, Jan. 2014.

[9] "GAITRite Systems - Portable Gait Analysis." [Online]. Available: http://www.gaitrite.com/. [Accessed: 02-Dec-2015].

[10] "Full Body Gait Analysis with Kinect - Microsoft Research." [Online]. Available: https://www.microsoft.com/en-us/research/publication/full-body-gait-analysis-with-kinect/. [Accessed: 07-Jul-2016].

[11] "Accuracy of the Microsoft Kinect^{TM} for measuring gait parameters during treadmill walking - Gait & Posture." [Online]. Available: http://www.gaitposture.com/article/S0966-6362(15)00462-2/abstract. [Accessed: 07-Jul-2016].

[12] S. J. M. Bamberg, A. Y. Benbasat, D. M. Scarborough, D. E. Krebs, and J. A. Paradiso, "Gait analysis using a shoe-integrated wireless sensor system," *IEEE Trans Inf Technol Biomed*, vol. 12, no. 4, pp. 413–423, Jul. 2008.

[13] M. Chen, B. Huang, and Y. Xu, “Intelligent shoes for abnormal gait detection,” in *IEEE International Conference on Robotics and Automation, 2008. ICRA 2008*, 2008, pp. 2019–2024.

[14] B. Mariani, M. C. Jiménez, F. J. G. Vingerhoets, and K. Aminian, “On-shoe wearable sensors for gait and turning assessment of patients with Parkinson’s disease,” *IEEE Trans Biomed Eng*, vol. 60, no. 1, pp. 155–158, Jan. 2013.

[15] A. Nsenga Leunkeu, T. Lelard, R. J. Shephard, P.-L. Doutrellot, and S. Ahmaidi, “Gait cycle and plantar pressure distribution in children with cerebral palsy: clinically useful outcome measures for a management and rehabilitation,” *NeuroRehabilitation*, vol. 35, no. 4, pp. 657–663, 2014.

[16] B. Huang, M. Chen, P. Huang, and Y. Xu, “Gait Modeling for Human Identification,” in *2007 IEEE International Conference on Robotics and Automation*, 2007, pp. 4833–4838.

[17] K. Kong and M. Tomizuka, “A Gait Monitoring System Based on Air Pressure Sensors Embedded in a Shoe,” *IEEE/ASME Transactions on Mechatronics*, vol. 14, no. 3, pp. 358–370, Jun. 2009.

[18] T. Liu, Y. Inoue, and K. Shibata, “A wearable ground reaction force sensor system and its application to the measurement of extrinsic gait variability,” *Sensors (Basel)*, vol. 10, no. 11, pp. 10240–10255, 2010.

[19] I. González, J. Fontecha, R. Hervás, and J. Bravo, “An Ambulatory System for Gait Monitoring Based on Wireless Sensorized Insoles,” *Sensors*, vol. 15, no. 7, pp. 16589–16613, Jul. 2015.

[20] Y. Wu, W. Xu, J. J. Liu, M.-C. Huang, S. Luan, and Y. Lee, “An Energy-Efficient Adaptive Sensing Framework for Gait Monitoring Using Smart Insole,” *IEEE Sensors Journal*, vol. 15, no. 4, pp. 2335–2343, Apr. 2015.

[21] N. Hegde and E. Sazonov, “SmartStep: A Fully Integrated, Low-Power Insole Monitor,” *Electronics*, vol. 3, no. 2, pp. 381–397, Jun. 2014.

[22] “WIISEL.” [Online]. Available: http://www.wiisel.eu/. [Accessed: 15-Jul-2015].

[23] A. Ferrari, P. Ginis, M. Hardegger, F. Casamassima, L. Rocchi, and L. Chiari, “A Mobile Kalman-Filter Based Solution for the Real-Time Estimation of Spatio-Temporal Gait Parameters,” *IEEE Transactions on Neural Systems and Rehabilitation Engineering*, vol. 24, no. 7, pp. 764–773, Jul. 2016.

[24] J. Klucken *et al.*, “Unbiased and Mobile Gait Analysis Detects Motor Impairment in Parkinson’s Disease,” *PLoS One*, vol. 8, no. 2, Feb. 2013.

[25] J. Barth *et al.*, “Stride Segmentation during Free Walk Movements Using Multi-Dimensional Subsequence Dynamic Time Warping on Inertial Sensor Data,” *Sensors*, vol. 15, no. 3, pp. 6419–6440, Mar. 2015.

[26] L. Wafai, A. Zayegh, J. Woulfe, S. M. Aziz, and R. Begg, “Identification of Foot Pathologies Based on Plantar Pressure Asymmetry,” *Sensors*, vol. 15, no. 8, pp. 20392–20408, Aug. 2015.

[27] M. J. Mueller *et al.*, “Forefoot structural predictors of plantar pressures during walking in people with diabetes and peripheral neuropathy,” *J Biomech*, vol. 36, no. 7, pp. 1009–1017, Jul. 2003.

[28] “Plantar Pressure Assessment | Physical Therapy Journal.” [Online]. Available: http://ptjournal.apta.org/content/80/4/399. [Accessed: 07-Jul-2016].

[29] E. S. Sazonov, T. Bumpus, S. Zeigler, and S. Marocco, “Classification of plantar pressure and heel acceleration patterns using neural networks,” in *2005 IEEE International Joint Conference on Neural Networks, 2005. IJCNN ’05. Proceedings*, 2005, vol. 5, pp. 3007–3010 vol. 5.

[30] S. J. Morris and J. A. Paradiso, “Shoe-integrated sensor system for wireless gait analysis and real-time feedback,” in *Engineering in Medicine and Biology, 2002. 24th Annual Conference and the Annual Fall Meeting of the Biomedical Engineering Society EMBS/BMES Conference, 2002. Proceedings of the Second Joint*, 2002, vol. 3, pp. 2468–2469 vol.3.

[31] R. M. Queen, B. B. Haynes, W. M. Hardaker, and W. E. Garrett, “Forefoot loading during 3 athletic tasks,” *Am J Sports Med*, vol. 35, no. 4, pp. 630–636, Apr. 2007.

[32] A. Gioftsidou, P. Malliou, G. Pafis, A. Beneka, G. Godolias, and C. N. Maganaris, “The effects of soccer training and timing of balance training on balance ability,” *Eur. J. Appl. Physiol.*, vol. 96, no. 6, pp. 659–664, Apr. 2006.

[33] M. J. Mueller, “Application of plantar pressure assessment in footwear and insert design,” *J Orthop Sports Phys Ther*, vol. 29, no. 12, pp. 747–755, Dec. 1999.

[34] R. Begg and M. Palaniswami, *Computational Intelligence for Movement Sciences: Neural Networks and Other Emerging Techniques*. Idea Group Inc (IGI), 2006.

[35] “zebris Medical GmbH Gait analysis.” [Online]. Available: http://www.zebris.de/english/medizin/medizin-ganganalyse.php#fdm. [Accessed: 01-Dec-2015].

[36] “F-Scan System,” *Tekscan*. [Online]. Available: https://www.tekscan.com/products-solutions/systems/f-scan-system. [Accessed: 01-Dec-2015].

[37] A. M. Tan, F. K. Fuss, Y. Weizman, Y. Woudstra, and O. Troynikov, “Design of Low Cost Smart Insole for Real Time Measurement of Plantar Pressure,” *Procedia Technology*, vol. 20, pp. 117–122, 2015.

[38] L. Shu, T. Hua, Y. Wang, Q. Qiao Li, D. D. Feng, and X. Tao, “In-shoe plantar pressure measurement and analysis system based on fabric pressure sensing array,” *IEEE Trans Inf Technol Biomed*, vol. 14, no. 3, pp. 767–775, May 2010.

[39] M. Saito *et al.*, “An in-shoe device to measure plantar pressure during daily human activity,” *Medical Engineering and Physics*, vol. 33, no. 5, pp. 638–645, Jun. 2011.

[40] “pedar.” [Online]. Available: http://www.novel.de/novelcontent/pedar. [Accessed: 01-Dec-2015].

[41] “SurroSense Rx,” *Orpyx Medical Technologies*. [Online]. Available: http://orpyx.com/pages/surrosense-rx. [Accessed: 04-Dec-2015].

[42] A. Coda and D. Santos, “Repeatability and Reproducibility of the F-Scan System in Healthy Children,” *Elyns Publishing Group*, vol. J Orth Rhe Sp Med 1(1): 104., 2015.

[43] Z. P. Luo, L. J. Berglund, and K. N. An, “Validation of F-Scan pressure sensor system: a technical note,” *J Rehabil Res Dev*, vol. 35, no. 2, pp. 186–191, Jun. 1998.

[44] H. Hamzah, N. A. A. Osman, and N. Hasnan, “Comparing Manufacturer’s Point Calibration and Modified Calibration Setup for F-Scan Insole Sensor System: A Preliminary Assessment,” in *4th Kuala Lumpur International Conference on Biomedical Engineering 2008*, D. N. A. A. Osman, D. F. Ibrahim, D. W. A. B. W. Abas, H. S. A. Rahman, and D. H.-N. Ting, Eds. Springer Berlin Heidelberg, 2008, pp. 424–427.

[45] P. M. Quesada, G. S. Rash, and N. Jarboe, “Assessment of pedar and F-Scan revisited,” *Clin Biomech (Bristol, Avon)*, vol. 12, no. 3, p. S15, Apr. 1997.

[46] C. Giacomozzi, “Appropriateness of plantar pressure measurement devices: A comparative technical assessment,” *Gait & Posture*, vol. 32, no. 1, pp. 141–144, May 2010.

[47] A. B. Putti, G. P. Arnold, L. A. Cochrane, and R. J. Abboud, “Normal pressure values and repeatability of the Emed ST4 system,” *Gait Posture*, vol. 27, no. 3, pp. 501–505, Apr. 2008.

[48] R. Ferber, T. Webber, B. Everett, and M. Groenland, “Validation of plantar pressure measurements for a novel in-shoe plantar sensory replacement unit,” *J Diabetes Sci Technol*, vol. 7, no. 5, pp. 1167–1175, Sep. 2013.

[49] T. Liu, Y. Inoue, and K. Shibata, “A wearable force plate system for the continuous measurement of triaxial ground reaction force in biomechanical applications,” *Measurement Science and Technology*, vol. 21, p. 085804, Aug. 2010.

[50] J. O. Hill, H. R. Wyatt, G. W. Reed, and J. C. Peters, “Obesity and the environment: where do we go from here?,” *Science*, vol. 299, no. 5608, pp. 853–855, Feb. 2003.

[51] J. A. Levine *et al.*, “Interindividual variation in posture allocation: possible role in human obesity,” *Science*, vol. 307, no. 5709, pp. 584–586, Jan. 2005.

[52] “S Health -Fitness Diet Tracker - Android Apps on Google Play.” [Online]. Available: https://play.google.com/store/apps/details?id=com.sec.android.app.shealth&hl=en. [Accessed: 02-Dec-2015].

[53] “iOS 9 - Health,” *Apple*. [Online]. Available: http://www.apple.com/ios/health/. [Accessed: 02-Dec-2015].

[54] “Apple Watch,” *Apple*. [Online]. Available: http://www.apple.com/watch/. [Accessed: 02-Dec-2015].

[55] “Fitbit Official Site for Activity Trackers & More.” [Online]. Available: https://www.fitbit.com/. [Accessed: 02-Dec-2015].

[56] “LG G Watch R | powered by android wear.” [Online]. Available: http://www.lg.com/global/gwatch/index.html#main. [Accessed: 02-Dec-2015].

[57] G. Uslu and S. Baydere, “RAM: Real Time Activity Monitoring with feature extractive training,” *Expert Systems with Applications*, vol. 42, no. 21, pp. 8052–8063, Nov. 2015.

[58] M.-È. Riou, F. Rioux, G. Lamothe, and É. Doucet, “Validation and Reliability of a Classification Method to Measure the Time Spent Performing Different Activities,” *PLoS ONE*, vol. 10, no. 6, p. e0128299, Jun. 2015.

[59] S. González, J. Sedano, J. R. Villar, E. Corchado, Á. Herrero, and B. Baruque, “Features and models for human activity recognition,” *Neurocomputing*, vol. 167, pp. 52–60, Nov. 2015.

[60] D. T. Gerd Krassnig, “User-friendly system for recognition of activities with an accelerometer.,” pp. 1–8, 2010.

[61] A. C. F. C. M J Mathie, “Detection of daily physical activities using a triaxial accelerometer,” *Medical & biological engineering & computing*, vol. 41, no. 3, pp. 296–301, 2003.

[62] B. G. C. M J Mathie, “Classification of basic daily movements using a triaxial accelerometer. Med Biol Eng Comput,” *Medical & biological engineering & computing*, vol. 42, no. 5, pp. 679–87, 2004.

[63] M. R. N. D. M. Karantonis, “Implementation of a Real-Time Human Movement Classifier Using a Triaxial Accelerometer for Ambulatory Monitoring,” *Information Technology in Biomedicine, IEEE Transactions on*, vol. 10, no. 1, pp. 156–167, 2006.

[64] N. D. Nishkam Ravi, “Activity Recognition from Accelerometer Data.,” *AAAI*, vol. 3, pp. 1541–1546, 2005.

[65] T. Ferguson, A. V. Rowlands, T. Olds, and C. Maher, “The validity of consumer-level, activity monitors in healthy adults worn in free-living conditions: a cross-sectional study,” *International Journal of Behavioral Nutrition and Physical Activity*, vol. 12, no. 1, p. 42, Mar. 2015.

[66] J.-M. Lee, Y. Kim, and G. J. Welk, “Validity of consumer-based physical activity monitors,” *Med Sci Sports Exerc*, vol. 46, no. 9, pp. 1840–1848, Sep. 2014.

[67] D. K. Spierer, M. Hagins, A. Rundle, and E. Pappas, “A comparison of energy expenditure estimates from the Actiheart and Actical physical activity monitors during low intensity activities, walking, and jogging,” *Eur. J. Appl. Physiol.*, vol. 111, no. 4, pp. 659–667, Apr. 2011.

[68] E. S. Sazonov, G. Fulk, J. Hill, Y. Schutz, and R. Browning, “Monitoring of posture allocations and activities by a shoe-based wearable sensor,” *IEEE Trans Biomed Eng*, vol. 58, no. 4, pp. 983–990, Apr. 2011.

[69] W. Tang and E. S. Sazonov, “Highly Accurate Recognition of Human Postures and Activities Through Classification With Rejection,” *IEEE Journal of Biomedical and Health Informatics*, vol. 18, no. 1, pp. 309–315, Jan. 2014.

[70] T. Zhang, G. D. Fulk, W. Tang, and E. S. Sazonov, “Using decision trees to measure activities in people with stroke,” in *2013 35th Annual International Conference of the IEEE Engineering in Medicine and Biology Society (EMBC)*, 2013, pp. 6337–6340.

[71] T. Zhang, J. Lu, G. Uswatte, E. Taub, and E. S. Sazonov, “Measuring gait symmetry in children with cerebral palsy using the SmartShoe,” in *2014 IEEE Healthcare Innovation Conference (HIC)*, 2014, pp. 48–51.

[72] E. S. Sazonov, N. Hegde, and W. Tang, “Development of SmartStep: an insole-based physical activity monitor,” *Conf Proc IEEE Eng Med Biol Soc*, vol. 2013, pp. 7209–7212, 2013.

[73] Nagaraj Hegde and Edward Sazonov, “SmartStep 2.0 – A completely wireless, versatile insole monitoring system,” in *2015 IEEE International Conference on Bioinformatics and Biomedicine (BIBM)*, 2015, pp. 746–749.

[74] B. Chen, X. Wang, Y. Huang, K. Wei, and Q. Wang, “A foot-wearable interface for locomotion mode recognition based on discrete contact force distribution,” *Mechatronics*.

[75] F. Kawsar, M. K. Hasan, R. Love, and S. I. Ahamed, “A Novel Activity Detection System Using Plantar Pressure Sensors and Smartphone,” in *Computer Software and Applications Conference (COMPSAC), 2015 IEEE 39th Annual*, 2015, vol. 1, pp. 44–49.

[76] N. Hegde, E. S. Sazonov, and E. Melanson, “Development of A Real Time Activity Monitoring Android Application Utilizing SmartStep,” in *2016 38th Annual International Conference of the IEEE Engineering in Medicine and Biology Society (EMBC)*, 2016.

[77] G. D. Fulk, S. R. Edgar, R. Bierwirth, P. Hart, P. Lopez-Meyer, and E. Sazonov, “Identifying activity levels and steps of people with stroke using a novel shoe-based sensor,” *J Neurol Phys Ther*, vol. 36, no. 2, pp. 100–107, Jun. 2012.

[78] U. Maurer, A. Smailagic, D. P. Siewiorek, and M. Deisher, “Activity recognition and monitoring using multiple sensors on different body positions,” in *International Workshop on Wearable and Implantable Body Sensor Networks (BSN’06)*, 2006, p. 4 pp.-116.

[79] S. R. Edgar, G. D. Fulk, and E. S. Sazonov, “Recognition of household and athletic activities using SmartShoe,” *Conf Proc IEEE Eng Med Biol Soc*, vol. 2012, pp. 6382–6385, 2012.

[80] N. Sazonova, R. C. Browning, and E. Sazonov, “Accurate prediction of energy expenditure using a shoe-based activity monitor,” *Med Sci Sports Exerc*, vol. 43, no. 7, pp. 1312–1321, Jul. 2011.

[81] K. L. Dannecker, N. A. Sazonova, E. L. Melanson, E. S. Sazonov, and R. C. Browning, “A comparison of energy expenditure estimation of several physical activity monitors,” *Med Sci Sports Exerc*, vol. 45, no. 11, pp. 2105–2112, Nov. 2013.

[82] “Lechal: http://lechal.com/insoles.html.” [Online]. Available: http://lechal.com/insoles.html. [Accessed: 03-Dec-2015].

[83] “Smart Shoe: https://us.vibram.com/article-smart-shoe.html,” *Vibram US*. [Online]. Available: https://us.vibram.com/article-smart-shoe.html. [Accessed: 03-Dec-2015].

[84] H. Gjoreski, B. Kaluža, M. Gams, R. Milić, and M. Luštrek, “Context-based ensemble method for human energy expenditure estimation,” *Applied Soft Computing*, vol. 37, pp. 960–970, Dec. 2015.

[85] E. V. Villanueva, “The validity of self-reported weight in US adults: a population based cross-sectional study,” *BMC Public Health*, vol. 1, no. 1, p. 11, Nov. 2001.

[86] N. A. Sazonova, R. Browning, and E. S. Sazonov, “Prediction of Bodyweight and Energy Expenditure Using Point Pressure and Foot Acceleration Measurements,” *Open Biomed Eng J*, vol. 5, pp. 110–115, Dec. 2011.

[87] P. Hellstrom, M. Folke, and M. Ekström, “Wearable Weight Estimation System,” *Procedia Computer Science*, vol. 64, pp. 146–152, 2015.

[88] I.-H. Khoo, P. Marayong, V. Krishnan, M. N. Balagtas, and O. Rojas, “Design of a biofeedback device for gait rehabilitation in post-stroke patients,” in *2015 IEEE 58th International Midwest Symposium on Circuits and Systems (MWSCAS)*, 2015, pp. 1–4.

[89] N. Hegde, G. D. Fulk, and E. S. Sazonov, “Development of the RT-GAIT, a Real-Time feedback device to improve Gait of individuals with stroke,” in *2015 37th Annual International Conference of the IEEE Engineering in Medicine and Biology Society (EMBC)*, 2015, pp. 5724–5727.

[90] L. Yang, P. S. Dyer, R. J. Carson, J. B. Webster, K. Bo Foreman, and S. J. M. Bamberg, “Utilization of a lower extremity ambulatory feedback system to reduce gait asymmetry in transtibial amputation gait,” *Gait Posture*, vol. 36, no. 3, pp. 631–634, Jul. 2012.

[91] L. Donovan, M. A. Feger, J. M. Hart, S. Saliba, J. Park, and J. Hertel, “Effects of an auditory biofeedback device on plantar pressure in patients with chronic ankle instability,” *Gait & Posture*, vol. 44, pp. 29–36, Feb. 2016.

[92] “NIHSeniorHealth: Falls and Older Adults - Causes and Risk Factors.” [Online]. Available: http://nihseniorhealth.gov/falls/causesandriskfactors/01.html. [Accessed: 02-Dec-2015].

[93] M. Schwenk, K. Hauer, T. Zieschang, S. Englert, J. Mohler, and B. Najafi, “Sensor-derived physical activity parameters can predict future falls in people with dementia,” *Gerontology*, vol. 60, no. 6, pp. 483–492, 2014.

[94] C. Doukas and I. Maglogiannis, “Advanced patient or elder fall detection based on movement and sound data,” in *Second International Conference on Pervasive Computing Technologies for Healthcare, 2008. PervasiveHealth 2008*, 2008, pp. 103–107.

[95] J. C. Ayena, L. D. Chapwouo T, M. J.-D. Otis, and B. A. J. Menelas, “An efficient home-based risk of falling assessment test based on Smartphone and instrumented insole,” in *2015 IEEE International Symposium on Medical Measurements and Applications (MeMeA)*, 2015, pp. 416–421.

[96] S. Y. Sim *et al.*, “Fall detection algorithm for the elderly using acceleration sensors on the shoes,” in *2011 Annual International Conference of the IEEE Engineering in Medicine and Biology Society, EMBC*, 2011, pp. 4935–4938.

[97] A. J. A. Majumder, I. Zerin, M. Uddin, S. I. Ahamed, and R. O. Smith, “smartPrediction: A Real-time Smartphone-based Fall Risk Prediction and Prevention System,” in *Proceedings of the 2013 Research in Adaptive and Convergent Systems*, New York, NY, USA, 2013, pp. 434–439.

[98] “Documents | WIISEL.” [Online]. Available: http://www.wiisel.eu/?q=content/documents. [Accessed: 20-Jun-2016].

[99] M. J.-D. Otis and B. J. Menelas, “Toward an augmented shoe for preventing falls related to physical conditions of the soil,” in *2012 IEEE International Conference on Systems, Man, and Cybernetics (SMC)*, 2012, pp. 3281–3285.

[100] M. Schirmer, J. Hartmann, S. Bertel, and F. Echtler, “Shoe Me the Way: A Shoe-Based Tactile Interface for Eyes-Free Urban Navigation,” in *Proceedings of the 17th International Conference on Human-Computer Interaction with Mobile Devices and Services*, New York, NY, USA, 2015, pp. 327–336.

[101] O. Bebek *et al.*, “Personal Navigation via High-Resolution Gait-Corrected Inertial Measurement Units,” *IEEE Transactions on Instrumentation and Measurement*, vol. 59, no. 11, pp. 3018–3027, Nov. 2010.

[102] N. Castaneda and S. Lamy-Perbal, “An improved shoe-mounted inertial navigation system,” in *2010 International Conference on Indoor Positioning and Indoor Navigation (IPIN)*, 2010, pp. 1–6.

[103] E. Foxlin, “Pedestrian tracking with shoe-mounted inertial sensors,” *IEEE Computer Graphics and Applications*, vol. 25, no. 6, pp. 38–46, Nov. 2005.

[104] N. S. Shenck and J. A. Paradiso, “Energy scavenging with shoe-mounted piezoelectrics,” *IEEE Micro*, vol. 21, no. 3, pp. 30–42, May 2001.

[105] G. Orecchini, M. M. Tentzeris, L. Yang, and L. Roselli, “#x201C;Smart Shoe #x201D;: An autonomous inkjet-printed RFID system scavenging walking energy,” in *2011 IEEE International Symposium on Antennas and Propagation (APSURSI)*, 2011, pp. 1417–1420.

[106] J. Zhao and Z. You, “A shoe-embedded piezoelectric energy harvester for wearable sensors,” *Sensors (Basel)*, vol. 14, no. 7, pp. 12497–12510, 2014.

[107] J. Kymissis, C. Kendall, J. Paradiso, and N. Gershenfeld, “Parasitic power harvesting in shoes,” in *Second International Symposium on Wearable Computers, 1998. Digest of Papers*, 1998, pp. 132–139.

[108] R. Meier, N. Kelly, O. Almog, and P. Chiang, “A piezoelectric energy-harvesting shoe system for podiatric sensing,” in *2014 36th Annual International Conference of the IEEE Engineering in Medicine and Biology Society (EMBC)*, 2014, pp. 622–625.

[109] “Internet of things,” *Wikipedia, the free encyclopedia*. 25-Jul-2016.

[110] “The rise and fall of the smart shoe – and why they could be on the way back: http://www.wareable.com/running/smart-shoes-875,” *Wareable*. [Online]. Available: http://www.wareable.com/running/smart-shoes-875. [Accessed: 05-Dec-2015].

[111] “MIT Media Lab: Affective Computing Group.” [Online]. Available: http://affect.media.mit.edu/projects.php. [Accessed: 26-Jul-2016].

[112] "ShiftWear: Customize your kicks." [Online]. Available: https://www.indiegogo.com/projects/shiftwear-customize-your-kicks/#/story. [Accessed: 05-Dec-2015].

[113] R. Wagner and A. Ganz, "PAGAS: Portable and accurate gait analysis system," in *2012 Annual International Conference of the IEEE Engineering in Medicine and Biology Society (EMBC)*, 2012, pp. 280–283.

[114] P. Lopez-Meyer, G. D. Fulk, and E. S. Sazonov, "Automatic Detection of Temporal Gait Parameters in Poststroke Individuals," *IEEE Trans Inf Technol Biomed*, vol. 15, no. 4, pp. 594–601, Jul. 2011.

[115] B. Mariani, M. C. Jiménez, F. J. G. Vingerhoets, and K. Aminian, "On-Shoe Wearable Sensors for Gait and Turning Assessment of Patients With Parkinson's Disease," *IEEE Transactions on Biomedical Engineering*, vol. 60, no. 1, pp. 155–158, Jan. 2013.

[116] I. P. I. Pappas, T. Keller, S. Mangold, M. R. Popovic, V. Dietz, and M. Morari, "A reliable gyroscope-based gait-phase detection sensor embedded in a shoe insole," *IEEE Sensors Journal*, vol. 4, no. 2, pp. 268–274, Apr. 2004.

[117] T. Liu, Y. Inoue, and K. Shibata, "Development of a wearable sensor system for quantitative gait analysis," *Measurement*, vol. 42, no. 7, pp. 978–988, Aug. 2009.

[118] W. Tao, T. Liu, R. Zheng, and H. Feng, "Gait Analysis Using Wearable Sensors," *Sensors (Basel)*, vol. 12, no. 2, pp. 2255–2283, Feb. 2012.

[119] "FF-1 - Wireless Flexible Force Sensor System." [Online]. Available: http://www.insenco-j.com/Flexible_Pressure_Sensor.htm. [Accessed: 18-May-2014].

[120] L. Shu, T. Hua, Y. Wang, Q. Li, D. D. Feng, and X. Tao, "In-Shoe Plantar Pressure Measurement and Analysis System Based on Fabric Pressure Sensing Array," *IEEE Transactions on Information Technology in Biomedicine*, vol. 14, no. 3, pp. 767–775, May 2010.

[121] P. H. Veltink, C. Liedtke, E. Droog, and H. van der Kooij, "Ambulatory measurement of ground reaction forces," *IEEE Transactions on Neural Systems and Rehabilitation Engineering*, vol. 13, no. 3, pp. 423–427, Sep. 2005.

[122] H. M. Schepers, E. H. F. Van Asseldonk, J. H. Buurke, and P. H. Veltink, "Ambulatory Estimation of Center of Mass Displacement During Walking," *IEEE Transactions on Biomedical Engineering*, vol. 56, no. 4, pp. 1189–1195, Apr. 2009.

[123] C. Zhou, J. Downey, D. Stancil, and T. Mukherjee, "A Low-Power Shoe-Embedded Radar for Aiding Pedestrian Inertial Navigation," *IEEE Transactions on Microwave Theory and Techniques*, vol. 58, no. 10, pp. 2521–2528, Oct. 2010.

[124] E. Foxlin, "Pedestrian tracking with shoe-mounted inertial sensors," *IEEE Computer Graphics and Applications*, vol. 25, no. 6, pp. 38–46, Nov. 2005.

[125] K. N. Winfree, I. Pretzer-Aboff, D. Hilgart, R. Aggarwal, M. Behari, and S. Agrawal, "An untethered shoe with vibratory feedback for improving gait of Parkinson's Patients: The PDShoe," in *2012 Annual International Conference of the IEEE Engineering in Medicine and Biology Society (EMBC)*, 2012, pp. 1202–1205.

[126] C. B. Redd and S. J. M. Bamberg, "A Wireless Sensory Feedback Device for Real-Time Gait Feedback and Training," *IEEE/ASME Transactions on Mechatronics*, vol. 17, no. 3, pp. 425–433, Jun. 2012.

[127] C. Mancinelli *et al.*, "A novel sensorized shoe system to classify gait severity in children with cerebral palsy," in *2012 Annual International Conference of the IEEE Engineering in Medicine and Biology Society (EMBC)*, 2012, pp. 5010–5013.

[128] E. S. Sazonov, G. Fulk, J. Hill, Y. Schutz, and R. Browning, "Monitoring of Posture Allocations and Activities by a Shoe-Based Wearable Sensor," *Biomedical Engineering, IEEE Transactions on*, vol. 58, no. 4, pp. 983–990, 2011.

[129] N. Sazonova, R. Browning, and E. Sazonov, "Accurate Prediction of Energy Expenditure Using a Shoe-Based Activity Monitor," *Medicine & Science in Sports & Exercise*, vol. 43, no. 7, pp. 1312–21, Jul. 2011.

[130] "DigiBarn Weird Stuff: Puma RS Computer Tennis Shoes (pedometer, 1980s)." [Online]. Available: http://www.digibarn.com/collections/weirdstuff/computer-tennis-shoes/. [Accessed: 20-Feb-2014].

[131] "Adidas 1 - Wikipedia, the free encyclopedia." [Online]. Available: http://en.wikipedia.org/wiki/Adidas_1. [Accessed: 20-Feb-2014].

[132] "Nike LunarGlide+ 4," *Nike.com*. [Online]. Available: http://www.nike.com/us/en_us/c/running/nike-running-lunarglide-plus. [Accessed: 20-Feb-2014].

[133] S. Edgar, T. Swyka, G. Fulk, and E. S. Sazonov, "Wearable shoe-based device for rehabilitation of stroke patients," *Conf Proc IEEE Eng Med Biol Soc*, vol. 2010, pp. 3772–3775, 2010.

[134] "TI BLE Stack," *Bluetooth low energy software stack and tools*. [Online]. Available: http://www.ti.com/tool/ble-stack.

[135] "ADXL346," *Ultralow Power Digital Accelerometer*. [Online]. Available: http://www.analog.com/static/imported-files/data_sheets/ADXL346.pdf.

[136] "Android BLE," *Bluetooth Low Energy*. [Online]. Available: http://developer.android.com/guide/topics/connectivity/bluetooth-le.html.

[137] "Measuring Bluetooth® Low Energy Power Consumption." [Online]. Available: http://www.ti.com/lit/an/swra347a/swra347a.pdf.

[138] "Vanadium rechargeable lithium batteries(VL series) | Lithium Batteries | Batteries & Energy Products | Industrial Devices | Panasonic Global." [Online]. Available: http://industrial.panasonic.com/www-cgi/jvcr13pz.cgi?E+BA+3+AAA4008+VL3032+7+WW. [Accessed: 29-May-2014].

[139] "CC2541 TPS62730EM Reference Design." [Online]. Available: http://www.ti.com/tool/cc2541-tps62730em-rd.

[140] "ADXL 362." [Online]. Available: http://www.analog.com/static/imported-files/data_sheets/ADXL362.pdf.

[141] "Home | Bluetooth Technology Special Interest Group." [Online]. Available: https://www.bluetooth.org/en-us. [Accessed: 14-Apr-2015].

[142] A. Darwish and A. E. Hassanien, "Wearable and Implantable Wireless Sensor Network Solutions for Healthcare Monitoring," *Sensors (Basel)*, vol. 11, no. 6, pp. 5561–5595, May 2011.

[143] P. Schonle, P. Bunjaku, S. Fateh, and Q. Huang, "Modular multi-sensor platform for portable and wireless medical instrumentation," in *2014 IEEE Biomedical Circuits and Systems Conference (BioCAS)*, 2014, pp. 165–168.

[144] D. Brunelli, E. Farella, L. Rocchi, M. Dozza, L. Chiari, and L. Benini, "Bio-feedback system for rehabilitation based on a wireless body area network," in *Fourth Annual IEEE International Conference on Pervasive Computing and Communications Workshops, 2006. PerCom Workshops 2006*, 2006, p. 5 pp.-531.

[145] A. Johansson, W. Shen, and Y. Xu, "An ANT Based Wireless Body Sensor Biofeedback Network for Medical E-Health Care," in *2011 7th International Conference on Wireless Communications, Networking and Mobile Computing (WiCOM)*, 2011, pp. 1–5.

[146] B. Najafi, A. Vaziri, and A.-R. Boloori, "Ambulatory system for measuring and monitoring physical activity and risk of falling and for automatic fall detection," US9005141 B1, 14-Apr-2015.

[147] Y. Hao and R. Foster, "Wireless body sensor networks for health-monitoring applications," *Physiol Meas*, vol. 29, no. 11, pp. R27-56, Nov. 2008.

[148] H. Baldus, K. Klabunde, and G. Müsch, "Reliable Set-Up of Medical Body-Sensor Networks," in *Wireless Sensor Networks*, H. Karl, A. Wolisz, and A. Willig, Eds. Springer Berlin Heidelberg, 2004, pp. 353–363.

[149] C. Gomez, J. Oller, and J. Paradells, “Overview and Evaluation of Bluetooth Low Energy: An Emerging Low-Power Wireless Technology,” *Sensors (Basel)*, vol. 12, no. 9, pp. 11734–11753, Aug. 2012.

[150] “Git at Google.” [Online]. Available: https://android.googlesource.com/platform/external/bluetooth/bluedroid/+/8dc42c603f5571047878640705eee18fa5396f11%5E%21/. [Accessed: 10-Dec-2015].

[151] *Trepn Profiler*. Qualcomm Innovation Center, Inc., 2015.

[152] “Specification | Adopted Documents | Bluetooth Technology Special Interest Group.” [Online]. Available: https://www.bluetooth.org/en-us/specification/adopted-specifications. [Accessed: 16-Dec-2015].

[153] “Cerebral Palsy Information Page: National Institute of Neurological Disorders and Stroke (NINDS).” [Online]. Available: http://www.ninds.nih.gov/disorders/cerebral_palsy/cerebral_palsy.htm. [Accessed: 20-Mar-2016].

[154] T. M. O’Shea, “Diagnosis, Treatment, and Prevention of Cerebral Palsy in Near-Term/Term Infants,” *Clin Obstet Gynecol*, vol. 51, no. 4, pp. 816–828, Dec. 2008.

[155] T. S. Park and J. H. Owen, “Surgical Management of Spastic Diplegia in Cerebral Palsy,” *New England Journal of Medicine*, vol. 326, no. 11, pp. 745–749, Mar. 1992.

[156] F. Heinen *et al.*, “European consensus table 2006 on botulinum toxin for children with cerebral palsy,” *Eur. J. Paediatr. Neurol.*, vol. 10, no. 5–6, pp. 215–225, Nov. 2006.

[157] K. Straub and J. E. Obrzut, “Effects of Cerebral Palsy on Neuropsychological Function,” *J Dev Phys Disabil*, vol. 21, no. 2, pp. 153–167, Jan. 2009.

[158] “Rehabilitation and Cerebral Palsy: Overview, Orthotic Devices, Physical Therapy,” Jan. 2016.

[159] E. Taub *et al.*, “Technique to improve chronic motor deficit after stroke,” *Arch Phys Med Rehabil*, vol. 74, no. 4, pp. 347–354, Apr. 1993.

[160] E. Taub, G. Uswatte, D. K. King, D. Morris, J. E. Crago, and A. Chatterjee, “A placebo-controlled trial of constraint-induced movement therapy for upper extremity after stroke,” *Stroke*, vol. 37, no. 4, pp. 1045–1049, Apr. 2006.

[161] E. Taub, A. Griffin, G. Uswatte, K. Gammons, J. Nick, and C. R. Law, “Treatment of congenital hemiparesis with pediatric constraint-induced movement therapy,” *J. Child Neurol.*, vol. 26, no. 9, pp. 1163–1173, Sep. 2011.

[162] E. Taub, G. Uswatte, V. W. Mark, and D. M. M. Morris, “The learned nonuse phenomenon: implications for rehabilitation,” *Eura Medicophys*, vol. 42, no. 3, pp. 241–256, Sep. 2006.

[163] G. Uswatte and E. Taub, “Implications of the learned nonuse formulation for measuring rehabilitation outcomes: Lessons from constraint-induced movement therapy,” *Rehabilitation Psychology*, vol. 50, no. 1, pp. 34–42, 2005.

[164] “UP by Jawbone | Find the best fitness tracker for you.” [Online]. Available: https://jawbone.com/up/trackers. [Accessed: 25-Jun-2016].

[165] E. S. Sazonov, G. Fulk, N. Sazonova, and S. Schuckers, “Automatic Recognition of postures and activities in stroke patients,” in *Annual International Conference of the IEEE Engineering in Medicine and Biology Society, 2009. EMBC 2009*, 2009, pp. 2200–2203.

[166] E. Sazonov, V. Krishnamurthy, O. Makeyev, R. Browning, Y. Schutz, and J. Hill, “Automatic recognition of postural allocations,” *Conf Proc IEEE Eng Med Biol Soc*, vol. 2007, pp. 4993–4996, 2007.

[167] “extrema.m, extrema2.m - File Exchange - MATLAB Central.” [Online]. Available: http://www.mathworks.com/matlabcentral/fileexchange/12275-extrema-m--extrema2-m. [Accessed: 12-Sep-2016].

[168] Flegal KM, Carroll MD, Ogden CL, and Curtin LR, “PRevalence and trends in obesity among us adults, 1999-2008,” *JAMA*, vol. 303, no. 3, pp. 235–241, Jan. 2010.

[169] L. Yang and G. A. Colditz, “Prevalence of Overweight and Obesity in the United States, 2007-2012,” *JAMA Internal Medicine*, vol. 175, no. 8, p. 1412, Aug. 2015.

[170] J. T. Cavanaugh, K. L. Coleman, J. M. Gaines, L. Laing, and M. C. Morey, “Using Step Activity Monitoring to Characterize Ambulatory Activity in Community-Dwelling Older Adults,” *Journal of the American Geriatrics Society*, vol. 55, no. 1, pp. 120–124, Jan. 2007.

[171] G. S. Gupta, S. C. Mukhopadhyay, M. Sutherland, and S. Demidenko, “Wireless Sensor Network for Selective Activity Monitoring In a Home for the Elderly,” in *2007 IEEE Instrumentation Measurement Technology Conference IMTC 2007*, 2007, pp. 1–6.

[172] D. González-Ortega, F. J. Díaz-Pernas, M. Martínez-Zarzuela, and M. Antón-Rodríguez, “A Kinect-based system for cognitive rehabilitation exercises monitoring,” *Computer Methods and Programs in Biomedicine*, vol. 113, no. 2, pp. 620–631, Feb. 2014.

[173] V. R. Reddy and T. Chattopadhyay, “Human Activity Recognition from Kinect Captured Data Using Stick Model,” in *Human-Computer Interaction. Advanced Interaction Modalities and Techniques*, M. Kurosu, Ed. Springer International Publishing, 2014, pp. 305–315.

[174] E. E. Stone and M. Skubic, “Fall Detection in Homes of Older Adults Using the Microsoft Kinect,” *IEEE Journal of Biomedical and Health Informatics*, vol. 19, no. 1, pp. 290–301, Jan. 2015.

[175] R. Schmelzer, “Physical activity monitoring and recording system and device,” US20120215328 A1, 23-Aug-2012.

[176] B. Ni, G. Wang, and P. Moulin, “RGBD-HuDaAct: A Color-Depth Video Database for Human Daily Activity Recognition,” in *Consumer Depth Cameras for Computer Vision*, A. Fossati, J. Gall, H. Grabner, X. Ren, and K. Konolige, Eds. Springer London, 2013, pp. 193–208.

[177] P. Hevesi, S. Wille, G. Pirkl, N. Wehn, and P. Lukowicz, “Monitoring Household Activities and User Location with a Cheap, Unobtrusive Thermal Sensor Array,” in *Proceedings of the 2014 ACM International Joint Conference on Pervasive and Ubiquitous Computing*, New York, NY, USA, 2014, pp. 141–145.

[178] T. van Kasteren, A. Noulas, G. Englebienne, and B. Kröse, “Accurate activity recognition in a home setting,” 2008, p. 1.

[179] M. Chan, E. Campo, and D. Est??ve, “Assessment of activity of elderly people using a home monitoring system:,” *International Journal of Rehabilitation Research*, vol. 28, no. 1, pp. 69–76, Mar. 2005.

[180] S. A. Prince, K. B. Adamo, M. E. Hamel, J. Hardt, S. C. Gorber, and M. Tremblay, “A comparison of direct versus self-report measures for assessing physical activity in adults: a systematic review,” *International Journal of Behavioral Nutrition and Physical Activity*, vol. 5, p. 56, 2008.

[181] P. S. Freedson and K. Miller, “Objective Monitoring of Physical Activity Using Motion Sensors and Heart Rate,” *Research Quarterly for Exercise and Sport*, vol. 71, no. sup2, pp. 21–29, Jun. 2000.

[182] S. C. Mukhopadhyay, “Wearable Sensors for Human Activity Monitoring: A Review,” *IEEE Sensors Journal*, vol. 15, no. 3, pp. 1321–1330, Mar. 2015.

[183] J. E. Berlin, K. L. Storti, and J. S. Brach, “Using Activity Monitors to Measure Physical Activity in Free-Living Conditions,” *Physical Therapy*, vol. 86, no. 8, pp. 1137–1145, Aug. 2006.

[184] J. Parkka, M. Ermes, P. Korpipaa, J. Mantyjarvi, J. Peltola, and I. Korhonen, “Activity classification using realistic data from wearable sensors,” *IEEE Transactions on Information Technology in Biomedicine*, vol. 10, no. 1, pp. 119–128, Jan. 2006.

[185] M. Ermes, J. PÄrkkÄ, J. MÄntyjÄrvi, and I. Korhonen, “Detection of Daily Activities and Sports With Wearable Sensors in Controlled and Uncontrolled Conditions,” *IEEE Transactions on Information Technology in Biomedicine*, vol. 12, no. 1, pp. 20–26, Jan. 2008.

[186] H. H. Publications, “Moderate exercise: No pain, big gains,” *Harvard Health*. [Online]. Available:

http://www.health.harvard.edu/newsletter_article/Moderate_exercise_No_pain_big_gains. [Accessed: 28-Oct-2016].

[187] C. Debes, A. Merentitis, S. Sukhanov, M. Niessen, N. Frangiadakis, and A. Bauer, "Monitoring Activities of Daily Living in Smart Homes: Understanding human behavior," *IEEE Signal Processing Magazine*, vol. 33, no. 2, pp. 81–94, Mar. 2016.

[188] L. Tao *et al.*, "A comparative home activity monitoring study using visual and inertial sensors," in *2015 17th International Conference on E-health Networking, Application Services (HealthCom)*, 2015, pp. 644–647.

[189] C. Moufawad el Achkar, C. Lenoble-Hoskovec, A. Paraschiv-Ionescu, K. Major, C. Büla, and K. Aminian, "Instrumented shoes for activity classification in the elderly," *Gait & Posture*, vol. 44, pp. 12–17, Feb. 2016.

[190] M. Benocci, L. Rocchi, E. Farella, L. Chiari, and L. Benini, "A wireless system for gait and posture analysis based on pressure insoles and Inertial Measurement Units," in *3rd International Conference on Pervasive Computing Technologies for Healthcare, 2009. PervasiveHealth 2009*, 2009, pp. 1–6.

[191] N. Hegde, M. Bries, and E. Sazonov, "A Comparative Review of Footwear-Based Wearable Systems," *Electronics*, vol. 5, no. 3, p. 48, Aug. 2016.

[192] K. P. Dowd, D. M. Harrington, and A. E. Donnelly, "Criterion and Concurrent Validity of the activPAL™ Professional Physical Activity Monitor in Adolescent Females," *PLOS ONE*, vol. 7, no. 10, p. e47633, Oct. 2012.

[193] "PAL Technologies Ltd." [Online]. Available: http://www.paltech.plus.com/products.htm. [Accessed: 01-Dec-2015].

[194] H. Peng, F. Long, and C. Ding, "Feature selection based on mutual information criteria of max-dependency, max-relevance, and min-redundancy," *IEEE Transactions on Pattern Analysis and Machine Intelligence*, vol. 27, no. 8, pp. 1226–1238, Aug. 2005.

[195] J. F. Knight and C. Baber, "A tool to assess the comfort of wearable computers," *Hum Factors*, vol. 47, no. 1, pp. 77–91, 2005.

[196] Y. Schutz, "The basis of direct and indirect calorimetry and their potentials," *Diabetes Metab. Rev.*, vol. 11, no. 4, pp. 383–408, Dec. 1995.

[197] I. of M. (US) C. on M. N. Research, S. J. Carlson-Newberry, and R. B. Costello, *Doubly Labeled Water for Energy Expenditure*. National Academies Press (US), 1997.

[198] S. E. Crouter, K. G. Clowers, and D. R. Bassett, "A novel method for using accelerometer data to predict energy expenditure," *Journal of Applied Physiology*, vol. 100, no. 4, pp. 1324–1331, Apr. 2006.

[199] H. Kumahara *et al.*, “The use of uniaxial accelerometry for the assessment of physical-activity-related energy expenditure: a validation study against whole-body indirect calorimetry,” *British Journal of Nutrition*, vol. 91, no. 2, pp. 235–243, Feb. 2004.

[200] F. Albinali, S. Intille, W. Haskell, and M. Rosenberger, “Using Wearable Activity Type Detection to Improve Physical Activity Energy Expenditure Estimation,” in *Proceedings of the 12th ACM International Conference on Ubiquitous Computing*, New York, NY, USA, 2010, pp. 311–320.

[201] N. Twomey, S. Faul, and W. P. Marnane, “Comparison of accelerometer-based energy expenditure estimation algorithms,” in *2010 4th International Conference on Pervasive Computing Technologies for Healthcare*, 2010, pp. 1–8.

[202] P. B. Júdice, M. T. Hamilton, L. B. Sardinha, T. W. Zderic, and A. M. Silva, “What is the metabolic and energy cost of sitting, standing and sit/stand transitions?,” *Eur. J. Appl. Physiol.*, vol. 116, no. 2, pp. 263–273, Feb. 2016.

[203] “How accurate are Fitbit trackers?,” *Fitbit Help*. [Online]. Available: https://help.fitbit.com/articles/en_US/Help_article/1136. [Accessed: 25-Dec-2016].

[204] K. Zhang, P. Werner, M. Sun, F. X. Pi-Sunyer, and C. N. Boozer, “Measurement of human daily physical activity,” *Obes. Res.*, vol. 11, no. 1, pp. 33–40, Jan. 2003.

[205] S. J. Strath, D. R. Bassett, D. L. Thompson, and A. M. Swartz, “Validity of the simultaneous heart rate-motion sensor technique for measuring energy expenditure,” *Med Sci Sports Exerc*, vol. 34, no. 5, pp. 888–894, May 2002.

[206] M. Ga, W. Kr, K. H, and ten H. F, “Assessment of energy expenditure by recording heart rate and body acceleration.,” *Med Sci Sports Exerc*, vol. 21, no. 3, pp. 343–347, 1989 1989.

[207] G. B. Spurr, A. M. Prentice, P. R. Murgatroyd, G. R. Goldberg, J. C. Reina, and N. T. Christman, “Energy expenditure from minute-by-minute heart-rate recording: comparison with indirect calorimetry.,” *Am J Clin Nutr*, vol. 48, no. 3, pp. 552–559, Sep. 1988.

[208] S. E. Crouter, J. I. Flynn, and D. R. Bassett, “Estimating physical activity in youth using a wrist accelerometer,” *Med Sci Sports Exerc*, vol. 47, no. 5, pp. 944–951, May 2015.

[209] D. R. Bassett, B. E. Ainsworth, A. M. Swartz, S. J. Strath, W. L. O’Brien, and G. A. King, “Validity of four motion sensors in measuring moderate intensity physical activity,” *Med Sci Sports Exerc*, vol. 32, no. 9 Suppl, pp. S471-480, Sep. 2000.

[210] A. M. Swartz, S. J. Strath, D. R. Bassett, W. L. O’Brien, G. A. King, and B. E. Ainsworth, “Estimation of energy expenditure using CSA accelerometers at hip and wrist sites,” *Med Sci Sports Exerc*, vol. 32, no. 9 Suppl, pp. S450-456, Sep. 2000.

[211] S. E. Crouter, J. R. Churilla, and D. R. Bassett, “Accuracy of the Actiheart for the assessment of energy expenditure in adults,” *Eur J Clin Nutr*, vol. 62, no. 6, pp. 704–711, Apr. 2007.

[212] “Sensoria Fitness: http://www.sensoriafitness.com/.” [Online]. Available: http://www.sensoriafitness.com/. [Accessed: 03-Dec-2015].

[213] J. Staudenmayer, D. Pober, S. Crouter, D. Bassett, and P. Freedson, “An artificial neural network to estimate physical activity energy expenditure and identify physical activity type from an accelerometer,” *Journal of Applied Physiology*, vol. 107, no. 4, pp. 1300–1307, Oct. 2009.

[214] A. G. Edwards, J. O. Hill, W. C. Byrnes, and R. C. Browning, “Accuracy of optimized branched algorithms to assess activity-specific physical activity energy expenditure,” *Med Sci Sports Exerc*, vol. 42, no. 4, pp. 672–682, Apr. 2010.

[215] “Refined Two-Regression Model for the ActiGraph Accelerometer : Medicine & Science in Sports & Exercise,” *LWW*. [Online]. Available: http://journals.lww.com/acsm-msse/Fulltext/2010/05000/Refined_Two_Regression_Model_for_the_ActiGraph.25.aspx. [Accessed: 22-Dec-2016].

[216] “COSMED - Validation Papers.” [Online]. Available: http://www.bodpod.com/en/science/validation-papers. [Accessed: 06-Dec-2016].

[217] E. L. Melanson, J. P. Ingebrigtsen, A. Bergouignan, K. Ohkawara, W. M. Kohrt, and J. R. B. Lighton, “A new approach for flow-through respirometry measurements in humans,” *Am J Physiol Regul Integr Comp Physiol*, vol. 298, no. 6, pp. R1571–R1579, Jun. 2010.

[218] “One-sample Kolmogorov-Smirnov test - MATLAB kstest.” [Online]. Available: https://www.mathworks.com/help/stats/kstest.html?requestedDomain=www.mathworks.com. [Accessed: 29-Dec-2016].

APPENDIX A IRB APPROVAL

THE UNIVERSITY OF ALABAMA | Office of the Vice President for Research & Economic Development
Office for Research Compliance

August 23, 2016

Edward Sazonov, Ph.D.
Electrical & Computer Engineering
College of Engineering
The University of Alabama
Box 870286

Re: IRB Protocol # 15-016-ME-R1
"A Longitudinal Assessment of Fall Risk: SmartStep Development"

Dr. Sazonov:

The University of Alabama Medical IRB recently met to consider your renewal application. The IRB voted to approve your protocol for a period of one year.

Your application will expire on August 11, 2017. You will receive a notice of the expiration date 90 days in advance. If your research will continue beyond this date, complete the renewal portions of the FORM: IRB Renewal Application. If you need to modify the study, please submit FORM: Modification of An Approved Protocol. Changes in this study cannot be initiated without IRB approval, except when necessary to eliminate apparent immediate hazards to participants. When the study closes, please complete the FORM: Request for Study Closure.

Please use reproductions of the IRB approved stamped consent form or information sheet to obtain consent [redacted]

Should [redacted] respondence regarding this application, please include the above [redacted]

Good luck with your research.

Sincerely,

J. Grier Stewart, MD, FACP
Medical IRB Chair

358 Rose Administration Building | Box 870127 | Tuscaloosa, AL 35487-0127
205-348-8461 | Fax 205-348-7189 | Toll Free 1-877-820-3066

AHRPP DOCUMENT
THE UNIVERSITY OF ALABAMA
HUMAN RESEARCH PROTECTION PROGRAM
UNIVERSITY OF ALABAMA INSTITUTIONAL REVIEW BOARD

Title of Research: A Longitudinal Assessment of Fall Risk: SmartStep development

Investigator(s): Edward Sazonov, PhD
IRB Approval #: **OSP #:**
Sponsor: None

<u>You are being asked to be in a research study.</u>

The name of this study is "A Longitudinal Assessment of Fall Risk: SmartStep development"

This study is being done by Edward Sazonov, PhD. He is a professor of Electrical and Computer Engineering at the University Of Alabama College Of Engineering.

Who is paying for this study?
This study is supported by the internal funding at the University of Alabama.

Is the researcher being paid for this study?
The researcher is not paid to conduct this study.

Is this research developing a product that will be sold, and if so, will the researcher profit from it?
This research is not developing a product to be sold, but a measurement device for research studying the risk of falling in elderly.

What is the purpose of this study—what is it trying to learn?
The objective of this research project is to build a sensor system that uses foot pressures and foot motion to identify and distinguish between different functional postures and activities. The sensor system consists of SmartStep insole monitoring system and a hand gesture sensor module. The sensor system is developed and built at University of Alabama and is an investigational device.
To validate the results of the proposed solution, the resultant data from the above sensor system will be compared against a commercially available sensor module – ActivePal, which the subject will be wearing during the study.

Based on the availability, a portable metabolic mask may be used in the study, which the participant is supposed to be wearing during the laboratory part.

- **Why is this study important—What good will the results do?**

The results will enable researchers to better analyze daily posture and activities in order to analyze the risk of falling in elderly. If the metabolic mask is used, then the study data can be used in developing energy expenditure models.

- **Why have I been asked be in this study?**

You have been asked to be in this study because you are a healthy individual within the age interval that is needed for the experiment.

- **What will I be asked to do in this study?**

If you agree to participate in this research project it will take approximately one and a half hours of your time in lab and then there will be a free living study part. The investigators will provide an insole that you'll wear in your shoes. The insoles feel just like any shoe insole. The insoles also contains electronics that collect information about the pressure under the foot and foot motion. A low-capacity battery powering the device is not capable of inflicting an electrical shock. Similar batteries are used in a variety of children toys, cell phones and other electronic appliances commonly available to general population. You will be also wearing a hand gesture sensor on the wrist and an activity tracker on your thigh. Based on the availability, you may be wearing a metabolic mask during the laboratory part of the study. You are isolated from the electronics of the sensors. The insole will not interfere with the normal use and support of the shoe. This sensor is an investigational device that is not approved by the FDA.

While wearing the monitor you will be asked to perform one of the following activities:

- Lie, sit or stand
- Walk/Jog on a treadmill
- Ascend/descend 3 flights of stairs
- Pedal a stationary bicycle
- Vacuum the floor and stack/shelve items
- Transition between posture and activities (for example, from sitting to standing)
- Walk in the hallways while changing direction and speed
- Drive your car
- Wear the sensor system while going back and perform all the activities as a usual day for 24 hours.

- **How much time will I spend being in this study?**
- **The time complete the study in lab is approximately two hours. And the free living part is 24 hours . You will be compensated $20.00 for participation in the study in lab and $20 for free living part. An additional $10 will be provided at the completion of both parts.**

- **Will being in this study cost us anything?**

No.

- **What are the benefits of being in this study?**

You will not benefit directly from this research. However, the results may help researchers and clinicians use this type of shoe sensor in the future to predict risk of falling in elderly.

What are the risks (dangers or harms) to me if I am in this study?

There are minimal risks associated with participation in this research project. The insole sensor does not interfere with a person's ability to walk, stand or sit so will not pose a risk of fall. There may be a risk of experiencing high heart rate or chest pains. To minimize these risks your heart rate will be continuously monitored and protocol stopped if your heart rate exceeds

80 % of your predicted maximum heart rate. The protocol can also be stopped at any time at your request. Other possible risks are likely to be fatigue, shortness of breath, or muscle soreness during or after the exercise trials. It is expected that when these symptoms occur, they will be minor and brief. We are using proper sanitization methods to all our sensors; however, in case there is any irritation and/or redness after wearing our sensor modules, you are advised to take them off immediately.

There is also the risk of release of personal information. All of the information collected during this study will be kept strictly confidential and used for research purposes only. Information obtained in this study is strictly confidential unless disclosure is required by law. All data will be secured in a locked filing cabinet and in a password protected computer, to which only the researchers will have access. Your name will not be recorded or used in the reporting of information in publications or conference presentations. When the results are presented in research proceedings it will be presented as a whole. Individual participants will not be able to be identified in any way. All individual information will be erased following this study.

How will my privacy be protected?
We will not tell anyone you are in this study. You do not have to answer any questions or give us any information that you do not want to. All individual information will be erased following this study. While wearing ActivePal sensor, which need to be attached to the thigh, you will be allowed to be alone to remove the lower body wear and attach the sensor module.

How will my confidentiality be protected?
The information collected will be kept confidential as much as is permitted by law. The data collected will be kept in a locked cabinet and in a password protected computer in a locked office. Any presentation of the results in scientific journals or meetings will be done in aggregate so that individual participants cannot be identified

Do I have to be in this study?
No. If you decide to be in this study it should be because you really want to volunteer. You can refuse to be in the study at all. You can also start the study and decide to stop at any time. If you refuse or if you start the study and then stop it, you will not receive the remuneration for your time.

If I do not want to be in the study, are there other choices?
If you do not want to be in this study, the other choice is to refuse. We will thank you for your time.

What if I have questions, suggestions, concerns, or complaints?
If you have questions about the study now, please ask them. If you have questions or concerns later, you can reach Dr. Sazonov at 315-244-2375. If you have questions about your rights as a person taking part in a research study, call Ms. Tanta Myles, The Research Compliance Officer of the University of Alabama at 205-348-8461.

What else do we need to know?

You do not give up any of your legal rights by signing this consent form.

You will be given a copy of this consent form to keep. Save it in case you want to review it later or you decide to contact the investigator or the university about the study.

The University of Alabama Institutional Review Board (IRB) is the committee that protects the rights of people in research studies. The IRB may review study records from time to time to be sure that people in research studies are being treated fairly and the study is being carried out as planned.

Also, the IRB conducts a survey of research participants about their experiences in a UA study. To complete it, ask the investigator for a copy or call IRB at (205) 348-8461. The survey can also be found on the IRB Outreach website at http://osp.ua.edu/site/PRCO_Welcome.html. The only identification requested is whether you are connected with UA or are from the outside community. Your response helps us improve our research protection program.

You may also ask questions, make suggestions, or file complaints and concerns at this website.

I have read this consent form. I have had a chance to ask questions. My questions have been answered. I understand what I will be asked to do. I freely agree to take part in it.

____ Date__________
Signature of Research Participant

____ Date__________
Signature of Investigator

APPENDIX B PUBLICATIONS

Journal Publications

SmartStep: A Fully Integrated, Low-Power Insole Monitor

Electronics 2014, 3, 381-397. Nagaraj Hegde, Edward Sazonov

A Comparative Review of Footwear Based Wearable Systems

Electronics 2016, 5(3), 48; doi:10.3390/electronics5030048, Nagaraj Hegde et.al

Posture and Activity Recognition and Energy Expenditure Estimation in a Wearable Platform

IEEE Journal of Biomedical and Health Informatics 05/2015; 19(4):1339-1346. DOI:10.1109/JBHI.2015.2432454, Edward Sazonov, Nagaraj Hegde et. Al

Conference Papers

Development of the RT-GAIT, a Real-Time Feedback Device to Improve Gait of Individuals with Stroke

IEEE Engineering in Medicine and Biology Society Conference, Milan, Italy, 08/2015. Nagaraj Hegde et.al

SmartStep 2.0 – A Completely Wireless, Versatile Insole Monitoring System

2015 IEEE International Conference on Bioinformatics and Biomedicine, Washington DC, November 2015. Acceptance rate: 18%. Nagaraj Hegde, Edward Sazonov

Development of A Real Time Activity Monitoring Android Application Utilizing SmartStep

IEEE Engineering in Medicine and Biology Society Conference, Orlando, FL, 08/2016. Nagaraj Hegde et.al

Development of SmartStep: An insole-based physical activity monitor

IEEE Engineering in Medicine and Biology Society Conference, Osaka, Japan, 07/2013. Edward Sazonov, Nagaraj Hegde.

SmartStep – A completely wireless, versatile insole monitor

Poster- IDTechEx Wearable USA conference, Santa Clara, CA 11/2015, Nagaraj Hegde et. al

SmartStep 2.0 insole monitor

Poster and Demo – Wireless Heath, Washington DC 9/2015, Nagaraj Hegde et. al

Book Chapter

Security issues in sdn/openflow

Network Innovation through OpenFlow and SDN: Principles and Design, CRC press, Nagaraj Hegde et al.

Papers under review

Implementation and Evaluation of an Android Bluetooth Low Energy Application for Multi-Sensor Interface

Article submitted to Pervasive and Mobile Computing, Elsevier, Nagaraj Hegde et.al

The Pediatric SmartShoe: Wearable Sensor System for Ambulatory Monitoring of Physical Activity and Gait

Under process for IEEE transactions on neuro engineering and rehabilitation, Nagaraj Hegde et.al

Monitoring Activities of Daily Living with Upper and Lower-body Worn Sensors

Under process for IEEE Journal of Biomedical and Health Informatics, Nagaraj Hegde et.al

Award

Texas Instruments North America Innovation Challenge 2016